The Dissertation Committee for Olga Zolochevska Certifies that this is the approved version of the following dissertation:

Epigenetic Modulation of Synaptic Resilience in Alzheimer's Disease

Committee:

Giulio Taglialatela, Ph.D., Supervisor

John Wiktorowicz, Ph.D.

Jere McBride, Ph.D.

Rakez Kayed, Ph.D.

Maria Micci, Ph.D.

Christopher Norris, Ph.D.

Dean, Graduate School

Epigenetic Modulation of Synaptic Resilience in Alzheimer's Disease

by

Olga Zolochevska, B.S., M.Ed., M.S.

Dissertation

Presented to the Faculty of the Graduate School of

The University of Texas Medical Branch

in Partial Fulfillment

of the Requirements

for the Degree of

Doctor of Philosophy

The University of Texas Medical Branch
November 2018

Acknowledgements

I would like to thank my mentor, Dr. Taglialatela, for his guidance during the years of my Ph.D. studies. I am indefinitely greatful for his support of all my professional and personal endeavors.

I would like to thank my science family for the insightful discussions, encouragement and sense of humor, which was greatly appreciated during the difficult times. Special thanks to David Briley, Claudia Marino and Whitney Franklin – your friendship added many bright colors to the routine. I also thank Salvo Saieva, Anna Fracassi, Wen Ru Zhang, Balaji Krishnan, Samantha Sheller-Miller and Liz Crofton.

I would also like to thank my committee members: Drs. Maria Adelaide Micci, Rakez Kayed, John Wiktorowicz, Christopher Norris and Jere McBride for their support and constructive critisism. Dr. David Niesel, Dr. Dorian Coppenhaver, Dr. Pomila Singh, Aurora Galvan and Debra Moncrief at UTMB.

Most importantly, I would like to thank my non-science family who had my back during these years. My husband, who had to suffer through proofreading of my abstracts and papers; who had to be the dog walker, the cook, the housekeeper and both mommy and daddy at times. My mom, who has been listening to my sciency monologues for many years and has not complained a single time. And last, but definitely not least, my daughter, the light of my life, for giving me inspiration and motivation to follow my dreams so that she can dream even bigger.

Epigenetic Modulation of Synaptic Resilience in Alzheimer's Disease

Publication No._____

Olga Zolochevska, Ph.D.

The University of Texas Medical Branch, 2018

Supervisor: Giulio Taglialatela

Some individuals, here referred to as Non-Demented with Alzheimer's Neuropathology (NDAN), retain their cognitive function despite the presence of amyloid plaques and tau tangles typical of symptomatic Alzheimer's Disease (AD). In NDAN, unlike AD, toxic amyloid beta (Aβ) oligomers do not localize to the postsynaptic densities (PSDs). Synaptic resistance to amyloid beta in NDAN may therefore enable these individuals to remain cognitively intact despite the AD-like pathology. The mechanisms responsible for this resistance remain unresolved and understanding such protective biological processes could reveal novel targets for the development of effective treatments for AD. The current work describes the use of a proteomic approach to compare the hippocampal postsynaptic densities of NDAN, AD and healthy age-matched persons to identify protein signatures characteristic for these groups. Subcellular fractionation followed by 2D gel electrophoresis and mass spectrometry were used to analyze the PSDs. Fifteen proteins were identified as the unique proteomic signature of NDAN PSDs, thus setting them apart from control subjects and AD patients. Using Ingenuity Pathway Analysis several microRNAs were identified as potential upstream regulators of the observed changes in the postsynaptic proteome of NDAN. MicroRNA-149, -4723 and -485 were confirmed to have differential expression in AD and NDAN hippocampi when compared to control. When tested *in vitro* (cellular system) and *in vivo* (wild-type mice) these microRNAs were capable of reducing Aβ oligomer binding possibly via modulating the key mRNAs. Remarkably, *in vivo* these protective effects were brain region- and sex-dependent. Taken together, our findings suggest that the unique protein signature at the NDAN PSDs is regulated by the selected microRNAs, while modulation of microRNA levels *in vitro* and *in vivo* has an effect on Aβ oligomer binding, further suggesting that a unique regulation of microRNAs in the NDAN subjects could be responsible for protection of synapses from Aβ toxicity, thus contributing to the retention of cognitive ability.

TABLE OF CONTENTS

List of Tables

List of Figures

List of Abbreviations

2DE	2D gel electrophoresis
AChE	acetylcholinesterase
AD	Alzheimer's Disease
ADC	AD Center
ANXA2	annexin 2
APOE	apolipoprotein ε
APP	amyloid precursor protein
Asc	ascorbate
Aβ	amyloid beta
BDNF	brain-derived neurotrophic factor
c-Abl	Abelson tyrosine-protein kinase 1
CAMK	calcium/calmodulin-dependent protein kinase
CDK	cyclin-dependent kinase
CDR	clinical dementia rating
CERAD	Consortium to Establish a Registry for Alzheimer's Disease
CKB	creatine kinase B
Clic6	chloride intracellular channel 6
CLTA	clathrin light chain A
CNP	2',3'-cyclic-nucleotide 3'-phosphodiesterase
CREB	cAMP response element-binding protein factor
DNM1	dynamin-1
DNMT1	DNA methyltransferase
ERK	mitogen-activated protein kinase
FC	frontal cortex
FDA	Food and Drug Administration
FDR	false discovery rate
GAPDH	glyceraldehyde-3-phosphate dehydrogenase
GFAP	glial fibrillary acidic protein

GluR2	glutamate receptor 2
GWAS	genome-wide SNP association study
H	hippocampus
HBB	hemoglobin
HBK	HEPES-buffered Krebs-like
HDAC	histone deacetylase
HSP90	heat shock protein 90
HTT	huntingtin
ICV	intracerebroventricular
IDE	insulin-degrading enzyme
IPA	Ingenuity Pathway Analysis
KRT	keratin
LTP	long-term potentiation
MALDI-TOF/TOF	matrix assisted laser desorption ionization-time of flight
MAP2	microtubule-associated protein 2
MAPT	microtubule-associated protein tau
MCI	mild cognitive impairment
MDH	malate dehydrogenase
Meg3	maternally expressed 3
miR	microRNA
MMSE	Mini-Mental State Examination
MS	mass spectrometry
nAChR	nicotinic acetylcholine receptor
NDAN	non-demented with Alzheimer's neuropathology
NDUFA5	NADH dehydrogenase [ubiquinone] 1 alpha subcomplex subunit 5
NDUFV1	NADH dehydrogenase [ubiquinone] flavoprotein 1
NEFM	neurofilament medium polypeptide
NFT	neurofibrillary tangle
NL-1	neuroligin-1
NMDAR	N-methyl-D-aspartate receptor
OHSU	Oregon Health and Science University

PC	pyruvate carboxylase
Pcdh20	protocadherin 20
PFN2	profilin 2
PiB	Pittsburg Compound B
PMF	peptide mass fingerprint
PMI	post-mortem interval
PP2A	protein phosphatase 2
PPP3CA	protein phosphatase 3, catalytic subunit, alpha isoform
PRDX5	peroxiredoxin-5
PrPc	prion protein
PSD	postsynaptic density
PSD95	postsynaptic density 95
PSEN	presenilin
qRT-PCR	quantitative real-time PCR
RhoGDI	Rho GDP-dissociation inhibitor 1
Rreb1	Ras responsive element binding protein 1
SEPT7	septin-7
SNAP25	synaptosomal-associated protein 25
SNCA	synuclein alpha
Snhg11	small nucleolar RNA host gene 11
SNP	single nucleotide polymorphism
Sp1	specificity protein 1
SPTAN1	spectrin alpha chain
STAR	Spliced Transcript Alignment to a Reference
STXBP1	syntaxin-binding protein 1
SYN1	synapsin-1
Syt17	synaptotagmin XVII
TNF-R	tumor necrosis factor receptor
Ttr	transthyretin
TUB	tubulin
UCHL1	ubiquitin carboxyl-terminal hydrolase isozyme L1

VAMP2	vesicle-associated membrane protein 2
VCL	vinculin
βME	beta-mercaptoethanol

CHAPTER 1. GENERAL INTRODUCTION

Alzheimer's Disease

Alzheimer's Disease (AD) is the most common form of dementia, affecting more than 5 million Americans [1]. Familial AD, representing a small subset of up to 5% cases, is associated with mutations in amyloid precursor protein (APP) and presenilin genes (PSEN1 and PSEN2) (reviewed by [2]). The etiology of sporadic AD, on the other hand, is complex and uncertain. Advanced age is the greatest risk factor for Alzheimer's, and over one third of people older than 85 have AD. Additionally, multiple other risk factors have been described: polymorphism of APOE (apolipoprotein ε4 carriers are more prone to AD development in a dose-dependent manner), gender (females are more susceptible), brain injury, cardiovascular health, physical activity and social interactions (reviewed by [2,3]). While available therapies are palliative and only temporarily improve cognition, there are no treatments that target pathological changes of AD. Currently there are five FDA (Food and Drug Administration) approved medications that are used to modulate cholinergic and glutamatergic circuits affected in AD [1].

In the clinic, AD is diagnosed through a series of medical tests which include assessment of mental status, physical and neurological exams, evaluation of medical history and additional tests (*e.g.* blood tests, brain imaging) [4,5]. One of the tests widely used is the Mini-Mental State Examination (MMSE), which assesses global cognitive function on a 0-30 scale (27-30 indicates a normal cognition) [6]. There is no single test to determine whether someone has AD. Unfortunately only at autopsy, neuropathologists can confirm AD diagnosis by evaluation of microscopic changes caused by the disease [7]. Based on the level of accumulation and distribution of neurofibrillary tangle (NFT) pathology (discussed below), one of six Braak stages

is assigned [8]. Braak I-II stages are characterized by changes in cortex, mild involvement of hippocampus and absence of isocortical changes. Mild to moderate damage of hippocampus and low isocortical involvement is typical for Braak III-IV. Stages V and VI are described by pathological changes in all components of hippocampus, isocortex, insula, orbitofrontal cortex, hypothalamus and substantia nigra [8].
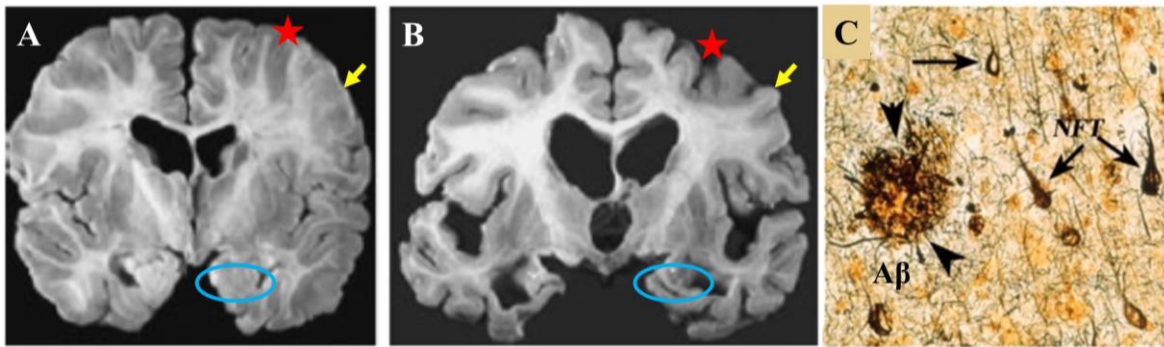
Figure 1.1:   Pathology of AD

Coronal sections of elderly nondemented individual (A) and AD patient (B) are shown. Widening of sulci (stars), shrinkage of gyri (arrows), significant shrinkage of hippocampus (circled) are typical changes during AD. Modified from Yaari and Corey-Bloom [9]. (C) Aβ plaques (arrowheads) and neurofibrillary tangles (arrows) in AD brain are revealed by the Bielschowsky silver stain. Modified from Nixon [10].

It can be appreciated that AD is a multifactorial disease that is characterized by cognitive decline and unique pathology, which is defined by the brain atrophy with widening of sulci and shrinkage of gyri (Fig. 1.1A, B) [9]. Noticeably, the hippocampus (Fig. 1.1A, B, circled), responsible for formation of new memories, is one of the most affected areas in the brain [11]. At the same time, at the microscopic level two main neurodegenerative processes, amyloidogenesis and NFT formation, are characteristic for AD brain (Fig.1.2C). However, these changes begin long before memory loss [12] with synapse loss being the most robust correlate of cognitive

decline in patients with AD [13,14]. Synapse loss is believed to occur at early stages of the disease before manifestation of the symptoms ([9,12] and reviewed by [13,15]), whereas cell death occurs at later stages [12]. Synaptic dysfunction can occur due to the presence of oligomeric forms of amyloidogenic proteins, in particular, two hallmark proteins of AD – amyloid beta (Aβ) and tau. Below, I briefly discuss these two proteins.

AMYLOID BETA PEPTIDE

A parent protein of Aβ, amyloid precursor protein (APP), is a 770 amino acids long, 87 kDa type I transmembrane glycoprotein, which is ubiquitously expressed and evolutionary conserved [16]. APP is important in synaptic transmission, learning and memory, and synaptic plasticity [17,18]. More than 20 years ago mutations in APP and APP-processing enzymes (presenilin-1 and -2, PSEN1/PSEN2) were linked to familial AD [17,18]. On the other hand, some polymorphisms in APP (for example, A673T) have a protective function against cognitive decline [19]. APP is located on chromosome 21, hence similar to AD pathology can be observed in later life of people with Down's syndrome.

APP can be cleaved by at least three enzymes: α-, β- and γ-secretases [16,20]. In the Non-amyloidogenic pathway, α-secretase cleaves within the Aβ sequence, generating non-toxic peptides. In the Amyloidogenic pathway, cleavage by β- and γ-secretases results in formation of Aβ (4 kDa peptide) and other peptides. γ-secretase has several recognition sites on Aβ peptide to yield 39-43 amino acid Aβ fragment [21]. Two main forms of Aβ are Aβ40 and Aβ42, which have different COOH-termini and aggregation propensity (Aβ42 has quicker kinetics).

The 4 kDa Aβ peptide, cleaved by β- and γ-secreatases, forms insoluble aggregates which have been shown to cause neurodegeneration [22]. Moreover, Aβ fragment can undergo multiple post-translation modification, which can affect its aggregation abilities (reviewed by [23]).

18

Misfolding of amyloid proteins into toxic aggregates involves few steps: monomer → paranuclei or small oligomers → large oligomers → protofibrils → fibrils [24]. Early oligomers formed during aggregation are the most toxic forms of misfolded Aβ, and have been shown to accumulate at the synapse [25–28]. Aβ oligomers are very "sticky" and can interact with multiple proteins and receptors, for example, α7-nAChR (α7-nicotinic acetylcholine receptor), AChE (acetylcholinesterase), PrPc (prion protein), NMDAR (N-methyl-D-aspartate receptor), TNF-R (tumor necrosis factor receptor), α2β1 and αVβ1 integrins, NL-1 (neuroligin-1) and others [29].

During Aβ oligomer interaction with the synapses, as reviewed by Sengupta *et al.*, they can exert their toxic function via multiple mechanisms [30]. For instance, Aβ oligomer association with the postsynaptic density (PSD) results in disturbed Ca^{2+} signaling in dendritic spines, which can affect multiple downstream pathways [31]. Furthermore, injection of Aβ oligomers into the CNS blocks long-term potentiation and disrupts cognitive function in rats [29]. Additionally, Aβ oligomers can cause membrane disruption, ion dysregulation, pore formation, inhibition of long-term potentiation, alterations in insulin signaling, toxic free radical formation, activation of astrocytes and recruitment of microglia [32] (reviewed by [23,30,33,34]. Aβ oligomers can also modify protein content at PSD thus inducing dendritic spine loss, and causing shrinkage of PSDs in cultured neurons [26,31]. Size of the PSD is proportional to the synapse strength, and therefore, Aβ-driven synapse damage can result in the loss of cognitive function due to dysruption of synapses. Moreover, Aβ toxicity can be dependent on size, aggregation state and diffusion of Aβ oligomers (reviewed by [30]). It was previously demonstrated that, contrary to Aβ oligomers, fibrillar Aβ is incapable of association

with the PSDs of primary hippocampal neurons (Fig. 1.2) [31]. In fact, there is no correlation

between presence of mature Aβ deposits with the cell loss or cognitive decline [18,25,35–37].
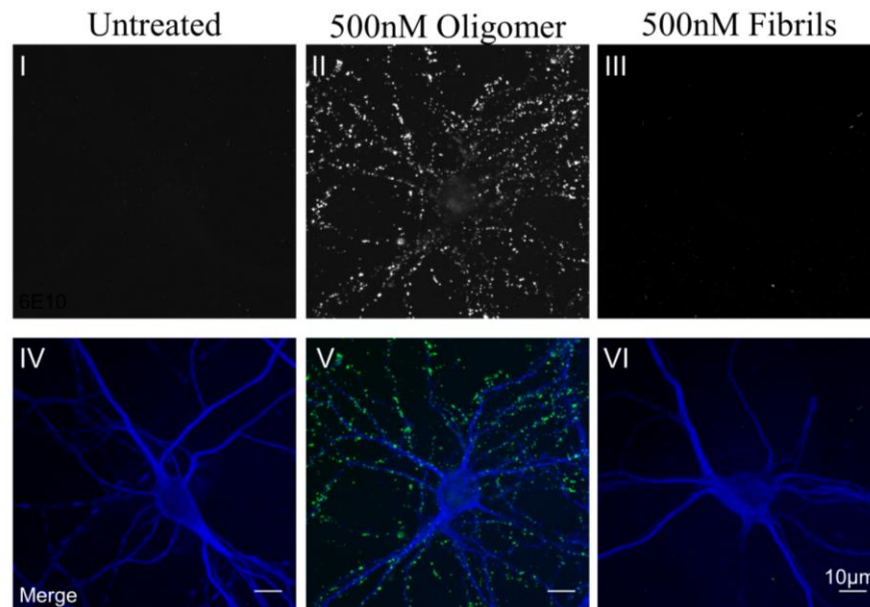
Figure 1.2. Aβ oligomers associate with the synapses

Oligomeric, but not fibrillar Aβ associates with dendritic processes of primary hippocampal neurons. Rat primary hippocampal neurons (day 17) were exposed to 500 nM oligomers or 500 nM fibrils (prepared in our laboratory) for 60 minutes then fixed and immunolabeled using 6E10 (green), which recognizes Aβ (I-III) and MAP2 (microtubule-associated protein 2; blue) antibodies. Merge is shown in (IV-VI) [31].

TAU PROTEIN

Tau protein is the main component of NFTs in AD and other tauopathies. Several neurodegenerative disorders (termed tauopathies) are characterized by the progressive accumulation of NFT lesions, however, AD is characterized by the co-presence of Aβ and tau depositions (reviewed by [38]). Microtubule-associated protein tau (MAPT) has six isoforms due to alternative splicing of exons 2, 3 and 10 [39]. These isoforms can contain either three (3R-tau)

or four (4R-tau) repeats of a conserved tubulin binding motif at the C-terminus, in addition to one or two acidic motifs at the N-terminus. The shortest isoform is 353 amino acids long and is the only isoform expressed in fetal human brain, while the longest tau isoform has 441 amino acids. The main fucntion of tau is stabilization of microtubules, however, many additional functions have been decribed, *i.e.* interactions with actin to promote polymerization, binding to other cytoskeleton proteins, plasma membrane and multiple signaling molecules (reviewed by [38]).

The exact mechanism of tau-driven toxicity is not entirely understood. While normally tau is a highly soluble protein, under pathological conditions it can aggregate to form oligomers that assemble into insoluble filaments and later form NFTs (reviewed by [38]). Tau can undergo multiple post-translational modifications, including phosphorylation, glycosilation, ubiquitination, truncation and others. Tau hyperphosphorylation is considered to be one of the early events in the pathogenesis of tauopathies. The phosphorylation state of tau is regulated by several kinases and proteases (reviewed by [38]). Hyperphosphorylated tau has reduced affinity for microtubules, which can result in the disassembly of the latter [40], thus potentially altering traffic of multiple cellular organelles and other cargoes to the synapses (reviewed by [41]). Additionally, tau hyperphosphorylation could be involved in neurodegeneration also due to increased fragmentation of Golgi and decreased mitochondria and rough endoplasmic reticulum (reviewed by [42]). Importantly, not only hyperphosphorylated [43] but also the truncated form of tau can form hetero-oligomers with normal tau, thus promoting its aggregation into fibrils (reviewed by [42]).

Pathologic tau was shown to accumulate in the spines (reviewed by [15]), where it can disrupt synaptic transmission and alter neurotransmitter receptor composition at the PSD [44]. It

21

can also co-localize with pre- and postsynaptic markers [45,46]. Interestingly, at the presynaptic site tau can immobilize presynaptic vesilces by binding directly to the vesicles and promoting actin polymerization to crosslink vesicles therefore restricting their release [47]. Similar to Aβ olgiomers, tau oligomers (and not fibrils) can induce neuronal damage and inhibit energy production by targeting mitochondria complex I, as reported by Lasagna-Reeves *et al.* [48]. However, compared to Aβ oligomers, less is known about tau-driven toxicity, and with continuing research additional mechanisms may be identified which will then allow for development of therapeutic interventions.

Aβ AND TAU OLIGOMERS SYNERGISTICALLY CAUSE SYNAPTIC TOXICITY

Several recent reports suggest that Aβ and tau can act together to impair dendritic spines in the hippocampus [25–28,49–51], however, the exact mechanisms of Aβ and tau toxic convergence are currently being elucidated. It was previusoly shown that both, Aβ and tau, can be released from neurons in response to synaptic activity (reviewed by [41]) and in AD brains they are known to co-localize within the synaptic terminals [45]. One of the potential common targets for both types of oligomers is the extrasynaptic NMDAR, which can be activated by Aβ, thus driving tau pathology [52]. Both Aβ and tau oligomers can also target synaptic mitochondria by affecting fission/fusion processes or directly targeting electron transport chain (reviewed by [41]). Furthermore, Aβ and tau oligomer-driven toxicity may cause apoptosis, disrupted Ca^{2+} homeostasis and toxic free radical formation [32,53,54]. Alterations in calcium homeostasis, in turn, can affect plasticity and cognition through the perturbation of Ca^{2+}/calmodulin-dependent protein kinase II-α (CAMKII) autophosphorylation [31]. Furthermore, association of amyloid oligomers with the PSD implicates dephosphorylation (deactivation) of CREB (cAMP response element-binding protein factor), which in turn affects transcription of genes regulating long-term

changes in synaptic strength [55]. Alterations in calcium ultimately lead to detrimental activation of calcineurin, which by itself can be sufficient to cause synapse loss (reviewed by [41]). Hence, calcineurin could be a potential common downstream target for both types of oligomers since both Aβ [55] and tau [56] have been shown to impinge upon the CAMK/CREB/calcineurin pathway. Furthermore, it is well documented that the long-term potentiation, a cellular mechanism for learning and memory, is inhibited by Aβ and tau olgiomers, either alone or in combination [51].

Despite this existing knowledge, however, it is still unclear if tau and Aβ act at the same level, molecularly-speaking, or if instead they initially target different processes that later converge onto a common downstream pathway. It has also been suggested that oligomers of different proteins may share a similar mechanism of toxicity due to their common conformation [57] (reviewed by [58]). Thus, α-synuclein oligomers were also shown to impair long-term potentiation and memory via a calcineurin-dependent mechanism [59].

To summarize, presence of soluble oligomeric species of Aβ and tau in the brain correlates with cognitive dysfunction [14,24,25,53,60] (reviewed by [13,15]), for which multiple molecular mechanisms are responsible. Soluble forms of Aβ and tau can initiate synaptic failure acting independently, however, there is growing evidence for a convergent mechanism. A schematic representation of oligomer-driven synaptotoxicity as a result of oligomer interactions with the membrane and synaptic proteins is shown in Fig. 1.3.
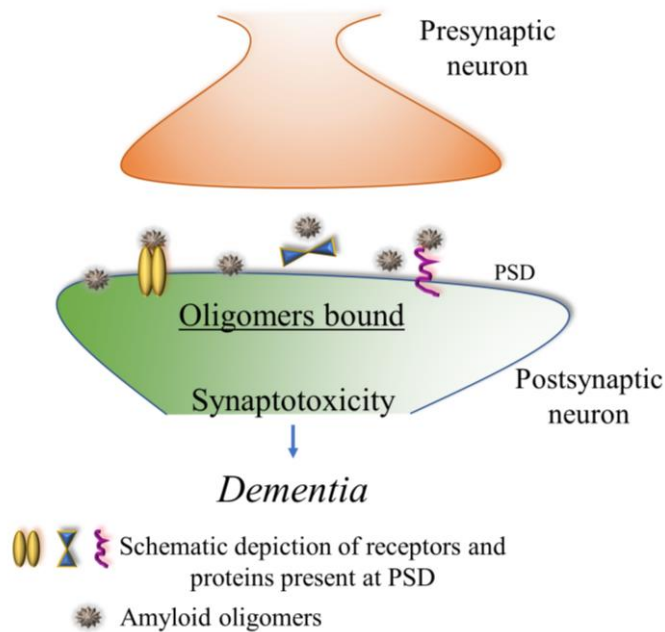
Figure 1.3. Aβ and tau oligomers bind AD hippocampal synapses

Diagrammatic representation of Aβ and tau oligomers interacting with the PSD in AD resulting in synaptic dysfunction and thus leading to dementia.

While there is currently no imaging technique available to detect loss of synapses due to oligomer toxicity in the brains of living people and potentially catch the disease at its early stages, detection of amyloid plaques and NFTs is possible. However, as discussed above, mature plaques and NFTs do not correlate with cognitive decline, and in fact, with the development of neuroimaging it has become clear that some individuals with AD-like neuropathology do not exibit any cognitive decline during their life (discussed in the next section) [12,35,61].

Non-Demented indivuduals with Alzheimer's Neuropathology

Probably the most well-known study of aging and AD – The Nun Study – was initiated in 1986 to include American members of the School Sisters of Notre Dame religious congregation [62]. As a result, a database with full medical record and brain bank with specimens from 678

participants (age 75-106) was created. This study included demented and non-demented participants and aimed to determine causes and prevention of AD, other brain diseases, and the mental and physical disability associated with the old age. Notably, one of the first conclusions from this study was that the presense of pathology is not sufficient for manifestation of AD since approximately one third of the participants met neuropathologic criteria for AD, however, were free of dementia until death [63]. Interestingly, this was not the first mention of cognitively intact individuals with high AD-like pathology at death. Throughout the years since the discovery of AD, this observation has been made by many researchers. For example, in 1937, Rothschild and Trainor reported no correlation between histopathological findings and intellectual impairment [64]. Decades later, in 1988 Katzman *et al.* described "a subgroup with preserved mental status and numerous neocortical plaques" [65]. For many years, due to the lack of official guidelines and scientific consensus these individuals were frequently either eliminated from the post-mortem research studies altogether, included in one group with control (due to the lack of cognitive impairement), or studies together with AD samples (due to the presence of pathology). Many examples can be found in literature, suggesting that systematic approaches and guidelines in studying such cases are needed. In 2011 the research recommendations for the study of cognitively intact indivuals with typical AD neuropathology were developed by the Alzheimer's Association workgroup in the diagnostic guidelines for Alzherimer's Disease, part of National Institute on Aging [61].

In our laboratory, we investigate this cohort of individuals that we refer to as Non-Demented with Alzheimer's Neuropathology (NDAN) [66,67]. Several research groups, including ours, are trying to understand the mechanisms involved in preservation of cognition in people with high levels of Aβ plaques and NFTs [18,35,61,66–74]. As shown in Fig. 1.4, NDAN

individuals and AD patients have comparable loads of pathological proteins (Aβ and tau) demonstrated by the post-mortem immunohistochemical staining of hippocampi. However, NDAN can resist the cognitive decline typically present in AD.
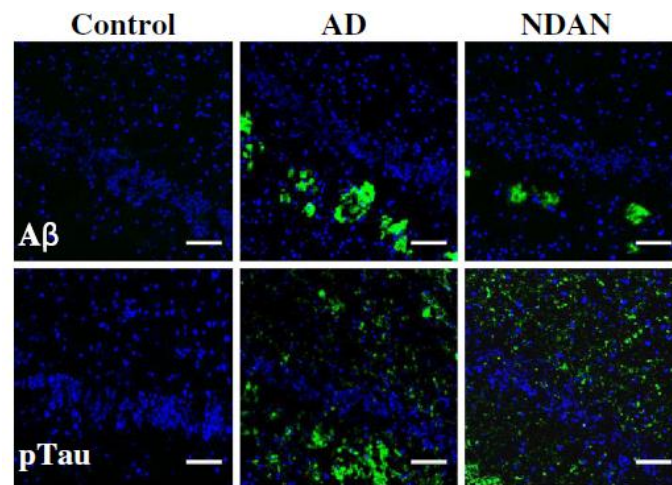
Figure 1.4. Immunohistochemical staining of control, AD and NDAN hippocampi

Data from our laboratory demonstrating Aβ plaques (top row) and phosphorylated tau (bottom row) in dentate gyrus of individuals classified as control (Braak 1, Plaque 3, MMSE 30), AD (Braak 6, Plaque 1, MMSE 2), or NDAN (Braak 6, Plaque 1, MMSE 27). DAPI-containing mounting medium was used to visualize nuclei (blue). 20x magnification, scale bar 100 μm [66].

Multiple mechanisms encompassing the ability to escape dementia by NDAN subjects have been proposed and are discussed in Chapter 2. Understanding the involved protective processes would lead to the development of novel and effective therapeutic strategies aimed at promoting resilience to amyloid toxicity in individuals with existing AD-like pathology. In our laboratory we study synaptic resilience to Aβ oligomers, which was first descibed by us (Fig. 1.5, [66]), and later confirmed by another group [75]. Postsynaptic densities of NDAN subjects are devoid of Aβ oligomers, thus allowing us to propose that the synaptic resilience to Aβ oligomers could explain why NDAN subjects remain cognitively intact.
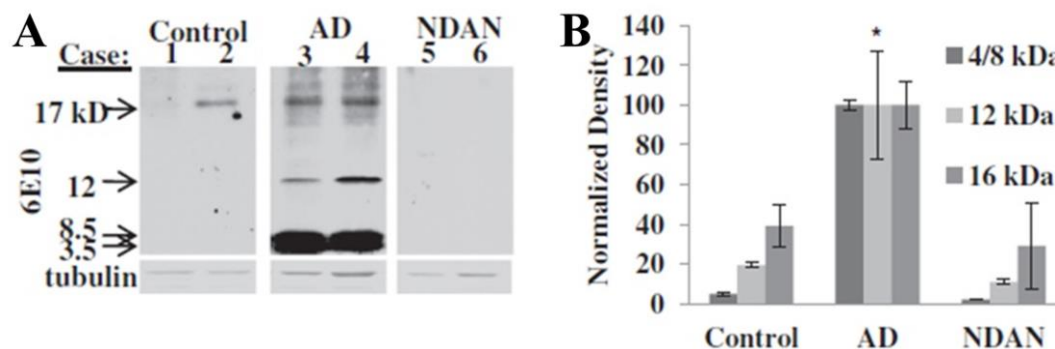
Figure 1.5. The Aβ oligomer rejection by postsynaptic densities in NDAN subjects

(A) Hippocampi from six different patients were evaluated for low molecular weight Aβ association synapses (40 μg protein each lane of a 10-20% tris-glycine gradient gel) [66]. (B) Densitometric analysis of each of the Aβ species (monomer/dimer = 4-8.5 kDa band, trimer = 12 kDa, and tetramer = 16 kDa) demonstrates that all Aβ species are increased in AD. The results are expressed as the mean ± SEM using propagation of error and normalized with AD = 100%. The asterisk denotes the values significantly higher than control (monomer/dimer, $p = 0.012$, trimer, $p =< 0.001$, and tetramer, $p = 0.014$; ANOVA; a Bonferroni correction was applied for the monomer/dimer and trimer density values) [66].

Objectives of the dissertation

NDAN individuals remain cognitively intact despite the CNS presence of substantial plaques and tangles consistent with what would be normally associated with fully symptomatic AD. In my work, I have focused on determining the mechanisms affording NDAN synapses the extraordinary resistance to Aβ oligomers, allowing the synapses to remain functional. I hypothesized that the postsynaptic density of NDAN subjects has a unique protein signature that protects synapses from detrimental binding of amyloid oligomers. I further proposed that the expression of some of these proteins is epigenetically regulated by specific microRNAs, thus allowing NDAN synapses to acquire resistance to amyloid oligomer binding and toxicity.

Therefore, the main objectives of this dissertation are 1) to identify the protein signatures of the postsynaptic densities in control, AD and NDAN subjects (Chapter 3), and 2) to determine

the upstream regulators (microRNAs) that could explain the unique protein set present at the PSDs of NDAN, and determine if these microRNAs protect against Aβ and tau oligomer binding (Chapter 4).

Altogether, the experimental data in this dissertation will help us understand the mechanisms responsible for natural preservation of cognitive function in NDAN and will thus lay a critical groundwork for the future development of novel effective therapies to treat AD centered on inducing brain resilience to the damaging effects of parthological amyloid proteins.

CHAPTER 2. MECHANISMS INVOLVED IN RESISTANCE TO COGNITIVE DECLINE

Introduction

Several research groups, including ours, have described individuals that remain cognitively intact in spite of having accumulation of Aβ and neurofibrillary tangles (NFTs) to an extent comparable to that normally observed in fully symptomatic Alzheimer's disease [69,70,72,73]. We refer to these individuals as "Non-Demented with Alzheimer's Neuropathology" (NDAN) [66]. Thus, NDAN individuals manifest AD-like pathology, however they remain cognitively intact. Due to the fact that AD-like pathology is observed in the brain of these individuals, they have also been termed "cognitively successful aging", "pathological aging", "asymptomatic AD", "resilient AD" and "preclinical AD" [18,69,76–78]. In this article we aim to review the current literature about non-demented subjects that manifest AD-like pathology.

Discussion

CLASSIFICATION OF AD AND NDAN

Latest progress in neuroimaging and advancement of other laboratory assays have allowed to effectively monitor the progression of AD neuropathology *in vivo*. Presence of Aβ aggregates in the brain of affected individuals can be correlated with structural and functional

alterations in mild cognitive impairement (MCI) and AD patients [61]. It is also recognized that a certain cohort of individuals with AD-like neuropathology do not become symptomatic during their lifetime. As we continue to learn more about early stages of AD, the need to redefine the disease emerges. At the same time we still need to discover more biomarkers that will help us define the severity of the disease and predict development of clinical symptoms, as well as define the individuals that will not progress to AD dementia. We will need to develop a set of biomarkers to determine the degree of synaptic loss, Aβ and tau accumulation, inflammation and other markers that could aid in more accurate diagnosis and prognosis of AD. In 2012, Alzheimer's Association workgroup in the diagnostic guidelines for Alzherimer's Disease, part of National Institute on Aging, suggested that during diagnosis we should separate those individuals that present with dementia and AD pathology from cognitively intact indivuals with typical AD neuropathology. The latter group of individuals can be described as "asymptomatic at risk for AD dementia", or "not normal, not MCI" [61]. It remains unknown, however, if these individuals would have developed AD should they have lived longer. Several studies describe the presence of Aβ aggreagates and other biomarkers in 20-40% of older individuals that are cognitively intact [65,79–86]. However, multiple studies demonstrate that these cognitively normal individuals have disrupted functional networks [87–89] and some brain atrophy [90]. Sperling *et al*. suggest that aberrant neural activity is associated with Aβ deposits and appears before cognitive impairment [89]. The same group has also noticed increased hippocampal activity which could indicate existence of compensatory mechanism. It is clear that more longitudinal studies are needed in order to describe different stages of asymptomatic and clinical AD.

POTENTIAL **COMPENSATORY MECHANISMS**

It has been established that Aβ deposition in cognitively normal individuals can be observed. Bjorklund *et al*. report that NDAN vs. AD individuals have comparable levels of Aβ plaques and NFTs, low molecular weight Aβ oligomers and Aβ$_{1-42}$ levels in their brains [66]. Also the pattern of distribution of plaques and tangles has been reported to be the same in AD and NDAN [79]. However, it is not yet clear if presence of Aβ plaques and NFTs in NDAN should be interpreted as an early event in AD pathogenesis (preclinical AD) or if there are mechanisms that are present in these people allowing them to counteract the toxicity of Aβ and tau, and therefore remain cognitively intact. Multiple groups report the results of PET imaging using Pittsburg Compound B (PiB) in healthy aged individuals, including those older than 85 years of age [86], which indicates that these subjects may indeed be resistant to Aβ toxicity. Understanding the protective mechanisms at play in these resistant individuals would be of great importance for the development of effective therapies. Below we review some of the proposed protective mechanisms that could be responsible for resistance to AD or significant delay of clinical symptoms in NDAN individuals.

Hippocampal volume

The volume of the hippocampus is a well-established criterion that allows for discriminating healthy and AD subjects. Gosche *et al*. performed a study involving 56 brains of nuns of the School Sisters of Notre Dame congregation and concluded that hippocampal volume correlates well with the AD neuropathology [91]. In their study, they also looked at brains of nuns who had significant AD neuropathology (44% of total number of cases) but were non-demented during their life. These non-demented subjects with Alzheimer's neuropathology had

some brain atrophy, which allowed the authors to conclude that hippocampal atrophy is not AD specific.

One of the hypotheses is that the presence of AD lesions in the brain may be insufficient to cause cognitive decline in these individuals due to larger brain reserve [70]. Some reports show that total brain and hippocampal volume are greater in cognitively intact subjects with high load of Aβ plaques and NFTs [12]. Additionally, higher number of synapses and enlargement of neuronal nuclei are hypothesized to correlate with preserved cognitive function [69,70,72]. In the study by Chetelat *et al*. the healthy individuals with high Aβ loads presented larger global and regional grey matter volumes when compared to cognitively impaired subjects with high Aβ [92].

Regulation of apoptosis has been suggested as one of the potential explanations for larger brain volume [70,93]. Large neuronal loss is typical for late stages of AD and is thought to be intitiated by the presense of plaques and tagles, however the execution of apoptosis may be different in NDAN. Indeed, one can argue that Aβ plaques and NFTs do not cause neuronal death, which is supported by phenomena observed in NDAN.

Other research groups found brain atrophy in non-demented individuals with high pathology. They reported that even though the atrophy is present, the progression rate is consistent with normal aging [90]. Some studies reported that hippocampal atrophy is not significant when compared to no pathology control [82]. And other studies did not find any difference in hippocampal volume [94]. The discrepancies in the results discussed here could be due to different participant inclusion/exclusion criteria, the assessment being done ante- or post-mortem and/or the acquisition parameters used in the MRI studies.

Cognitive reserve

"Cognitive reserve" represents the ability of the brain to engage alternate networks or cognitive strategies to manage the effects of pathology [61]. This hypothesis leads to two predictions: aged individuals with more education are expected to demonstrate less cognitive impairment when compared to people with less education, and, on the other hand, comparison of subjects with similar cognitive status would reveal more severe changes in brain structures in those subjects who have higher education due to the fact that original cognitive reserve can provide a "buffer" that will allow these individuals to resist dementia [95–98]. This can explain why there are several studies reporting higher atrophy in cognitively intact individuals who have AD neuropathology.

In several studies, high socioeconomic status has been associated with resistance to AD [99]. Fotenos *et al*. report that individuals with higher socioeconomic status are able to withstand the typical AD pathology for extended time due to unknown mechanisms [100]. Even though the non-demented people with AD pathology demonstrated reduced brain volume when followed in this longitudinal study, they did not manifest cognitive decline. Some participants began to show early signs of dementia, however individuals with higher socioeconomic status remained non-demented throughout the study [100].

Ngandu *et al*., based on their study of a Finnish cohort, conclude that level of education is not associated with other risk factors for dementia and less education correlates with higher risk for dementia [101]. It is, however, hard to determine if the cognitive reserve is innate, or if it is set during childhood years or later during adulthood. Another possibility is that more years of education allow people to make better choices regarding their lifestyle, thus leading to better overall health and decreased risks for dementia [101].

Brain reserve

The hypothesis of greater brain reserve refers to the ability of the brain to resist the pathological insult, possibly due to greater synaptic density or larger number of healthy neurons. High brain reserve can be associated with up to 50% reduction in prevalence of dementia [102].

In 1988 Katzman *et al*. have described a group of individuals "nondemented with Alzheimer's changes" which have higher number of large neurons when compared to age-matched healthy control and AD brains; they also reported higher brain weight when compared to control and AD [65]. They find these individuals to be intermediate between control and AD and they hypothesized that "nondemented with Alzheimer's changes" subjects are able to escape shrinkage of large neurons that usually occurs during aging. A possible explanation for these results is that larger brains and greater number of neurons since early in the life of these protected individuals would provide a "reserve" allowing them to cope with age-associated losses.

SantaCruz *et al*. report non-demented individuals to have heavier brains when compared to demented AD patients [103]. Interestingly, individuals with higher socioeconomic status or those with larger brains are less likely to develop dementia, whereas, having both high education and larger brain does not provide an advantage to lower the risk of dementia [104].

It may require more pathology for the individuals with greater brain reserve to manifest clinical dementia [105,106]. By the time the dementia is detectable in those with higher brain reserve, most likely the brain has already accumulated substantial pathology, which results in the observation that those individuals with greater brain reserve die sooner after AD diagnosis [107]. Along these lines, there is also some evidence that people with higher education and IQ experience quicker cognitive decline [108–110].

In concordance with the reserve theory, higher levels of leisure activity prior to the manifestation of clinical symptoms of AD are linked to more severe neuropathology and progression of the disease [111].

Insulin resistance

The link between insulin resistance and progression of AD has been established [112]. Insulin resistance is a characteristic of type II diabetes mellitus and it is also present in AD [113,114]. Insulin, a key player in CNS signaling, has been proposed as a therapeutic target for AD. Insulin prevents binding of Aβ oligomers to the synapse thus improving cognitive performance in patients with early AD [115,116]. Aβ oligomer binding ability to synapses decreases due to insulin-dependent reduction of binding sites [115]. By preventing the binding, insulin provides protection from Aβ-induced synapse retraction, oxidative stress and insuin receptor loss [115]. When used *in vivo*, the insulin-sensitizing drug rosiglitazone has shown some promising results in mouse models of AD and some clinical trials in early AD patients [117–119]. In a small preliminary clinical trial, rosiglitazone showed beneficial effects in terms of cognitive improvement during the treatment period; however, the effect was short-lived, ceasing as soon as the treatment was withheld [119]. This suggests that insulin-sensitizing medications can affect the symptoms of AD, but not the underlying pathology. Unfortunately, phase III clinical trials with insulin-sensitizing drugs have returned negative results [120,121].

Insulin signaling increases the levels of insulin-degrading enzyme (IDE), which can degrade insulin and also monomeric Aβ [122,123]. IDE was found to be increased in AD when compared to NDAN, which suggests that degradation of insulin is increased in AD and, consequently, glucose metabolism impaired in affected brain cells [18].

Levels of key insulin signaling elements downstream of activated insulin receptors that are decreased in AD [114,124], are maintained in NDAN hippocampi, and in some cases even higher than control (Taglialatela, unpublished). Using Western blotting we have measured several markers of the insulin signaling pathway, including insulin receptor, insulin receptor substrate 2, pAkt and pGSK-3β in post-synaptic densities (PSDs) in control, AD and NDAN hippocampi. We observed a high degree of activation of all four proteins in NDAN that was significantly greater than AD and exceeded the levels observed in controls. Silva *et al*. reported higher pAkt in NDAN when compared to AD, which is consistent with our findings [93]. Collectively these results suggest that NDAN individuals have increased insulin sensitivity at the PSD when compared to AD.

Synaptic health

The number of synapses has been shown to be positively correlated with cognitive testing results, while Aβ oligomers have been suggested as a potent cause of synaptic loss in AD [125]. The mechanism of Aβ synaptotoxicity is not fully understood, but it is hypothesized that Aβ oligomer association with the PSD results in disturbed Ca^{2+} signaling in dendritic spines, which can affect multiple downstream pathways [31]. Aβ oligomers can interact with multiple proteins and receptors at the PSD, including α7-nAChR (α7-nicotinic acetylcholine receptor), AChE (acetylcholinesterase), PrPc (prion protein), NMDAR (N-methyl-D-aspartate receptor), TNF-R (tumor necrosis factor receptor), α2β1 and αVβ1 integrins, NL-1 (neuroligin-1) and others [29]. Association of Aβ oligomers with the PSD implicates dephosphorylation (deactivation) of CREB (cAMP response element-binding protein factor), which in turn affects transcription of genes regulating long-term changes in synaptic strength [55].

Synapses are the most vulnerable neuronal structures in AD and, interestingly, the number of synapses and levels of synaptic markers are preserved in NDAN [18,125–127]. Low molecular weight Aβ species are present at PSDs of AD brains, however they are rejected by NDAN synapses [66]. Absense of Aβ oligomers at the PSD of NDAN can be potentially explained by regulation of Zn^{2+} homeostasis [128]. Aβ oligomers can be targeted to the synapses by synaptic Zn^{2+} [129]. Bjorklund *et al*. report that AD brains have significantly higher Zn^{2+} levels, while NDAN samples have more than control, but less than AD [128]. Additionally, levels of pCREB, an indicator of synaptic health, were similar in control and NDAN, however significantly reduced in AD [66]. This observation suggests that synaptic integrity is indeed preserved in NDAN. To further understand if the PSD of NDAN subjects possesses additional protective mechanisms, we have performed proteomic analysis of PSDs of control, AD and NDAN (described in detail in Chapter 3, [130]). We have determined a set of proteins that are unique to PSD of NDAN subjects, further suggesting that critical structural/biochemical changes at the NDAN synapse can contribute to its resistance to Aβ impact.

Neurogenesis

Neurogenesis in adult human brain was first described in 1998 in cancer patients who had received BrdU for diagnostic purposes [131]. Proliferating progenitor neural cells were found in the subventricular zone of the lateral ventricles, and the granule cell layer, and subgranular zone of the dentate gyrus, which served as a confirmation of continuously active neurogenesis in humans [131]. The newly formed neurons have been shown to integrate into existing networks (reviewed in [132]). There are many factors that can alter neurogenesis. As reviewed by Farin *et al*., aging, stress, antidepressants, exercise, neurotrophic factors can all play a role in neurogenesis in adult organism [133]. Levels of neurotrophic factors are altered in AD

[134,135], including brain-derived neurotrophic factor (BDNF), which is known to play a role in regulation of basal level of neurogenesis [136]. We found increased levels of BDNF (Taglialatela, unpublished) and neurogenesis in NDAN [67], which could both contribute to preserved cognition in these resistant individuals.

Dysregulation of cell cycle (an important determinant in neurogenesis) has also been reported in AD [93]. Markers of cell cycle progression (Cdk4, cyclin D, pRb, E2F1, Cdk1 and Cyclin B) are elevated and those of cell cycle inhibition – decreased (Cdk5 and p27) in AD when compared to control and NDAN [93]. Cell cycle regulation in NDAN is similar to control, which suggests that NDAN individuals possess a compensatory mechanism that allows them to retain control of cell cycle and thus neurogenesis [93].

Oxidative stress

Oxidative stress and damage induced by free radicals has been hypothesized to cause synaptic loss in AD brains [4,137–139]. It has been suggested that oxidative damage is a very early event, which can lead to neuronal dysfunction and AD independently or in conjunction with other factors [140]. Silva *et al*. have measured levels of oxidative DNA damage, DNA repair pathway activity, cell cycle and cell death in healthy aged population, as well as AD and non-demented subjects with AD pathology [93]. They have demonstrated that control and NDAN subjects cluster very closely together for all studied parameters, whereas in most cases AD manifests significant changes when compared to the other two groups. Furthermore, levels of oxidative DNA damage as measured by 8-hydroxyguanine and λ-H2AX (both established markers of DNA damage) were significantly higher in AD when compared to control [93]. DNA repair proteins (P53, BRCA1 and PTEN) were significantly elevated in control and NDAN when compared to AD, which indicates the DNA repair pathway is a possible compensatory

mechanism in NDAN allowing these individuals to maintain proper cognitive functioning and, therefore, resist memory impairment [93]. Additionally, we have assessed in NDAN and AD brains levels of APE1 and XRCC1, proteins involved in DNA repair pathway (Taglialatela, unpublished). APE1 levels were higher in control and NDAN when compared to significantly lower levels in AD. XRCC1, on the other hand, was significantly increased in NDAN when compared to control however it was significantly lower that AD, which is in agreement with the findings by Silva *et al*. of activated DNA repair pathway in NDAN.

Neuroinflammation and glial activation

Neuroinflammation is an important component of the events through which Aβ and tau manifest their detrimental neurodegenerative effects on the brain. Lue *et al.* report that, similar to controls, NDAN brains have significantly lower levels of inflammatory markers C5b-9 and LN3 when compared to AD [126]. Consistent with preserved cognitive ability, absence of inflammation in the brains of NDAN subjects can indicate a potential compensatory mechanism.

Maarouf *et al.* describe no differences in levels of inflammatory TNF-α cytokine and GFAP in AD vs. NDAN [18]. GFAP is elevated in regions with high pathology in AD brains, which is thought to indicate a response to trauma, chemical injury, neuroinflammation, and astrogliosis in dementia [141–143]. Interestingly, a significant increase in S100B level was found in NDAN when compared to AD [18]. S100B is produced by astrocytes and plays a role in protein degradation, cell movement, proliferation and differentiation, cytoskeleton assembly, regulation of transcription factors and enzyme activities and receptor functions [144–146]. S100B is considered to be a neuroprotective factor for cholinergic neurons during oxygen and glucose deprivation [147], and therefore the moderate increase in S100B levels observed by Maarouf *et al.* can be interpreted as a protective effect in NDAN.

AD brains are characterized by significant increases in the number of activated astrocytes and microglia when compared to control and NDAN [148]. Reactive glia in the brain of AD patients can be very toxic to neuronal function, and lack of such activation in NDAN might indicate the lack of synaptic and neuronal damage [148].

Genetic advantage

Genetic mutations can provide an ability to resist a particular disease. Silva *et al*. describe significant changes in genes involved in energy metabolism, cell cycle, DNA synthesis and repair, inflammatory signaling, and transcriptional regulation in AD and NDAN vs. control [78]. While reporting that AD and NDAN subjects are overall transcriptionally similar, Silva *et al*. describe six genes which allowed them to distinguish these two groups, suggesting that differential expression of specific genes could represent a possible compensatory mechanism in NDAN to resist dementia [78]. Consistent with this possibility, multiple transcriptional changes were also observed in control vs. AD and NDAN by Liang *et al*. [74]. Of these, several could be hypothesized as representing potential compensatory mechanisms underscoring NDAN resistance to dementia: inhibition of NFT formation (changes in tau expression and tau kinases), inhibition of Aβ clearance pathway (lower levels of BACE1, presenilin 1 and 2), and changes in learning and memory processes [74].

Kramer *et al*. have utilized NDAN subjects to determine if there is a genetic mutation that promotes cognitive health in these individuals despite presence of AD neuropathology [73]. A genome-wide SNP (single nucleotide polymorphism) association study (GWAS) was conducted based on samples from non-demented subjects with and without NFT pathology [73]. There was no difference in education level and APOEε4 allele distribution between the two groups. Three reelin SNPs were found to be associated with higher AD pathology [73]. Reelin is an

extracellular matrix protease that regulates microtubule function in neurons, plays a role in tau phosphorylation [149–151], and can protect against Aβ-induced decrease in long-term potentiation [152]. Reelin expression is elevated in hippocampal pyramidal neurons in AD and NDAN, which suggests that upregulation of reelin may be a compensatory mechanism in response to Aβ or tau-driven neuronal stress, even prior to dementia onset [73]. The same authors propose that SNPs in the reelin gene lead to disruptions in tau phosphorylation resulting in formation of NFTs [73].

Epigenetic factors

Epigenetic modifications can occur long before the diagnosis of Alzheimer's Disease, and therefore development of sensitive diagnostic tools is crucial to detect the changes [153]. Epigenetic alterations include DNA methylation and hydroxymethylation, histone modifications, chromatin remodeling and regulation of gene expression by non-coding RNAs [153]. Epigenetic changes can be induced by exposure to certain environmental toxicants, and sometimes these modifications can be reversed using therapeutics that target specific enzymes or factors that control them. Moreover, changes in gene expression due to epigenetics are observed during aging and in several diseases, such as depression, schizophrenia, glioma, Rett syndrome, alcohol dependence, autism, epilepsy, multiple sclerosis and stress [153]. Some of these modification, such as DNA methylation and histone acetylation, have been shown to participate in memory formation [154]. In fact, studies involving monozygotic twins found that AD twin had reductions in methylation levels when compared to non-AD twin [153], emphasizing that epigentic changes in AD are important in the disease progression [153–158].

Various epigenetic mechanisms have been studies in AD, however, not much is known about NDAN epigenetic status. Only one study describing multiple small non-coding RNAs,

microRNAs (miRs), has been published up to date. In this work, the authors describe several miRs known to regulate neurogenesis that were shown to be decreased in the dentate gyrus of NDAN when compared to AD and MCI [67]. MiRs' role in AD pathology has been previously investigated [159–167]. For example, miR-107 and miR-23b decrease with the progression of pathology [168], whereas the expression profile of several miRs (27a, 132, 124, 143) is different between brain regions affected by the disease [169]. One additional study involving NDAN subjects is decribed in this dissertation in Chapter 4, where three miRs (149, 485 and 4723) were found to be downregulated in hippocampi of NDAN when compared to control and AD. Thus, miRs pose as an attractive target for research with therapeutic potential in AD, however, more research is needed to better characterize these molecules and their regulation in NDAN.

Conclusion

Over the years, numerous studies have included non-demented individuals with Alzheimer neuropathology as a part of the control non-demented group when investigating Alzheimer's disease. NDAN subjects perform similar to healthy aged individuals that have no AD pathology. However, there are currently no biomarkers that can distinguish NDAN from healthy aged population with no AD pathology. NDAN individuals are able to preserve their cognitive function while maintaining normal levels of several biochemical and functional markers that are normally degraded in fully symptomatic AD. While several studies, including those described in this chapter, report close clustering of biochemical and functional markers in control and NDAN, there are some discrepancies in the reported data which could be explained by different selection criteria used among different research groups to classify an individual as NDAN. Considering the clinical importance of understanding the involved mechanisms, there is

still a pressing need for standardized inclusion criteria that would fully encompass the characteristics of NDAN subjects.

Here we have discussed potential mechanisms involved in preservation of cognitive function in NDAN individuals. Regardless whether NDAN are resistant to AD-related dementia, or whether they have extraordinarily delayed the onset of cognitive decline, understanding the involved molecular mechanisms would represent a significant step toward developing a new therapeutic concept for AD centered on inducing cognitive resistance in spite of the occurrence of overt AD neuropathology.

CHAPTER 3. POSTSYNAPTIC PROTEOME OF NDAN

Introduction

Synaptic dysfunction in AD is observed as a result of Aβ oligomers association with the PSD [26]. At the PSD, Aβ oligomers oppose expression of long-term potentiation (LTP), modify protein content and induce dendritic spine shrinkage and eventually loss [26,31,32]. Since the size of the PSD is proportional to the strengh of the synapse, Aβ-driven synapse damage can result in the loss of cognitive function. In AD, plasticity and cognition are affected through the perturbation of Ca^{2+}/calmodulin-dependent protein kinase II-α (CaMKII) autophosphorylation [31]. Association of Aβ oligomers with the PSD implicates dephosphorylation (deactivation) of CREB (cAMP response element-binding protein factor), which in turn affects transcription of genes regulating long-term changes in synaptic strength [170].

We have previously reported that NDAN synapses reject Aβ oligomers, which could explain why NDAN subjects remain cognitively intact. Our laboratory has demonstrated for the first time that the PSD of NDAN subjects is free of Aβ oligomers [66]. Based on this observation, we hypothesized that there might be unique changes in protein expression levels at the PSDs of NDAN subjects that specifically mark the ability of their PSDs in the hippocampus to reject binding of toxic Aβ oligomers. To test our hypothesis, in the present work we performed proteomic anaysis of the PSDs isolated from healthy control, AD and NDAN individuals. The

protein levels in AD and NDAN were compared to control, in addition to direct NDAN vs. AD comparison. As a result, we identified a unique PSD protein signature of NDAN which consists of fifteen proteins, setting them apart from control and AD.

Methods

CASE SUBJECTS

Frozen mid-hippocampus tissue was obtained from the Oregon Brain Bank at Oregon Health and Science University (OHSU) in Portland, OR. Donor subjects were enrolled and clinically evaluated in studies at the NIH-sponsored Layton Aging and AD Center (ADC) at OHSU. Subjects were participants in brain aging studies at the ADC and received annual neurological and neuropsychological evaluations, with a clinical dementia rating (CDR) assigned by an experienced clinician. Controls and NDAN had normal cognitive and functional examinations with CDR<1. The AD subjects were diagnosed by a clinical team consensus conference, met the National Institute for Neurological and Communicative Disorders and Stroke-Alzheimer's Disease and Related Disorder Association diagnostic criteria for clinical AD, had a CDR of greater than 1.0 and neuropathologic confirmation at autopsy (after informed consent). Tissue use conformed to institutional review board-approved protocols. Neuropathologic assessment conformed to National Institute on Aging-Reagan consensus criteria. All brain tissue was examined by a neuropathologist for neurodegenerative pathology including neurofibrillary tangles and neuritic plaques. Using standardized CERAD (Consortium to Establish a Registry for Alzheimer's Disease) criteria [171], cases were assigned an amyloid score based on the deposition of amyloid plaques in the brain (0 = no plaques, 1 = sparse plaques, 2 = moderate plaques and 3 = dense plaques) and a Braak stage (0–6; with 6 being the

most severe) indicative of the level and location of hyperphosphorylated tau tangles [8]. In addition to the pathological information detailed above, demographical data were received along with the frozen tissue. These included age, sex and MMSE score [171] for each case. Several AD patients presented with relatively high MMSE scores, which is attributable to multiple factors: 1) the last MMSE was collected several months prior to death, 2) the diagnosis is mainly based on consensus CDR assessments and several tests beyond MMSE, 3) even milder impairments sometimes led to the diagnosis of AD with the understanding that this was earlier-stage disease. When these scores are looked at as a whole, it can be appreciated that these patients do tend to be in earlier stages of dementia, both in terms of their clinical ratings and in terms of their pathologies, with intermediate (3-4) versus high (5-6) Braak scores.

Hippocampal regions from twenty-four cases were used for proteomic analysis using 2D gel electrophoresis (eight samples per group were pooled). An independent set of fifteen samples (five cases per group) different from those assayed by 2D gel electrophoresis was used for validation of protein levels using immunoblotting.

SYNAPTIC FRACTIONATION

For proteomic studies, synaptic fractionation was performed as described previously [6,128,172]. Briefly, hippocampal tissue was homogenized in 0.32 M sucrose solution containing 1x Protease Inhibitor Cocktail (MilliporeSigma, St. Louis, MO) and Halt Phosphatase Inhibitor Cocktail (Life Technologies, Inc., Carlsbad, CA) using a Dounce glass homogenizer. Synaptosomes were isolated using a sucrose gradient and ultracentrifugation (100,000 x g for 3 hrs at 4°C). Synaptic junctions were obtained by incubating the synaptosomes in pH = 6 buffer (1 M Tris in 0.1 mM $CaCl_2$) and then centrifuging at 40,000 x g for 30 min at 4°C. The supernatant (containing synaptic vesicles) and the pellet were collected separately. The pellet

was solubilized and incubated in pH = 8 buffer (20 mM Tris, 1% Triton X-100 in 0.1 mM $CaCl_2$) and then centrifuged at 40,000 x g for 30 min at 4°C to generate the PSD pellet. This pellet was solubilized in 1% SDS.

To confirm protein changes using immunoblotting, the isolation of synaptosomes was performed using Syn-PER Synaptic Protein Extraction Reagent (ThermoFisher Scientific, Waltham, MA) as described previously [173], followed by ultracentrifugation to obtain PSD fractions. Similarly to sucrose gradient protocol described above, the hippocampal tissue was homogenized using a Dounce glass homogenizer in Syn-PER Reagent and centrifuged at 1,200 x g for 10 min at 4ºC. The supernatant containing synaptosomes was collected and centrifuged at 15,000 x g for 20 min at 4ºC. The supernatant (cytosolic fraction) and pellet (synaptosomes) were collected separately. Synaptic junctions were obtained by incubating the synaptosomes in pH = 6 buffer (as described above) and then centrifuging at 40,000 x g for 30 min at 4°C. The supernatant (containing synaptic vesicles) and the pellet were collected separately. The pellet was solubilized and incubated in pH = 8 buffer (as described above) and then centrifuged at 40,000 x g for 30 min at 4°C to generate the PSD pellet. This pellet was solubilized in 1% SDS.

PROTEOMICS

Control, NDAN and AD samples were processed for proteomic analysis as described previously (for examples, see [174,175]) . Triplicate samples from control, AD and NDAN PSD (200 µg) were extracted with 7 M urea, 2 M thiourea, 2% CHAPS and 50 mM Tris pH 7.5, treated with sodium ascorbate (Asc) to reverse S-nitrosylation and then dialyzed against the urea buffer to remove Asc, which interferes with labeling. Protein concentrations were determined with the Lowry method and cysteines (cysteic acid) determined by amino acid analysis (Model L8800, Hitachi High Technologies America, Pleasanton, CA). Proteins from the tissues were

47

then labeled with BODIPY® FL *N*- (2-aminoethyl) maleimide (Life Technologies, Inc., Carlsbad, CA) at 60-fold excess cysteine to BODIPY FL-maleimide (Beckton Dickinson, Franklin Lakes, NJ) as published previously [176]. After quenching the labeling reactions with 10x molar excess β-mercaptoethanol (βME, Beckton Dickinson, Franklin Lakes, NJ), 200 µg labeled proteins in 0.5% IPG buffer pH 3-10 (GE Healthcare, Chicago, IL) were loaded onto a 11 cm pH 3-10 IPG strip (GE Healthcare, Chicago, IL) and proteins were focused according to the previously published protocol [177]. After focusing, the IPG strips were equilibrated in 6 M Urea, 2% SDS, 50 mM Tris, pH 8.8, 20% glycerol for 30 min at room temperature, applied to an 8-16% Tris-glycine-SDS gel and run at 150V x 2.25 hrs at 4°C. The gels were fixed for 1 hr in 10% methanol, 7% acetic acid and washed overnight in 10% ethanol. Finally, gels were imaged on a Typhoon Trio Imaging System (GE Healthcare, Chicago, IL; excitation λ = 480/40 nm & emission λ = 535/50 nm). We have previously demonstrated that this covalent sulfhydryl alkylation method using an uncharged thiol-reactive dye exhibits excellent specificity for cysteine thiols – little to no modification of other amino acid residues, does not impact protein electrophoretic mobility – for spot matching with unlabeled proteins, and accomplishes highly accurate and reproducible quantification – by virtue of its specificity and saturating concentration over protein thiols [174,176].

PROTEIN QUANTIFICATION AND IMAGE ANALYSIS

The 2D gel electrophoresis (2DE) images were analyzed using SameSpots software (TotalLab, Ltd. Newcastle Upon Tyne, UK). The software performs pixel-to-pixel matching before spot detection, ensuring that spot boundaries are the same for all gels, and eliminating errors that accumulate in the reference gel(s) as the number of gels within one experiment increases. Once the pixel matching and spot detection is complete, a reference gel is selected

according to several criteria, including quality and number of spots. Subsequent to automatic spot detection, spot filtering is manually performed and spots with an area of less than 250 pixels are filtered out, and spots with a volume (intensity) / area ratio of less than 375 pixels (whose abundance is insufficient for mass spectrometry (MS) identification) are also filtered. Typically, some manual spot editing is required to correct for spots that are not split correctly, not detected, or split unnecessarily during the automated detection process. The matching of spots between the gels is manually reviewed and adjusted as necessary. The software normalizes spot volumes using a calculated bias value based on the assumption that the great majority of spot volumes represent no change in abundance (ratio control to experimental = 1.0) (TotalLab documentation).

Ratiometric calculation from BODIPY-fluorescence units was conducted for quantifying differential protein abundance for the samples, and parametric t-test performed on log 2 normalized abundance ratios.

MASS SPECTROMETRY AND PROTEIN IDENTIFICATION

Selected 2DE spots that exhibited significant differential prevalence ($p \leq 0.05$) were picked robotically (ProPick II, Digilab, Ann Arbor, MI), and trypsin digested. In brief, gel spots were incubated at 37°C for 30 min in 50 mM NH_4HCO_3, dehydrated twice for 5 min each in 100 µl acetonitrile, dried, and proteins were digested in-gel at 37°C overnight with 10 µl of trypsin solution (1% trypsin in 25 mM ammonium bicarbonate). Peptide mixtures (1 µl), obtained after tryptic digestion, were directly spotted onto a target plate with 1 µl of alpha-cyano-4-hydroxycinnamic acid matrix solution (5 mg/ml in 50% acetonitrile) and analyzed by matrix assisted laser desorption ionization-time of flight (MALDI-TOF/TOF) MS using the ABI 4800 Proteomics Analyzer (AB Sciex, Foster City, CA). The Applied Biosystems software package

included the 4000 Series Explorer (v.3.6 RC1) with Oracle Database Schema (v.3.19.0) and Data

Version (3.80.0) to acquire and analyze MS and MS/MS spectral data. The instrument was

operated in a positive ion reflectron mode with the focus mass set at 1700 Da (mass range: 850-

3000 Da). For MS data, 1000-2000 laser shots were acquired and averaged from each protein

spot. Automatic external calibration was performed by using a peptide mixture with the reference

masses 904.468, 1296.685, 1570.677, and 2465.199. Following MALDI MS analysis, MALDI

MS/MS was performed on several (5-10) abundant ions from each protein spot. A 1 kV positive

ion MS/MS method was used to acquire data under post-source decay conditions. The instrument

precursor selection window was +/- 3 Da. Automatic external calibration was performed by

using reference fragment masses 175.120, 480.257, 684.347, 1056.475, and 1441.635 (from

precursor mass 1570.700).

AB Sciex GPS Explorer[TM] (v.3.6) software was employed in conjunction with MASCOT

(v.2.2.07) to search the UniProt human protein database (last accessed: June 7, 2015; 87,656

sequences 35,208,664 residues) by using both MS and MS/MS spectral data for protein

identification. Protein match probabilities were determined by using expectation values and/or

MASCOT protein scores. The MS peak filtering included the following parameters: a mass range

of 800 Da to 3000 Da, minimum S/N filter = 10, mass exclusion list tolerance = 0.5 Da, and

mass exclusion list for some trypsin and keratin-containing compounds included masses (Da)

842.51, 870.45, 1045.56, 1179.60, 1277.71, 1475.79, and 2211.1. The MS/MS peak filtering

included the following parameters: minimum S/N filter = 10, maximum missed cleavages = 1,

fixed modification of carbamidomethyl (C), variable modifications due to oxidation (M),

precursor tolerance = 0.2 Da, MS/MS fragment tolerance = 0.3 Da, mass = monoisotopic, and

peptide charges = +1. The significance of a protein match, based on the peptide mass fingerprint

(PMF) in the MS and the MS/MS data from several precursor ions, is presented as expectation values ($p < 0.001$).

In addition, where MALDI protein confidence scores left ambiguous identification, the trypsin digested protein spots were analyzed by nano-LC-MS/MS using a Thermo Scientific Orbitrap Fusion MS (Thermo Fisher Scientific, Waltham, MA), coupled with a Dionex Ultimat 3000 nanoHPLC with a 40 well standard auto sampler. The samples were injected onto a nanotrap (100 µm i.d. x 1 cm, C18 PepMap 100), followed by a C18 reversed-phase (RP) home-packed column (SB-C18, ZORBAX, 5 micron from Agilent, Santa Clara, CA) at a flow rate of 400 nL/min with 60 min LC gradient (5% AcN, 0.1% trifluoroacetic acid (TFA) to 100% AcN, 0.1% TFA). The RP column was further eluted for several min with 90% AcN and TFA to minimize intersample contamination. Mass spectrometer parameters include the following: spray tip voltage at +2.2 kV, Fourier-transform MS mode for MS acquisition of precursor ions (resolution 120,000); ITMS mode for subsequent MS/MS of top 10 precursors selected; same ions were excluded for 15 sec; MS/MS was accomplished via collision induced dissociation.

Data analysis was performed using the MASCOT server by interrogating the total organism database. The selected analytical parameters included: the enzyme as trypsin; maximum missed cleavages = 2; variable modifications included oxidation (methionine); precursor ion mass tolerance was set at 5 ppm; fragment ion mass tolerance was 0.6 Da. The significance of a protein match is based on peptide expectation values and the numbers of peptides found (≥ 2). The default significance threshold is $p \leq 0.05$ to achieve a false discovery rate (FDR) of less than 1.0%. Protein identifications were accepted if they could be established at 95.0% probability to achieve an FDR [178] of less than 1.0%.

Western blot analysis was performed on the PSD fractions isolated using Syn-PER Reagent, followed by ultracentrifugation to enrich for PSD as described above. Separation of the proteins in the samples obtained was done by 12% SDS- polyacrylamide gel electrophoresis. The separated proteins were transferred to a nitrocellulose membrane (Bio-Rad Laboratories, Hercules, CA) and incubated with PSD95, CAMK2A, GAPDH, UCHL1 and PFN (all 1:1,000; Cell Signaling Technology, Danvers, MA) antibodies overnight. Actin (1:1,000; Cell Signaling Technology, Danvers, MA) was used as a loading control. The membrane was incubated with proper fluorescent secondary antibodies (1:10,000) (LI-COR Biosciences, Lincoln, NE) and scanned using Odyssey infrared fluorescent imaging system (LI-COR Biosciences, Lincoln, NE). The band densities were analyzed using ImageJ software, normalizing using the densities of the loading control obtained by reprobing the membranes for actin. All fifteen samples were run on the same blot. Differences between groups were assessed using Student's t-test.

Results

PROTEINS IDENTIFIED

The goal of this study was to determine if the unique ability of NDAN postsynaptic densities (PSDs) to reject Aβ oligomer binding can be explained by a unique protein signature that sets NDAN aside from AD and healthy age-matched control individuals. PSD fractions from three experimental groups (control, AD and NDAN) were used in a discovery-mode proteomics, the cases were pooled in order to increase the likelihood that the proteins identified would be universal to the experimental group, while decreasing the inter-individual variability. Case subject data is provided in Table 3.1. In order to analyze the PSD proteome, we determined the

ratios of expression levels in three different ways: AD vs. control, NDAN vs. control and NDAN vs. AD.

Table 3.1: Demographic data of the cases used in the proteomics study
PMI – post-mortem interval, MMSE – mini-mental state exam.

Case number	Diagnosis	Age, yrs	Sex	PMI, hrs	Braak stage	MMSE
1525	Control	88	F	3	1	28
1716	Control	>89	M	5	1	29
1944	Control	>89	F	8	3	29
1957	Control	>89	F	8	3	30
1965	Control	>89	F	5.5	2	26
1977	Control	>89	F	4	3	28
2337	Control	86	M	28.5	3	26
2376	Control	>89	M	4	3	26
	Average	92	3/5	8.3	2.4	27.8
1791	AD	>89	M	10	4	19
2010	AD	87	F	6	4	23
2126	AD	>89	F	9	4	26
2146	AD	>89	F	9.5	4	30
2157	AD	>89	M	11.5	4	12
2221	AD	>89	F	15.5	4	29
2315	AD	>89	M	4	4	28
2330	AD	>89	F	4.5	4	28
	Average	95	3/5	8.8	4.0	24.4
697	NDAN	>89	M	5	4	29
1095	NDAN	88	M	3	5	29
1179	NDAN	89	F	2.5	4	27
1362	NDAN	>89	F	48	4	27
1644	NDAN	76	F	30	5	30
1677	NDAN	>89	F	18	6	30
1686	NDAN	87	F	3	4	29
1845	NDAN	86	M	5	4	29
	Average	90	3/5	14.3	4.5	28.8

Seven hundred and twenty-seven individual spots were detected on Coomassie-stained 2DE of isolated PSDs (Fig. 3.1). Three hundred and forty most abundant spots were collected for protein digestion. Following digestion, the resulting peptides were separated by liquid chromatography and the amino acid sequences were determined. Using MS/MS we identified 122 proteins that have the p-value ≤ 0.05 in at least one comparison (*i.e.* AD vs. control, NDAN vs. control, or NDAN vs. AD) and MALDI protein score cut-off ≥ 62. In the Supplementary table 3.1 we have additionally included 10 proteins that presented with the p-values greater than 0.05, however, are relevant and contribute to the discussion.
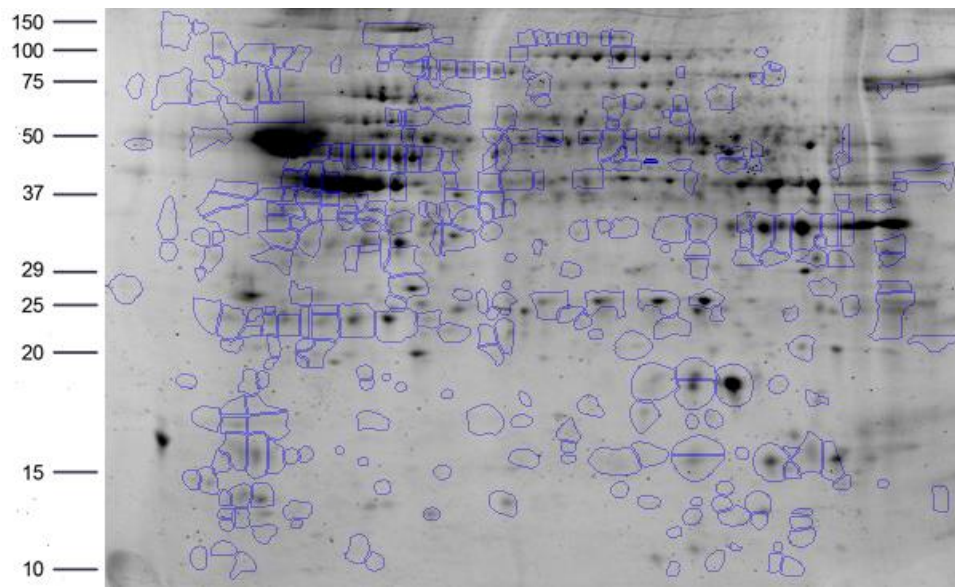
Figure 3.1. Representative 2DE of proteins identified

The highlighted spots were excised and analyzed in the present study. The x-axis is calibrated in pH units, while y-axis is calibrated in mass units (kDa).

Since the goal of this work was to determine differences between AD and NDAN that would reflect their diverse cognitive status and synaptic vulnerability to Aβ oligomers, we selected proteins that were statistically changed (cut-off ≥ ±1.5 fold) in NDAN vs. AD,

regardless of whether they were changed in either group as compared to controls. Following this criterion, thirty-one proteins with the fold change of at least ±1.5 in NDAN vs. AD were chosen for further analysis (Table 3.2). Using this set of 31 proteins we then looked at AD vs. control and NDAN vs. control (Fig. 3.2) to determine if the changed protein would fall into any of the following categories:

1) progression of neuropathology – proteins that have more pronounced change in either AD, or NDAN when compared to control;

2) unique to AD – proteins that change in AD vs. control, but not in NDAN vs. control;

3) unique to NDAN – proteins that change in NDAN vs. control, but not in AD vs. control.
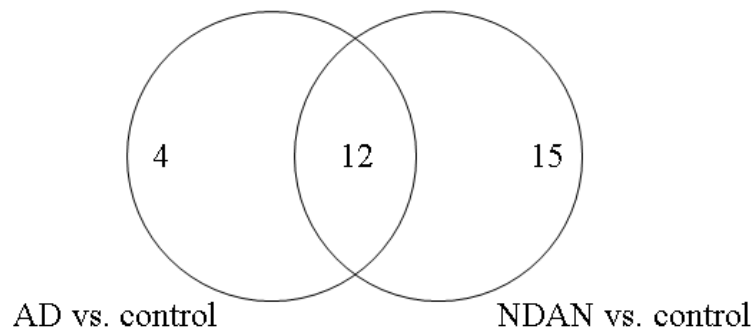
Figure 3.2. Venn diagram of the protein changes in NDAN vs. AD

The diagram includes the total number of proteins with significant differential expression in NDAN vs. AD, including the number of proteins that change in AD vs. control and NDAN vs. control.

Table 3.2:   Postsynaptic density proteins identified using MS/MS that have ± 1.5 fold change in NDAN vs.AD

Protein name	Gene ID	Accession Number	Theoretical pI	Measured pI	Theoretical Mw, kDa	Measured Mw, kDa	MS ID protein score	AD vs. control	NDAN vs. AD	NDAN vs. control
Actin, cytoplasmic 2	ACTG1	P63261	5.31	6.31	42	15	78	-1.50	-1.49	-2.23
Annexin (Fragment)	ANXA2	H0YN42	5.56	8.03	29	30	141	1.55	1.83	2.85
Calcium/calmodulin-dependent protein kinase type II subunit alpha	CAMK2A	Q9UQM7	6.61	5.84	54	17	115	1.43	1.98	2.83
Calreticulin	CALR	P27797	4.29	4.65	48	71	70	-1.15	-2.85	-3.27
Creatine kinase B-type	CKB	P12277	4.29	6.93	48	17	70	1.05	-1.98	-1.88
Creatine kinase B-type (Fragment)	CKB	G3V4N7	4.89	5	24	20	116	1.09	-2.80	-2.57
Glial fibrillary acidic protein	GFAP	P14136	5.42	5.39	50	46	1010	-1.44	2.58	1.79
Glial fibrillary acidic protein	GFAP	P14136	5.42	5.34	50	46	950	-1.23	2.18	1.77
Glial fibrillary acidic protein	GFAP	P14136	5.42	5.28	50	46	969	-1.32	2.15	1.63
Glial fibrillary acidic protein	GFAP	P14136	5.42	5.43	50	46	1050	-1.25	2.12	1.69
Glial fibrillary acidic protein	GFAP	P14136	5.42	5.18	50	46	863	-1.02	2.06	2.02
Glial fibrillary acidic protein	GFAP	P14136	5.42	5.07	50	37	915	-1.48	1.53	1.03
Glial fibrillary acidic protein	GFAP	E9PAX3	5.42	4.98	50	18	374	1.27	-1.98	-1.56

Protein name	Gene ID	Accession Number	Theoretical pI	Measured pI	Theoretical Mw, kDa	Measured Mw, kDa	MS ID protein score	AD vs. control	NDAN vs. AD	NDAN vs. control
Glial fibrillary acidic protein	GFAP	P14136	5.42	5.06	50	34	850	-1.44	-2.07	-2.97
Glial fibrillary acidic protein	GFAP	E9PAX3	5.42	5	50	20	400	-1.12	-4.32	-4.84
Glial fibrillary acidic protein (Fragment)	GFAP	K7EJU1	5.6	5.61	28	21	339	-4.13	2.00	-2.07
Glyceraldehyde-3-phosphate dehydrogenase	GAPDH	E7EUT4	8.57	9.17	36	32	88	-6.19	6.55	1.06
Hemoglobin subunit beta	HBB	P68871	6.74	7.35	16	13	170	1.26	2.90	3.66
Hemoglobin subunit beta	HBB	P68871	6.74	7	16	14	70	1.68	1.84	3.09
Hemoglobin subunit beta	HBB	P68871	6.74	7.34	16	14	212	1.75	1.67	2.92
Isoform 1 of Vinculin	VCL	P18206-2	5.83	5.88	117	118	322	1.03	1.92	1.97
Isoform 2 of Glial fibrillary acidic protein	GFAP	P14136-2	5.42	5.09	50	36	223	-2.19	2.42	1.10
Isoform 2 of Glial fibrillary acidic protein	GFAP	P14136-2	5.42	5.16	50	35	92	-1.91	1.70	-1.12
Isoform 2 of Glial fibrillary acidic protein	GFAP	P14136-2	5.42	5.17	50	38	885	-1.12	1.63	1.46
Isoform 2 of Glial fibrillary acidic protein	GFAP	P14136-2	5.42	5.23	50	46	945	1.02	1.63	1.66
Isoform 2 of Glial fibrillary acidic protein	GFAP	P14136-2	5.42	5.5	50	46	974	-1.08	1.60	1.48
Isoform 2 of Glial fibrillary acidic protein	GFAP	P14136-2	5.42	5.07	50	37	790	-1.53	1.56	1.02

Protein name	Gene ID	Accession Number	Theoretical pI	Measured pI	Theoretical Mw, kDa	Measured Mw, kDa	MS ID protein score	AD vs. control	NDAN vs. AD	NDAN vs. control
Isoform 2 of Glial fibrillary acidic protein	GFAP	P14136-2	5.42	5.16	50	49	828	-1.19	1.53	1.28
Isoform 2 of Glial fibrillary acidic protein	GFAP	P14136-2	5.42	5.74	50	48	284	2.04	-1.60	1.27
Isoform 3 of Dynamin-1	DNM1	Q05193-3	6.57	4.93	96	20	346	-1.23	1.69	1.38
Isoform 3 of Dynamin-1	DNM1	Q05193-3	6.57	4.88	96	19	300	-1.35	-1.60	-2.16
Isoform 3 of Peroxiredoxin-5, mitochondrial	PRDX5	P30044-3	9.12	7.7	17	15	154	1.29	-1.77	-1.37
Isoform 3 of Ras-related protein Rap-1b	PAR1B	P61224-3	8.72	6.37	19	19	112	-1.19	1.92	1.62
Isoform CNPI of 2',3'-cyclic-nucleotide 3'-phosphodiesterase	CNP	P09543-2	8.73	9.11	45	40	97	-1.66	1.82	1.10
Isoform Cytoplasmic+peroxisomal of Peroxiredoxin-5, mitochondrial	PRDX5	P30044-2	6.73	7.75	17	16	143	1.31	-2.27	-1.73
Isoform IB of Synapsin-1	SYN1	P17600-2	9.88	9.17	70	75	271	1.16	-1.72	-1.48
Isoform IB of Synapsin-1	SYN1	P17600-2	9.88	8.87	70	74	290	1.17	-2.00	-1.71
Isoform Non-brain of Clathrin light chain A	CLTA	P09496-2	4.45	4.69	24	30	62	-1.01	-3.31	-3.34
Keratin, type I cytoskeletal 10	KRT10	P13645	5.13	5.33	59	102	78	-1.04	-1.80	-1.87
Keratin, type I cytoskeletal 9	KRT9	P35527	5.14	6.14	62	17	95	-1.37	1.55	1.13

Protein name	Gene ID	Accession Number	Theoretical pI	Measured pI	Theoretical Mw, kDa	Measured Mw, kDa	MS ID protein score	AD vs. control	NDAN vs. AD	NDAN vs. control
Keratin, type I cytoskeletal 9	KRT9	P35527	5.14	4.82	62	13	213	-1.21	-1.56	-1.89
Keratin, type II cytoskeletal 1	KRT1	P04264	8.15	7.55	66	12	181	1.32	-1.54	-1.17
Keratin, type II cytoskeletal 1	KRT1	P04264	8.15	4.66	66	35	63	-1.14	-1.81	-2.07
Keratin, type II cytoskeletal 1	KRT1	P04264	8.15	5.54	66	17	130	1.33	-3.10	-2.33
Malate dehydrogenase, mitochondrial	MDH2	P40926	8.92	8.94	36	30	228	1.67	1.77	2.97
NADH dehydrogenase [ubiquinone] 1 alpha subcomplex subunit 5	NDUFA5	F8WAS3	5.75	5.5	13	13	237	-3.21	-1.44	-4.62
NADH dehydrogenase [ubiquinone] flavoprotein 1, mitochondrial (Fragment)	NDUFV1	E9PQP1	8.51	8.26	51	46	105	2.77	-1.47	1.88
Neurofilament medium polypeptide	NEFM	E7EMV2	4.76	5.4	79	50	210	-1.28	1.50	1.17
Profilin-2	PFN2	C9J0J7	9.26	5.76	10	14	126	1.80	-1.54	1.17
Profilin-2	PFN2	C9J0J7	9.26	5.06	10	13	78	1.01	-2.08	-2.06
Pyruvate carboxylase, mitochondrial	PC	P11498	6.37	6.28	130	119	96	1.12	-1.59	-1.42
Rho GDP-dissociation inhibitor 1 (Fragment)	ARHGDIA	J3KTF8	5.37	5.02	22	20	185	1.18	-1.77	-1.50
Septin-7	SEPT7	F5GZE5	8.76	8.68	51	45	84	1.48	-1.66	-1.12

Protein name	Gene ID	Accession Number	Theoretical pI	Measured pI	Theoretical Mw, kDa	Measured Mw, kDa	MS ID protein score	AD vs. control	NDAN vs. AD	NDAN vs. control
Spectrin alpha chain, non-erythrocytic 1	SPTAN1	Q13813	5.22	5.38	285	134	439	1.22	-1.91	-1.56
Syntaxin-binding protein 1	STXBP1	P61764	6.5	5.52	68	31	171	1.12	2.00	2.24
Tubulin alpha-1A chain (Fragment)	TUBA1A	F8VRZ4	5.44	5.09	12	22	67	-2.13	1.56	-1.37
Tubulin alpha-1B chain (Fragment)	TUBA1B	F8VVB9	5.03	5.54	28	46	91	-1.31	2.04	1.55
Tubulin alpha-1B chain (Fragment)	TUBA1B	F8VVB9	5.03	5.29	28	33	342	-1.26	-1.66	-2.09
Tubulin alpha-1B chain (Fragment)	TUBA1B	F8VVB9	5.03	5.23	28	33	128	-1.32	-2.97	-3.93
Tubulin beta-2A chain	TUBB2A	Q13885	4.78	5.45	50	34	139	1.19	-1.84	-1.55
Tubulin beta-4A chain	TUBB4A	P04350	4.78	4.81	50	16	62	-1.20	-1.84	-2.20
Tubulin beta-6 chain (Fragment)	TUBB6	K7ESM5	5.49	5.26	37	12	123	-1.59	-2.51	-4.01
Ubiquitin carboxyl-terminal hydrolase isozyme L1	UCHL1	D6R974	5.67	5.15	17	20	133	1.04	-2.47	-2.37

We also found several sets of protein spots on the 2DE with different isoelectric points and/or sizes that were identified as the same protein ("protein trains") (Table 3.3). The differences in theoretical and detected isoelectric points, with little to no change in sizes, could suggest post-translational modifications of the protein, while differences in protein size could indicate post-translational modifications and/or protein cleavage.

Table 3.3:   Proteins detected in trains of spots on the 2DE

Protein	Theoretical pI	Theoretical Mw, kDa	Measured pI	Measured Mw	Fold change in NDAN vs. AD
Isoform 3 of dynamin-1, DNM1	6.57	96.04	4.88	19	-1.6
			4.93	20	1.96
Glial fibrillary acidic protein, GFAP	5.42	49.88	5	20	-4.32
			5.06	34	-2.07
			4.98	18	-1.98
			5.07	37	1.53
			5.18	46	2.06
			5.43	46	2.12
			5.28	46	2.15
			5.34	46	2.18
			5.39	46	2.58
Isoform 2 of glial fibrillary acidic protein, GFAP	5.53	50.28	5.74	48	-1.6
			5.16	49	1.53
			5.07	37	1.56
			5.5	46	1.6
			5.23	46	1.63
			5.17	38	1.63
			5.16	35	1.7
			5.09	36	2.42
Hemoglobin subunit beta, HBB	6.74	16	7.34	14	1.67

Protein	Theoretical pI	Theoretical Mw, kDa	Measured pI	Measured Mw	Fold change in NDAN vs. AD
			7	14	1.84
			7.35	14	2.9
Keratin type I cytoskeletal 9, KRT9	5.14	62.06	4.82	13	-1.56
			6.14	17	1.55
Keratin type II cytoskeletal 1, KRT1	8.15	66.04	5.54	17	-3.1
			4.66	35	-1.81
			7.55	12	-1.54
Profilin-2, PFN2	9.26	9.84	5.06	13	-2.08
			5.76	14	-1.54
Isoform cytoplasmic + peroxiredoxin-5, mitochondrial, PRDX5	6.73	17	7.75	16	-2.27
Isoform 3 of peroxiredoxin-5, mitochondrial, PRDX5	9.12	17	7.7	15	-1.77
Isoform IB of synapsin-1, SYN1	9.88	70.03	8.87	74	-2
			9.17	75	-1.72
Tubulin alpha-1B chain, TUBA1B	5.03	27.55	5.23	33	-2.97
			5.29	33	-1.66
			5.54	46	2.04

VALIDATION OF SELECTED PROTEIN TARGETS

To validate the protein changes observed using the 2DE we selected four target proteins based on the fold change and availability of commercial antibodies. Additionally, we included one protein (PSD95) that was not changed in our proteomic dataset. Validation was performed on a different set of hippocampal samples (five cases per group) different from those used for proteomics (Table 3.4) that were analyzed individually.

Table 3.4:   Demographic data of the cases used for validation of protein levels using
              immunoblotting

PMI – post-mortem interval, MMSE – mini-mental state exam.

Case number	Diagnosis	Age, yrs	Sex	PMI, hrs	Braak stage	MMSE
2467	Control	>89	F	4.5	3	28
2553	Control	>89	M	4	2	28
2682	Control	>89	F	9	2	29
2755	Control	>89	F	18	2	29
2953	Control	>89	M	2.5	3	27
	Average	97	2/3	8	2	28
2272	AD	>89	F	5	6	20
2312	AD	87	F	2.5	6	19
2316	AD	83	M	13	5	N/A
2317	AD	88	M	4.5	6	N/A
2374	AD	>89	M	24	6	N/A
	Average	88	3/2	10	6	20
2322	NDAN	>89	F	14	4	29
2474	NDAN	>89	F	8	4	28
2491	NDAN	82	M	17	4	27
2556	NDAN	>89	M	12	4	28
2753	NDAN	>89	M	12	4	28
	Average	89	3/2	13	4	28

For validation using immunoblotting we selected CAMK2A, GAPDH, UCHL1 and PFN proteins (Fig. 3.3). Blotting for CAMK2A was not consistent with the proteomics results (Table 3.5), possibly due to inter-individual variability which was more pronounced in AD. Nonetheless, in direct comparison of NDAN vs. AD, we noted a same trend for increased levels of this protein (1.23), which however did not reach the same fold change (1.98 in proteomics).

Table 3.5: Densitometry analysis of Western blots for PSD95, CAMK2A, GAPDH, UCHL1 and PFN

Data are presented as mean +/- standard error of 5 cases per group; statistical significance was determined by Student's t-test.

Protein name	AD vs. Control	p-value	NDAN vs. AD	p-value	NDAN vs. Control	p-value
PSD95	-1.35 ± 0.07	0.025	1.14 ± 0.04	0.237	-1.18 ± 0.04	0.069
CAMK2A	-1.44 ± 0.13	0.081	1.23 ± 0.08	0.350	-1.17 ± 0.09	0.271
GAPDH	-1.03 ± 0.03	0.627	-1.18 ± 0.06	0.248	-1.21 ± 0.12	0.191
UCHL1	2.67 ± 0.76	0.091	-2.86 ± 0.47	0.062	-1.07 ± 0.23	0.892
PFN	3.49 ± 0.84	0.024	-2.65 ± 0.56	0.043	1.32 ± 0.32	0.492
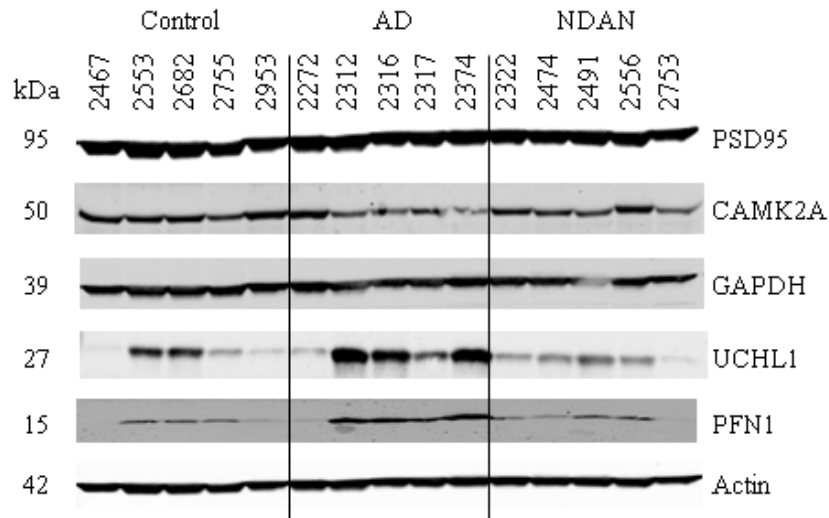
Figure 3.3. Confirmation of proteomic changes for selected proteins

Five cases per group were assayed individually. Case information is provided in Table 3.4.

Assessment of GAPDH levels revealed no change across experimental groups (Fig. 3.3 and Table 3.5), which could be explained by the presence of four isoforms in the proteomic dataset, three of which had no change in NDAN vs. AD, that could mask the detection of changes in only one out of the four isoforms detected by the immunoblotting antibody.

UCHL1 (Fig. 3.3 and Table 3.5) presented with some inter-individual variability, overall confirming the proteomics data (NDAN vs. AD: -2.47 in proteomics and -2.86 in densitometry analysis of immunoblotting).

Similarly, immunoblotting and proteomics quantification of PFN demonstrated a similar decrease of protein levels in NDAN vs. AD (Fig. 3.3 and Table 3.5).

Levels of PSD95 were not changed significantly across three groups (Fig. 3.3 and Table 3.5) as determined by immunoblotting, confirming the proteomic data.

In the following discussion some of the proteins we have identified are usually found in the presynaptic terminals. Our samples were prepared using a PSD-enrichment protocol, therefore, some of the presynaptic proteins were identified during the proteomic analysis. We elected to present these results as the presynaptic proteins contribute to the observed changes at the synaptic level.

MAIN UPSTREAM REGULATORS

The thirty-one proteins were analyzed using Ingenuity Pathway Analysis (IPA) to determine main upstream regulators and pathways. Five upstream elements were identified as regulators of the changes that were observed: MAPT (microtubule-associated protein tau), PSEN1 (presenilin 1), APP (amyloid precursor protein), HTT (huntingtin) and D-glucose. MAPT, PSEN1, APP and HTT are known to play a role in Alzheimer's Disease pathogenesis ([53,179,180]; reviewed by [181–183]). Multiple studies with ^{18}F-fluorodeoxyglucose demonstrate that in AD there is a progressive reduction of glucose metabolism which correlates with severity of the disease (reviewed by [184]). Impaired glucose metabolism in the brain is one of the pathophysiological features that frequently precedes clinical manifestation in AD (reviewed by [184]).

CANONICAL PATHWAYS AND MOLECULAR AND CELLULAR FUNCTIONS

IPA was used to identify pathways that the 31 changed proteins collectively represent or are a part of. The top canonical pathways returned by the IPA were: remodeling of epithelial adherens junctions ($p = 5.14*10^{-12}$), epithelial adherens junction signaling ($p = 1.07*10^{-9}$), phagosome maturation ($p = 1.18*10^{-9}$), 14-3-3 mediated signaling ($p = 2.49*10^{-8}$), axonal guidance signaling ($p = 2.42*10^{-6}$), and gap junction signaling ($p = 3.75*10^{-6}$).

The molecular and cellular functions identified by IPA included cellular assembly and organization, cellular function and maintenance, and cell morphology. Interestingly, eleven proteins from our dataset cluster into the nervous system development and function pathway. This is consistent with our previous findings showing that when compared to AD and MCI, NDAN individuals have higher rate of neurogenesis in the dentate gyrus, which is positively correlated to their ability to escape (or significantly delay) dementia [67].

PANTHER [185–187] was used to analyze relevant proteins by function (Fig. 3.4). Table 3.6 describes identified proteins in NDAN vs. AD by functional category.
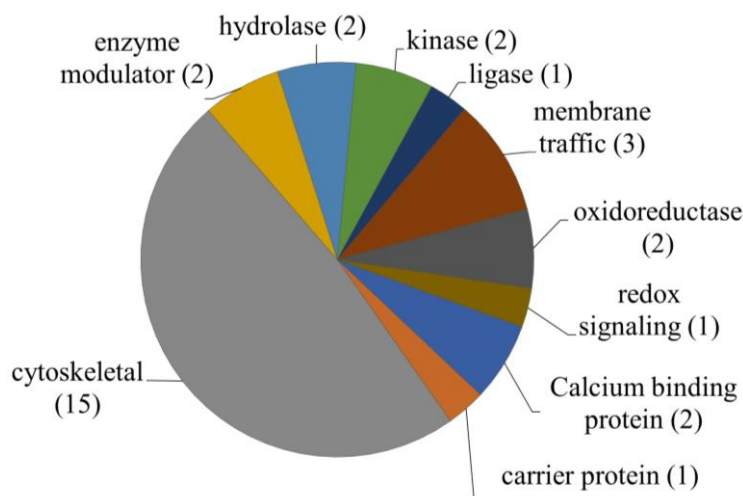
Figure 3.4. Pie chart representing the PANTHER classification of proteins based on protein class The number of proteins in each category is shown in parenthesis.

66

Discussion

PROTEIN FUNCTION AND PATHWAY ANALYSIS

The samples employed in this study consisted of PSD-enriched hippocampal fractions; the purity of PSD fractions prepared according to our protocol was previously described [66]. The proteomic methodology for this study was chosen for the superior quantitative aspects, but due to technical limitations of extraction and the 2DE methodology, hydrophobic or transmembrane proteins are not reliably represented in our dataset. Future studies focusing on transmembrane proteins will complement this initial work that therefore centers on soluble, non-transmembrane proteins. Among the 31 proteins that have significantly different levels in NDAN vs. AD, fifteen form a unique expression pattern in NDAN, setting these individuals aside from both age-matched healthy controls and AD patients. Existence of the unique protein "signature" at the PSD of NDAN cases suggests that these non-demented subjects should not be considered pre-symptomatic AD, but rather individuals who are clearly distinct from both control and those who have clinical manifestation of the disease.

The unique protein expression signature in our dataset represents several pathways that converge onto junction signaling, phagosome maturation and 14-3-3 pathway. Additionally, twenty proteins from our dataset were clustered by IPA into the neurological disease pathway, which reveals that these proteins are closely related to each other and have been previously shown by other investigators to be implicated in brain diseases (Fig. 3.5). This latter observation corroborates the notion that relevant mechanisms may be acting at the NDAN synapses to mediate their resilience to neurodegeneration and associated dementia.
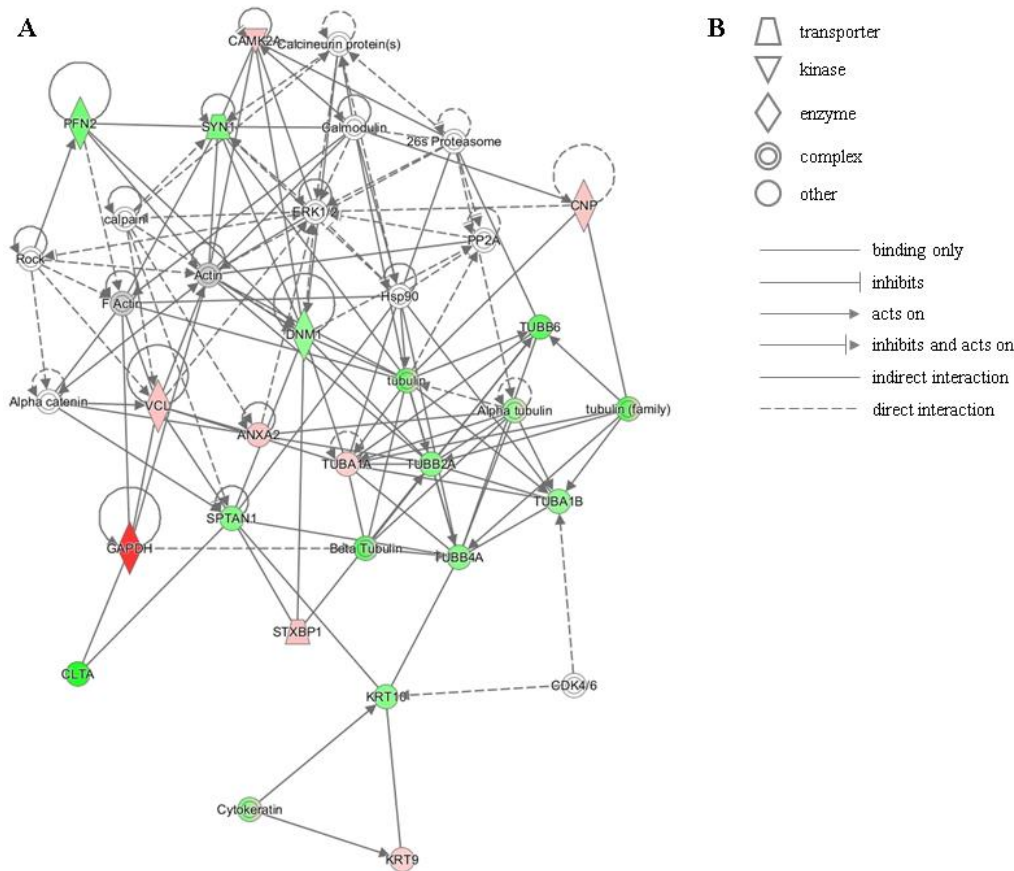
Figure 3.5. IPA identifies twenty proteins from our dataset that are associated with the
neurological disease network

(A) Upregulated (red) or downregulated (green) proteins from our dataset are highlighted in the
network. Solid and dashed lines indicate direct and indirect correlation between proteins,
respectively. CAMK2A – calcium/calmodulin-dependent protein kinase type II subunit alpha;
PFN2 – profilin-2; SYN1 – synapsin-1; CNP - 2',3'-cyclic-nucleotide 3'-phosphodiesterase;
PP2A – protein phosphatase 2; ERK1/2 – mitogen-activated protein kinase 1/2; DNM1 –
dynamin-1; Hsp90 – heat shock protein 90; TUBB6 – tubulin beta-6 chain; VCL – vinculin;
ANXA2 – annexin 2; TUBA1A – tubulin alpha-1A chain; TUBB2A – tubulin beta-2A chain;
TUBA1B – tubulin alpha-1B chain; TUBB4A – tubulin beta-4A chain; SPTAN1 – spectrin alpha
chain, non-erythrocytic 1; GAPDH – glyceraldehyde-3-phosphate dehydrogenase; CLTA –
clathrin light chain A; STXBP1 – syntaxin-binding protein 1; KRT10 – keratin, type I
cytoskeletal 10; CDK4/6 – cyclin-dependent kinases 4/6; KRT9 – keratin, type I cytoskeletal 9.
(B) Figure legend for the IPA network. Nodes in the network are depicted by different shapes
that represent various functional classes of the proteins. Arrows/lines represent different
molecular relationships in the IPA network.

PROGRESSION OF NEUROPATHOLOGY – PROTEINS WITH A MORE PRONOUNCED CHANGE IN EITHER AD OR NDAN

We found higher levels (1.83 fold) of annexin 2 (ANXA2) at the PSDs of NDAN subjects (1.55 AD vs. control, 2.85 NDAN vs. control). ANXA2 belongs to a group of soluble, hydrophilic proteins which can bind to negatively charged phospholipids in a Ca^{2+}-dependent manner [188]. ANXA2 has Ca^{2+}-dependent filament bundling activity and can participate in membrane vesicle aggregation, where it forms membrane-membrane or membrane-cytoskeleton connections by interacting with F-actin [188]. Notably, decreased levels of F-actin have been associated with synapse structural instability in AD (reviewed by [189]). ANXA2 has been demonstrated to modulate the activity of membrane channels, including Cl^- and Ca^{2+}; in addition, ANXA2 functions as a GLUT-4 transporter upon insulin stimulation [190]. Furthermore, ANXA2 interaction with tau modulates the tau mobility in the tips of neurites [191]. Therefore, higher levels of ANXA2 present in NDAN synapses could be indicative of preserved synaptic structure, function and insulin responsiveness.

Calcium/calmodulin-dependent protein kinase type II subunit alpha (CAMK2A) is a serine/threonine protein kinase and is required for hippocampal long-term potentiation (LTP) and spatial learning (as reviewed by [192]). Exposure to Aβ oligomers decreases the CAMK2 pool at the synapse [193]. CAMK2A-containing neurons are selectively lost in the CA1 of hippocampus in AD patients [194]. CAMK2 serves as a molecular switch for LTP and is capable of long-term memory storage [195]. CAMK2A levels are increased by 1.98 fold in NDAN when compared to AD (1.43 AD vs. control, 2.83 NDAN vs. control), which could indicate that robust CAMK2 upregulation is a necessary event to provide resistance of synapses to AD-related disruption as seen in NDAN, an event that may occur to an insufficient extent in symptomatic AD. The functionality of CAMK2A is measured by the subcellular localization and phosphorylation at

69

Thr286 [196], which were not assessed in this study. However, our previous study demonstrated that in AD the PSD immunoreactivity of the p(Thr286)CAMK2 is shifted away from the dendritic spines as it accumulates at the neuron's cell body in an Aβ oligomer-dependent phenomenon ([31], reviewed by [192]), and therefore, present results of CAMK2A levels at the PSD could reflect the compartmentalization of this protein.

Hemoglobin (HBB) was increased in NDAN vs. AD, a phenomenon consistently observed for each of the detected isoforms: 1.67 (1.75 AD vs. control, 2.92 NDAN vs. control), 1.84 (1.68 AD vs. control, 3.09 NDAN vs. control) and 2.9 fold (1.26 AD vs. control, 3.66 NDAN vs. control), which could suggest multiple scenarios. First, increased levels of HBB can indicate a response to hypoxia in the brain. Indeed, decreased expression of hemoglobin in AD was observed in neurons containing NFTs [197]. Furthermore, nitric oxide and its metabolites have high affinity for HBB, and HBB can be considered a protectant from oxidative and nitrosative stress [198]. Besides nitric oxide scavenging, HBB is capable of binding Aβ and enhancing its aggregation ability due to the presence of the iron core; HBB was previously shown to localize to amyloid plaques in AD brains [199]. It is thus possible that in NDAN HBB is promoting Aβ removal from the synapses which is supportive of our previous findings [66]. On the other hand, HBB presence at the synapse could be due to leaky blood-brain barrier, which has been shown to occur in the aged and diseased CNS ([200,201], reviewed by [202]). However, mRNAs for hemoglobin α- and β-chains were previously detected in rat and human neuronal cultures [203,204], whereas human brain sections stained for HBB showed a granular pattern in the cytoplasm without localization to specific compartments [203,205], collectively suggesting a possible role of local HBB within neurons.

Malate dehydrogenase (MDH) is the terminal enzyme of the TCA cycle; its function is to catalyze the conversion of L-malate to oxaloacetate, which requires NAD as a cofactor [206]. In our dataset we found an increase in MDH2 at the PSD of 1.77 fold in NDAN as compared to AD patients (1.67 AD vs. control, 2.97 NDAN vs. control). While it has been reported that MDH levels can be elevated during caloric restriction in mice [207], a diet regimen known to reduce age-associated CNS deficits (reviewed by [208,209]), the physiological significance of increased MDH at the synapses remains to be established [207].

Tubulin alpha-1A (-2.13 AD vs. control, -1.37 NDAN vs. control, 1.56 fold in NDAN vs. AD) and beta-6 (-1.59 AD vs. control, -4.01 NDAN vs. control, -2.51 fold in NDAN vs. AD) have significantly different abundance in NDAN vs. AD (Table 3.3). Tubulin alpha and beta are the main components of microtubules which are very dynamic structures. Microtubules undergo rapid growth and disassembly which could potentially explain the protein level variability in our dataset, as well as the possibility of multiple post-translational modifications (reviewed by [210]).

Interestingly, the majority of proteins in this category presented with higher fold change in NDAN vs. control, than in AD vs. control. It is therefore tempting to speculate that these proteins participate in the protective phenotype in NDAN, which is also observed in AD to a limited extent and is therefore possibly ineffective (and/or abortive).

PROTEIN CHANGES UNIQUE TO AD

2',3'-cyclin-nucleotide 3'-phosphodiesterase (CNP) levels in AD were found to be -1.66 fold decreased vs. control. Our data is in agreement with previously published findings by Reinikainen *et al.* where they describe decreased CNP activity in hippocampus of AD patients [211]. Activity of CNP can be used as a measure of myelination of axons and lower levels of

CNP in AD could be indicative of the loss of myelination of hippocampal neurons [212]. CNP hydrolyses 2',3'-cyclic nucleotides to create 2'-derivatives [213]. CNP can regulate tubulin polymerization and microtubule distribution [214], as microtubules use CNP as a linker, which allows them to connect to the plasma membrane. Additionally, CNP stimulates F-actin reorganization, which is essential for filopodia and lamellipodia formation [214]. CNP levels were unchanged in NDAN vs. control and were decreased in AD, which once again supports the idea that NDAN synapses remain healthy.

Glyceraldehyde-3-phosphate dehydrogenase (GAPDH) was found to be dramatically downregulated in AD vs. control (-6.19 fold). As reviewed by Butterfield *et al*., in addition to glycolytic activity, GAPDH performs many other functions: DNA and RNA binding, transcription regulation, kinase, catalysis of microtubule formation and polymerization, vesicular transport and interaction with multiple molecules and proteins, including NO, huntingtin and APP [215]. In addition, GAPDH can undergo multiple post-translational modifications: oxidation, phosphorylation, S-nitrosylation, as well as direct or indirect interaction with oxidative species. GAPDH can interact with Aβ [216], and has been found to be a major component of amyloid plaques and NFTs in AD brains [215]. Aβ, on the other hand, was shown to stimulate inactivation of GAPDH in addition to promoting its nuclear translocation and pro-apoptotic function [215]. GAPDH levels are decreased in AD which can indicate reduced glucose metabolism [217]. GAPDH has been suggested to be a potent target to prevent neurodegeneration in AD brains, due to ability of GAPDH to serve as scaffold for APP, Aβ40 and Aβ42, and tau protein [215,216]. Levels of GAPDH in NDAN are unaltered when compared to control, which distinguishes NDAN from AD and can indicate better overall brain health of NDAN individuals.

Neurofilament medium polypeptide (NEFM) was measured at -1.28 in AD vs. control, which indicates a trend towards decrease in AD. Overall in NDAN vs. AD NEFM was changed by 1.5 fold (1.17 in NDAN vs. control). Neurofilaments play a role in establishing and maintenance of the 3D structure of axons [218]. NEFM is essential for the formation of the cross-bridge, stabilization, and extension of filament network [218,219]. NEFM tail and its phosphorylation are required for radial growth of large myelinated motor axons [218]. Neurofilaments allow neurons to maintain their shape and are required for axon growth [220]. Neurofilaments can interact with microtubules, certain receptors that are located at the PSD and many other proteins that are transported along neurofilaments.

We found that the level of septin-7 (SEPT7) was increased by 1.48 fold in the PSD of AD patients as compared to control subjects while remaining unchanged in NDAN vs. control. Septins are evolutionary conserved cytoskeletal GTPases. Septins can be found in NFTs, dystrophic neurites in senile plaques and neuropil threads in AD brains [221]. Some septin species are also found in granular or fine fibrillary deposits in neuronal soma [221]. Formation of septin fibrils suggests that aggregation of this protein may accompany NFT formation. In order to function properly, septins form filaments following a process regulated by GTP hydrolysis [221]. Dysregulation of normal septin assembly in neurons may result in affected vesicular transport and structural integrity, leading to accelerated neurodegeneration. Interactions with phospholipids, microtubules and actin can influence septin assembly [222]. Septin assemblies can modulate the distribution of surface proteins and receptors and can also play a role in clathrin-mediated endocytosis [222]. It is thought that septins can serve as scaffolds for submembranous structures, assisting in neuronal polarity and vesicle trafficking [222]. SEPT7, in particular, can be located on the cytoplasmic side of presynaptic membranes and in endfeet of

astroglia [223]. As reviewed by Mostowy and Cossart, SEPT7 plays a role in actin dynamics, axon growth, cell shape, chromosome segregation, cytokinesis, dendrite formation, DNA repair, membrane trafficking and microtubule regulation in addition to serving as a scaffolding protein [222].

PROTEIN CHANGES UNIQUE TO NDAN

Calreticulin, a key upstream regulator of calcineurin [224], is a chaperone protein that can be found in several organelles in neurons and glial cells [225]. It is known to interact with APP, Aβ and Ca^{2+} [224,226–230]. Calreticulin was found at lower levels (-3.27 fold) at the PSDs in NDAN when compared to control. While lower levels of calreticulin have been shown to be associated with decreased calcineurin activity [231,232], increased calcineurin has been reported in the AD brain and correlates with disease severity [233,234]. Furthermore, we have previously shown that calcineurin mediates the toxic action of Aβ oligomers at synapses and that pharmacological inhibition of calcineurin protects from AD-related memory deficits in both experimental animals and humans ([32,235–237]; reviewed by [170]). Furthermore, we found that calcineurin levels are unaltered in the brain of NDAN subjects as compared to demented AD patients (Taglialatela *et al.*, unpublished observation). Therefore, reduced calreticulin levels at the synapses in NDAN individuals may be one of the mechanisms maintaining low calcineurin, thus contributing to preservation of synaptic integrity in the face of the presence of toxic amyloid oligomers.

Clathrin was downregulated in NDAN vs. control (-3.34 fold). Clathrin plays an important role in sorting and recycling of the proteins at the synaptic membrane [238]. While the protein levels of clathrin in AD are preserved when compared to control, the regulation of clathrin transport is known to be impaired in AD brains [238]. Under normal conditions clathrin

is transported from neuronal perikarya to axonal terminals, with the highest concentration of clathrin found at the synaptic terminals [238]. However, Nakamura *et al.* report that in AD the amount of clathrin at synaptic terminals is decreased, while NFTs and neuronal perikarya have detectable levels of clathrin [238]. In the growth cones, repulsive Ca^{2+} signals cause asymmetric clathrin-mediated endocytosis via calcineurin [239]. Calcineurin activation results in clathrin- and dynamin-dependent endocytosis. Additionally, Aβ42 reduces axonal density by promotion of clathrin-mediated endocytosis in the growth cones, which results in a growth cone collapse due to Ca^{2+} signaling, and calcineurin and calpain activation [240]. Moreover, inhibition of clathrin-mediated endocytosis was demonstrated to rescue the Aβ42-induced toxicity [240]. Reduction of clathrin levels at PSD in NDAN in comparison to AD could thus be another contributing factor to the ability of NDAN synapses to withstand the toxic hit by Aβ which in AD results in increased endocytosis and growth cone retraction.

Creatine kinase B (CKB) levels were decreased at the PSDs of NDAN vs. control (-2.57 and -1.88 fold). The CKB family of enzymes is involved in the regulation of the ATP and ADP levels by reversible transfer of phosphate onto creatine to form phosphocreatine, which can provide energy when ATP concentrations drop [241,242]. Additionally, CKB is identified as a part of slow axonal transport [243]. CKB-deficient cells show significantly increased fraction of motile mitochondria [241] . While initial evidence suggests that synaptic mitochondria in NDAN have less DNA damage through a preserved mitochondrial DNA repair system (Taglialatela *et al.*, unpublished observation), we have not yet analyzed mitochondria function in NDAN vs. AD, nevertheless, it has been reported that mitochondria are severely impaired in AD [244,245]. Interestingly, two subunits of the mitochondrial membrane respiratory chain complex I were detected in our dataset. NADH dehydrogenase [ubiquinone] 1 alpha subcomplex subunit 5

(NDUFA5) and NADH dehydrogenase [ubiquinone] flavoprotein 1 (NDUFV1) did not meet the ±1.5 fold cut-off criteria in NDAN vs. AD, however, they were measured at -1.44 and -1.47 fold changes, respectively. Collectively these findings indicate the dysregulation of mitochondrial function in the presence of AD-like pathology. Mitochondria function and ATP generation in the brain can be affected by the improper glucose metabolism since Krebs cycle and oxidative phosphorylation of glucose occur in mitochondria (reviewed by [184]).

Activity of pyruvate carboxylase (PC) is tightly regulated. PC activity can be downregulated by insulin, which reduces the carbon flux when the glucose levels are high [246]. Lower levels of PC in NDAN (-1.59 fold vs. AD) could be explained by the fact that NDAN subjects, unlike AD, have preserved insulin responsiveness (Taglialatela *et al.*, unpublished observation). One of the important roles of PC pathway is detoxification of ammonia from the brain, during which glutamine synthetase catalyzes formation of glutamine from ammonia and glutamate. Conversion of pyruvate to oxaloacetate replenishes the TCA cycle, which is utilized during detoxification of ammonia or oxidation of glutamate [247].

Synapsin 1 (SYN1) is downregulated in NDAN vs. control (-1.71 and -1.48 fold). SYN1 is a member of a family of neuron-specific phosphoproteins that can be localized pre- and postsynaptically [248,249]. SYN1 plays a role in regulation of axonogenesis, synaptogenesis and regulation of nerve terminal function in mature synapses [249]. SYN1 is differentially distributed in different regions of the hippocampus. It is suggested that presynaptic SYN1 (approximately 60% of total SYN1) becomes associated with synaptic vesicles, while the postsynaptic 40% of this protein possibly represent the newly synthesized protein that will be transported to the nerve terminals [248].

Syntaxin binding protein 1 (STXBP1) is upregulated in NDAN vs. control (2.24 fold). Syntaxin 1 and STXBP1 form a complex in 1:1 ratio [250]. STXBP1 can act as a chaperone for syntaxin [251]. Proteins of the STXBP1 family can interact with Rabs, small GTPases, and together they may play a role in vesicle trafficking and membrane fusion [251]. STXBP1 proteins can also contribute to the specificity of membrane trafficking. It has been suggested that protein kinase C regulates the STXBP1-syntaxin interaction [251]. Syntaxin bound to STXBP1 cannot interact with other proteins, which indicates that STXBP1 can play a role in determining the binding partners for syntaxin and further complex formation [251]. We have not detected syntaxin in the current proteomics set, therefore, we cannot unequivocally conclude if the higher levels of STXBP1 correlate with those of syntaxin as part of the complex that these proteins are known to form.

Donovan *et al.* reported increased levels of ubiquitin carboxyl-terminal hydrolase isozyme L1 (UCHL1) in AD when compared to healthy individuals [252]; we found a decrease in UCHL1 levels at the PSD in NDAN (-2.37 NDAN vs. control). UCHL1 can associate with free ubiquitin in neurons, which suggests that this interaction is important for maintenance of the free ubiquitin pool in neuronal cells [253,254]. UCHL1 is expressed mostly by neurons and neuroendocrine cells, and it was found in Lewy bodies [255] and NFTs [256]. Interestingly, Lombardino *et al.* showed that replaceable neurons have lower levels of UCHL1 when compared to non-replaceable neurons [257], which can be in concordance with the increased neurogenesis in NDAN [67] – one of the hypothesis behind NDAN preserved cognitive function.

Several proteins involved in actin dynamics were uniquely affected in NDAN. Actin and other cytoskeletal proteins are responsible for changes in spine morphology. Dendritic spine dynamics are determined by actin cytoskeleton organization [258]. Ability of spines to change

their structure allows for synaptic plasticity and plays an important role in memory formation [258]. Therefore, it is not unreasonable to argue that the changes in this class of proteins described below and uniquely observed in NDAN subjects are intimately associated with their preservation of synaptic integrity and cognitive ability ([66,69,70,72], reviewed by [170,259]). Cytoplasmic actin 2 showed a trend for downregulation in NDAN when compared to AD (-1.49 fold). Actin is responsible for stabilization of synaptic boutons in addition to modulation of bouton's structure to adjust to postsynaptic signaling [258]. The interaction between actin and profilins is essential for proper actin polymerization [260]. Profilins provide actin monomers to the barbed-end polymerization of actin filaments [258]. We found profilin 2 to be downregulated in NDAN when compared to control by -2.06 fold. We further found vinculin (VCL) to be upregulated in NDAN vs. control by 1.97 fold. VCL plays an important role in focal adhesion strengthening and stabilization due to its interaction with actin and talin [261]. At the leading edge of focal adhesion, VCL coordinates actin organization and dynamics. VCL determines the architecture of the leading edge by engaging actin flow to the extracellular matrix at maturing focal adhesion [261]. Vinculin binds to actin directly; however, vinculin also has an effect on actin dynamics independent of direct binding [261,262]. Interestingly, stabilization and maturation of focal adhesion are two distinct processes, as VCL inhibits the maturation of focal adhesion, but stimulates the stabilization [261].

Keratin type I cytoskeletal 10 (KRT10) is downregulated in NDAN vs. control by -1.87 fold. Changes in KRT10 in tear proteome were reported by Kalló *et al.* in AD patients [263]. Keratins are normally abundant in epidermal tissue, however, several other research groups have identified keratin 1 and 9 in samples of blood and CSF (keratin 1 and 9 are discussed in section Protein isoforms).

Significant decreases in tubulin beta-2A and 4A were observed in NDAN vs. control (-1.55 and -2.2, respectively). As discussed above in "Progression of neuropathology" section, tubulin is a major component of microtubules and is a very dynamic protein.

NDAN PSDs have higher levels of Ras-related protein Rap-1b (1.62 in NDAN vs. control). Rap1B, a small GTP-binding protein [264], in growth cones of hippocampal neurons is required for axonal development and growth [265]. Rap1B works together with Cdc42, whereas Rho and Rac function as antagonists to regulate extension of axons and neurites [258]. Cdc42 is a member of Rho GTPase family that plays a role in differentiation of oligodendrocytes, axon outgrowth, and neuronal polarity and migration (reviewed by [266]). Rap1B is reported to regulate plasma membrane Ca^{2+} transport, enhancing protein kinase C activity which is needed at the tip of axon [265]. Consequently, Rap1B possibly functions as a positioning factor for protein kinase C [265] and increased Rap-1b at NDAN synapses could support the notion that NDAN synapses retain proper function.

Another molecule, Rho GDP-dissociation inhibitor 1 (RhoGDI), from the same pathway was downregulated in our dataset (-1.5 fold in NDAN vs. control). Levels of RhoGDI are typically in balance and roughly equivalent to combined levels of RhoA, Rac1 and Cdc42 [267]. RhoGDI functions as stabilizer for Rho proteins, protecting them from degradation [267]. Due to the complex regulation of RhoA/Rac1 cell signaling and the fact that we have not detected RhoA, Rac1, or Cdc42 in the PSD fractions – the exact meaning of altered RhoGDI levels in the NDAN PSD remains unclear. On the other hand, Cdc42/RhoA/Rac1 network is involved in actin assembly/disassembly in response to extracellular stimuli [268,269] and our data indicate that this signaling pathway regulation differs in NDAN vs. AD as can be inferred by the levels of some key players of this network, including RhoGDI and Rac1.

As reviewed by Yan and Jeromin, remodeling and degradation and overall metabolism of spectrin (SPTAN1) play a role in the maintenance of membranes and cytoskeleton, protein cleavage, recycling and degradation [270]. SPTAN1 was downregulated in NDAN vs. control (-1.56 fold). Interactions between spectrin and other membrane-anchored proteins allow for proper trafficking and dynamics of proteins within the lipid bilayer. In the brain, SPTAN1 is estimated to comprise approximately 3% of total membrane protein content, being present in neuronal cell bodies, dendrites and postsynaptic terminals [270]. Additionally, SPTAN1 can localize to plasma membrane, microtubules, mitochondria, endoplasmic reticulum and nuclear envelope. In AD, SPTAN1 and its breakdown products are increased and have been proposed to be used as biomarkers in AD patients [270–272]. At the PSD, spectrin functions as a connector between integral membrane proteins and actin (reviewed by [273]). SPTAN1/synaptosomal membrane interaction is inhibited by Ca^{2+}/calmodulin [274]. Spectrin interaction with NMDAR mediates the regulation of NMDAR activity, which can be the basis for plasticity-induced changes in spines (reviewed by [273]).

We detected multiple cytoskeletal proteins as well as their regulators to be altered in NDAN vs. AD, which could indicate active remodeling of the synapses. Our findings concur with the observations reported by others regarding preserved synaptic integrity in NDAN [18,125,127,275]. Collectively these results suggest that the complex regulation of structural proteins in NDAN contributes to Aβ resistance.

PROTEIN ISOFORMS

Dynamin-1 (DNM1) is a large neuron-specific GTPase that is present at presynaptic terminals, where it is involved in synaptic vesicle budding off the membrane and recycling for future release [276]. DNM1 expression is dependent on CREB1 level [277]. DNM1 plays a role

in formation of associative memory in hippocampus [278]. Dynamin in complex with other presynaptic proteins (*e.g.*, synapthophysin) participates in plasticity by modulating the efficiency of vesicle release. When DNM1 was knocked down in AD animal models, Aβ levels were lowered possibly due to regulation of BACE1 internalization [279]. Conversely, in tissue culture (hippocampal neurons) application of Aβ causes the decrease of DNM1 levels via calpain-mediated proteolysis [276]. Interestingly, this reduction of DNM1 occurs prior to synapse loss in cultured hippocampal neurons, which suggests the intriguing hypothesis that synapses become dysfunctional first and later the synapse retraction/loss occurs. In our dataset we have identified 2 protein spots for DNM1 on 2DE with fold change of 1.69 and -1.6 in NDAN vs. AD. It remains to be established if the DNM1 undergoes a post-translational modification which could explain different levels of this protein in our dataset.

We have detected several isoforms of glial fibrillary acidic protein (GFAP), which can be expressed by several cell types in the brain, including neurons [280]. In concordance with other published studies [281], we have identified several horizontal "trains" of GFAP on the 2DE in our study (18 spots on the gel) (Table 3.3), which could indicate protein cleavage and/or degradation, co-translational or post-translational modifications that can affect the structure and function of GFAP. GFAP can undergo many post-translational modifications, such as phosphorylation, sulfation, glycosylation, oxidation, acetylation and other [282]. Each modification can result in different alteration of GFAP function and/or localization, although the exact mechanisms are still under investigation.

Keratin type I cytoskeletal 9 (1.55 and -1.56 fold in NDAN vs. AD) and keratin type II cytoskeletal 1 (-3.1, -1.54 and -1.81 fold in NDAN vs. AD) are expressed at significantly different levels in NDAN vs. AD (Table 3.3). Notably, keratin 9 was identified by multiple

research groups in the CSF and has been even proposed as a biomarker for AD [283–285]. Furthermore, keratin 1 was identified in 5xFAD mouse hippocampi using proteomics [286], and keratin 1 and 9 show different expression patterns in other neurodegenerative disorders [287].

Several isoforms of tubulin alpha-1B with fold change of 2.04, -1.66, and -2.97 were significantly different between NDAN and AD. The possible significance of tubulins in the maintenance of synaptic function/stability in NDAN vs. AD has been discussed earlier.

Peroxiredoxins (PRDX) play a role in protection from oxidative stress, cell differentiation, proliferation, immune response and apoptosis [288]. In our data set we find lower levels of PRDX5 (-1.77 and -2.27 fold) at the PSD of NDAN vs. AD which can potentially indicate decreased oxidative stress in the brains of these individuals [93]. PRDX5 can neutralize hydrogen peroxide, alkyl hydroperoxides and peroxynitrite [289,290] and its expression is increased during oxidative stress [291]. Peroxynitrite can alter the mitochondrial electron transport chain, therefore, efficient neutralization of peroxynitrite can be neuroprotective [291].

Conclusion

In summary, we used subcellular fractionation combined with 2DE and mass spectrometry protein identification to study the postsynaptic density proteome of the hippocampus from cognitively intact NDAN subjects in comparison to demented AD patients. We identified 15 unique proteins that set NDAN apart from AD, thus supporting the notion that NDAN individuals are distinct from both control subjects and AD patients, and should likely not be considered pre-AD. The subset of proteins identified in our study can be further investigated in order to establish the mechanisms responsible for preservation of cognitive function in NDAN despite the presence of AD pathology. Additional analysis of post-translational modifications

would be of interest as it can yield more insights into the protective mechanisms at play in NDAN, which in turn can result in development of novel therapeutic targets.

CHAPTER 4. EPIGENETIC REGULATION OF THE SYNAPTIC RESILIENCE TO AMYLOID BETA OLIGOMERS

Introduction

Stemming from our previous report describing the presence of a unique postsynaptic proteome in NDAN individuals [130], this study aimed to determine the upstream transcriptional regulators that could explain the unique protein signature at the PSDs of NDAN. We discovered three microRNAs (miRs) that are expressed at different levels in control, AD and NDAN and could be involved in providing resistance to AD-like pathology.

Alterations in miR levels have been associated with AD previously (reviewed by [164,165]) due to the link between multiple families of miRs and hallmark pathological processes in AD, as well as other neurodegenerative disorders (reviewed by [166,167]). MiRs are non-coding 18-22 nucleotide-long single-stranded RNAs that can target multiple messenger RNAs (mRNAs) via Watson-Crick base pairing, leading to their degradation or translational repression. MiRs are involved in multiple biological pathways and their expression is regulated by enzymes which process and stabilize mature miRs, or by epigenetic mechanisms such as DNA methylation or histone modifications [292]. While miRs are essential for organism development, their expression profile changes with age and they are found to be dysregulated in several diseases, including AD [159–163]. It is hypothesized that in neurodegenerative diseases, miRs can modulate the levels of toxic proteins by modulating the expression of their mRNAs or by regulating mRNA of proteins that regulate the levels of toxic proteins [293].

Therefore, in this study we tested the hypothesis that a global action of miRs allows NDAN synapses to acquire resistance to Aβ and tau oligomer binding. Using both *in vitro* and *in*

vivo approaches, we demonstrate here that these specific miRs decrease Aβ, but not tau, oligomer association with the synapses, possibly by modifying the hippocampal transcriptome.

Methods

CASE SUBJECTS

Frozen mid-hippocampus tissue was obtained from the Oregon Brain Bank at Oregon Health and Science University (OHSU) in Portland, OR. Donor subjects were enrolled and clinically evaluated in studies at the NIH-sponsored Layton Aging and AD Center (ADC) at OHSU. Subjects were participants in brain aging studies at the ADC and received annual neurological and neuropsychological evaluations, with a clinical dementia rating (CDR) assigned by an experienced clinician. Controls and NDAN had normal cognitive and functional examinations with CDR < 1. The AD subjects were diagnosed by a clinical team consensus conference, met the National Institute for Neurological and Communicative Disorders and Stroke-Alzheimer's Disease and Related Disorder Association diagnostic criteria for clinical AD, had a CDR of greater than 1.0 and neuropathologic confirmation at autopsy (after informed consent). Tissue use conformed to institutional review board-approved protocols. Neuropathologic assessment conformed to National Institute on Aging-Reagan consensus criteria. All brain tissue was examined by a neuropathologist for neurodegenerative pathology including neurofibrillary tangles and neuritic plaques. Using standardized CERAD criteria [171], cases were assigned an amyloid score based on the deposition of amyloid plaques in the brain (0 = no plaques, 1 = sparse plaques, 2 = moderate plaques and 3 = dense plaques) and a Braak stage (0–6; with 6 being the most severe) indicative of the level and location of hyperphosphorylated

tau tangles [8]. In addition to the pathological information detailed above, demographical data were received along with the frozen tissue.

RNA ISOLATION AND REAL-TIME PCR

RNA was isolated using Trizol Reagent (Life technologies, Carlsbad, CA) according to the manufacturer's protocol. Tissue was placed in Trizol and homogenized using the Polytron homogenizer (ThermoFisher Scientific, Waltham, MA). Chloroform was then added, and the samples were spun down at 12,000 rpm for 15 min at 4ºC. The aqueous phase was transferred to a new tube containing isopropanol. The samples were centrifuged at 12,000 rpm for 10 min at 4ºC. Pellet was washed with ice cold 80% ethanol and air-dried. The samples were resuspended in 40 µl nuclease free water. The RNA concentration was measured using NanoDrop 2000c (ThermoFisher Scientific, Waltham, MA).

miR qPCR: Reverse transcription was performed using miScript II RT Kit (Qiagen, Hilden, Germany) according to manufacturer's protocol. Briefly, 0.5 µg RNA was reverse-transcribed in 20 µl reaction volume containing 4 µl 5x HiSpec buffer, 2 µl 10x miScript Nucleics mix and 2 µl miScript Reverse transcriptase. The mix was incubated at 37ºC for 1 hr, then at 95ºC for 5 min and placed on ice. The reverse transcribed miR mix was diluted with nuclease free water to a final concentration of 3 ng/µl. Real-time PCR was performed to quantitate miR in control, AD and NDAN. miScript SYBR Green PCR Kit (Qiagen, Hilden, Germany) was used according to manufacturer's protocol. Briefly, the reaction was performed in 25 µl final volume in each well containing 3 ng reverse transcribed miR, 1x SYBR Green, reverse and forward primers (Qiagen, Hilden, Germany). The reaction was performed in Mastercycler epgradient S (Eppendorf, Hamburg, Germany). The samples were incubated at 95ºC for 15 min to activate the polymerase followed by 40 cycles of amplification: 94ºC for 15

sec, 55ºC for 30 sec and 70ºC for 30 sec. Standard melting curve was performed at the end. All samples were run in duplicate and levels of miRs were normalized to U6 snRNA. The relative fold change in expression of target miRs was determined using the comparative cycle threshold method ($2^{-\Delta\Delta Ct}$).

mRNA qPCR: cDNA was made using amfiRivert Platinum cDNA Synthesis Master Mix (GenDEPOT, Katy, TX) according to manufacturer's protocol. Briefly, 0.5 µg RNA was first incubated at 70ºC for 5 min and then chilled on ice. The cDNA reaction mix was prepared with the Buffer and Enzyme mixes provided in the kit. cDNA was made using the following conditions: 25ºC for 5 min, followed by incubation at 42ºC for 60 min and finally 15 min at 70ºC.

The primer sequences were obtained from the PrimerBank (pga.mgh.harvard.edu/primerbank, Harvard, Cambridge, MA) to measure expression of genes of interest. Quantitative real-time PCR (qRT-PCR) was performed to measure mRNA levels. Each well of 96-well plate for qRT-PCR contained 20 ng RNA, 1 mM oligo and 1x KAPA SYBR FAST Universal qPCR kit (KAPA Biosystems, St. Louis, MO). All samples were run in duplicate, standard melting curve was performed at the end. Measured mRNA values were normalized to the expression level of actin. The relative fold change in expression of mRNAs was determined using the comparative cycle threshold method ($2^{-\Delta\Delta Ct}$).

CELL CULTURE AND TRANSFECTION

SH-SY5Y cells (ATCC, Manassas, VA) were cultured in Eagle's minimum essential medium with non-essential acids and Ham's F12 medium and 10% FBS at 5% CO_2. The day before transfection the cells were plated in a 6-well plate at 20,000 cells/well. Selected miRs as well as negative control (ThermoFisher Scientific, Waltham, MA) were dissolved in nuclease-

free water to a final concentration of 50 µM. The transfection was performed using Lipofectamine2000 (ThermoFisher Scientific, Waltham, MA) according to manufacturer's protocol. Briefly, in separate tubes, the miRs and Lipofectamine2000 were diluted in serum-free/antibiotic-free medium and incubated at room temperature for 5 min. Diluted Lipofectamine2000 was added to each tube containing miR drop-wise, inverted several times and incubated for 20 min at room temperature to allow for complex formation. Each well received 50 nM of miR. The growth media was replaced 24 hours post-transfection. The cells were collected 48 hours post-transfection. Each well also received control siRNA tagged with FAM (ThermoFisher Scientific, Waltham, MA) to control for transfection efficiency.

Aβ OLIGOMER PREPARATION

Aβ oligomer preparation is a technique, used routinely by our laboratory [66]. Briefly, lyophilized Aβ1-42 aliquots (Department of Biophysics and Biochemistry, Yale University, New Haven, CT) were dissolved in 200 µl of 1,1,1,3,3,3-hexafluoro-2-propanol and then added to 700 µl of distilled deionized H_2O in microcentrifuge tubes. Loosely capped tubes were stirred on a magnetic stirrer in a fume hood for 48 hrs and then aliquoted and stored at -80ºC. In order to prepare labeled Aβ oligomers, a small aliquot of HiLyte^{TM} Fluor 647-labeled Aβ1-42 (AnaSpec, Fremont, CA) was added to the HFP-Aβ mix described above. Western and dot blot analysis using A-11 antibodies (Aβ oligomer specific) are used to determine the quality of oligomerization (as previously described by [28]).

EX VIVO Aβ OLIGOMER BINDING AND FLOW CYTOMETRY

The SH-SY5Y cells were lifted with 10 mM EDTA, spun down and resuspended in 3% BSA in PBS. In order to measure Aβ oligomer association with the cellular surface, the cells

were incubated with 2 μM HiLyte^{TM} Fluor 647-labeled Aβ oligomers for 30 min at room temperature in dark. To remove all unbound oligomers the cells were washed in 3% BSA in PBS by centrifugation at 1,250 x g for 5 min at 4ºC. The pellet was resuspended in 4% PF in PBS and incubated at room temperature for 10 min. The samples were then washed in PBS and resuspended in PBS without Ca^{2+}/Mg^{2+}, and analyzed using Guava easyCyte flow cytometer (MilliporeSigma, Burlington, MA). In order to assess the Aβ oligomer interaction with cellular surface those cells manifesting green fluorescence (siRNA-FAM, described above) and binding Aβ oligomers (red fluorescence) were analyzed.

To determine the amount of Aβ oligomers associated with the synaptosomes (synaptosome isolation is described below), two million synaptosomes were incubated with 2.5 μM HiLyteTM Fluor 647-labeled Aβ oligomers for 1 hr at room temperature in dark. The samples were washed three times in HBK buffer to remove all unbound Aβ oligomers and resuspended in PBS without Ca^{2+}/Mg^{2+}. The samples were analyzed using Guava easyCyte flow cytometer (MilliporeSigma, Burlington, MA). Standard size polystyrene particles (Spherotech, Inc., Lake Forest, IL) were used to set up size 1-5 μm gate for synaptosomes analyses.

ANIMALS

Eleven to thirteen weeks old wild-type male and female C57B6 mice were purchased from the Jackson Laboratory (Bar Harbor, ME). Health care for all animals was provided by the animal care specialists under a supervision of the facilities manager. The care and maintenance were provided for the animal colony on daily basis to ensure the safe and healthy environment. Each animal was used under an animal protocol approved by the Institutional Animal Care and Use Committee of the University of Texas Medical Branch, ensuring that the animals received the minimal amount of pain/discomfort. All animals were housed under USDA standards (12:12

hr light/dark cycle, food and water ad libitum) at the University of Texas Medical Branch vivarium.

ICV INJECTIONS

Male and female mice were injected intracerebroventricularly (ICV) with miRs (scrambled, 149, 485 and 4723) (ThermoFisher Scientific, Waltham, MA) dissolved in artificial cerebrospinal fluid. Seven animals per group were used.

ICV injection is a technique routinely used by our laboratory [32]. Briefly, mice were anesthetized with isoflurane. The ICV injections were performed according to the freehand injection method described by Clark *et al.* [294]. 29-gauge needle was held with hemostatic forceps to leave 4 mm of the needle tip exposed. The needle was connected to a 25 µl Hamilton syringe via 0.38 mm polyethylene tubing. The injection volume was set at 2 µl to deliver 1 nmole of miR; infusion rate was set at 1 µl/min using electronic programmable microinfuser (Harvard Apparatus, Cambridge, MA). After the injection, the needle was left in place for 1 min. The mouse was allowed to recover while lying on a heated pad under warm light. Twenty-four hours post-injection mice were euthanized by using deep anesthesia followed by cervical dislocation. Mouse brain was quickly collected and stored at -80ºC for further analysis.

ISOLATION OF SYNAPTOSOMES

Synaptosomes were isolated using Syn-PER Reagent (Thermo Fisher Scientific, Waltham, MA) according to the manufacturer's protocol. Briefly, approximately 30 mg of tissue was homogenized using Dounce glass homogenizer in presence of Halt Protease Inhibitor Cocktail (Thermo Fisher Scientific, Waltham, MA) and Phosphatase Inhibitor Cocktail (MilliporeSigma, Burlington, MA). The homogenate was spun down at 1,200 x g for 10 min at

4ºC. The supernatant was centrifuged at 15,000 x g for 20 min at 4ºC to obtain the pellet of synaptosomes. The pellet was then resuspended in HBK (HEPES-buffered Krebs-like) buffer as described before [172]. The concentration of synaptosomes was determined using flow cytometry. The samples were stored at -80ºC until use. Synaptosome preparations are routinely analyzed by Western blot and electron microscopy to ensure the quality of the preparation, as we have previously reported [172].

TAU OLIGOMER PREPARATION

Recombinant tau oligomers were prepared by Dr. Rakez Kayed's laboratory as previously described [295]. Briefly, recombinant tau monomer protein was added to PBS to obtain a concentration of 0.3 mg/ml. Aβ42 oligomer seeds were then added to the tau mixture and incubated on an orbital shaker for 1 hr at room temperature. Produced tau oligomers were used as seeds in a second batch of tau monomers to prepare a new batch of tau oligomers. This protocol was repeated three times to ensure the elimination of the original Aβ seeds resulting in the production of tau oligomers. Each batch of oligomers is tested using dot blot with T22, a tau oligomer-specific antibody, Western blot analysis and atomic force microcopy to verify the quality of tau oligomer preparation.

EX VIVO TAU OLIGOMER BINDING TO SYNAPTOSOMES

Synaptosomes were isolated from mice receiving ICV injections of miRs as described above. Ten million synaptosomes were incubated with 2 µM of tau oligomers for 1 hr at room temperature. The samples were then centrifuged and washed three times with the HBK buffer to remove any unbound tau oligomers. The concentration of synaptosomes was measured again

using flow cytometry and equal amounts of synaptosomes were analyzed by tau5 ELISA as described below.

Tau ELISA

Tau levels were measured by ELISA using the total tau antibody tau5 (Thermo Fisher Scientific, Waltham, MA). Following the *ex vivo* incubation with tau oligomers as described above, the samples were incubated at 4ºC overnight on an ELISA plate with the coating buffer 0.05 M sodium bicarbonate (pH 9.6). The plates were then washed with Tris-buffered saline with low Tween 20 (0.01%) (TBS-low T) followed by blocking with 10% nonfat milk for 2 hr at room temperature. The plates were washed one more time followed by an incubation with tau5 antibody (1:1000 in 5% nonfat milk in TBS-low T) for 1 hr at room temperature. Following a washing step, horseradish peroxidase-conjugated anti-mouse IgG (1:1000 in 5% nonfat milk in TBS-low T; MilliporeSigma, Burlington, MA) was added to the plate and incubated for 1 hr at room temperature. The plates were washed with TBS-low T and room temperature 3,3,5,5-tetramethylbenzidine (TMB-1 component substrate; MilliporeSigma, Burlington, MA) was added. After 15 min in dark, 2 M HCl was added to stop the reaction and the plate was read at 450 nm.

RNA-Seq

Library Construction and Sequencing: Quality of the purified RNA was assessed by visualization of 18S and 28S RNA bands using an Agilent BioAnalyzer 2100 (Agilent Technologies, CA); the electropherograms were used to calculate the 28S/18S ratio and the RNA Integrity Number. Poly-A+ RNA was enriched from total RNA (~1 μg) using oligo dT-attached magnetic beads. Bound RNA was fragmented by incubation at 94ºC for eight minutes in 19.5 μl

of fragmentation buffer (Illumina, San Diego, CA). First and second strand synthesis, adapter ligation and amplification of the library were performed using the Illumina TruSeq RNA Sample Preparation kit as recommended by the manufacturer (Illumina, San Diego, CA). "Index tags" incorporated into the adapters were used to track samples. Library quality was evaluated using an Agilent DNA-1000 chip on an Agilent 2100 Bioanalyzer. Quantification of library DNA templates was performed using qPCR and a known-size reference standard. Sequencing was performed by the UTMB Next Generation Sequencing Core Facility on an Illumina NextSeq 550 with 3 samples per group. Sequencing conditions were paired-end 75 base in the High-Output mode.

RNA-Seq Analysis: The alignment of NGS sequence reads to the mouse mm10 reference genome was performed using the Spliced Transcript Alignment to a Reference (STAR) program, version 2.5.4b [296], using the ENCODE standard options as recommended by the developer. The UCSC version of the mouse reference sequence and annotation files were downloaded from the iGenomes website maintained by Illumina (https://support.illumina.com/sequencing/sequencing_software/igenome.html). The "-quantMode GeneCounts" STAR option was used to count the number or reads mapping to each gene. Differential gene expression was analyzed with the program DESeq2, version 1.18.1, running in R version 3.4.3 [297]. A table of read counts per gene per sample was provided to DESeq2 and differential expression between conditions was tested using the standard analysis vignette provided by the authors.

STATISTICAL ANALYSIS

PCR data were log2 transformed before statistical analysis. The results were expressed as mean ± standard error unless otherwise noted. Data analysis was completed using GraphPad

Prism version 7.05 for Windows (GraphPad Software, La Jolla, California, www.graphpad.com). One-way or Two-way ANOVA was performed, followed by either Dunnett's or Sidak's multiple comparisons test (specified in the results). A p value of less than 0.05 was considered statistically significant.

Results

UPSTREAM REGULATORS OF POSTSYNAPTIC PROTEOME CHANGES IN NDAN

We have recently reported the unique protein signature present at the postsynaptic densities of NDAN when compared to AD and age-matched control individuals [130]. As part of these studies, we utilized a bioinformatics approach (Ingenuity Pathway Analysis, IPA) to determine the upstream regulators of the observed changes. The Upstream Regulators tool of the IPA can identify key upstream players which could drive the changes observed at the protein level. Following this approach, three miRs were identified as major drivers of the proteome changes observed at the PSDs of NDAN subjects: miR-4723, miR-149 and miR-485. Notably, a literature search revealed that these miRs are all involved in regulation of synaptic genes.

MiR-149 (Fig. 4.1A) regulates Specificity protein 1 (Sp1) [298], APP (amyloid precursor protein), BACE1 (beta-secretase 1), tau, HDAC1/2 (histone deacetylase 1 and 2), huntingtin and DNMT1 (DNA methyltransferase) [299]. MiR-485 (Fig. 4.1B) regulates the expression of BACE1, tau, dendritic spine density and number, PSD95 (postsynaptic density protein 95) clustering, surface GluR2 (glutamate receptor 2), and the miniature excitatory postsynaptic currents frequency [300–302]. MiR-4723 (Fig. 4.1C) regulates c-Abl (Abelson tyrosine-protein kinase 1) [303], which can also be regulated directly by Aβ oligomers [304]; c-Abl can regulate the expression of synaptic genes via HDAC2 [305].

94
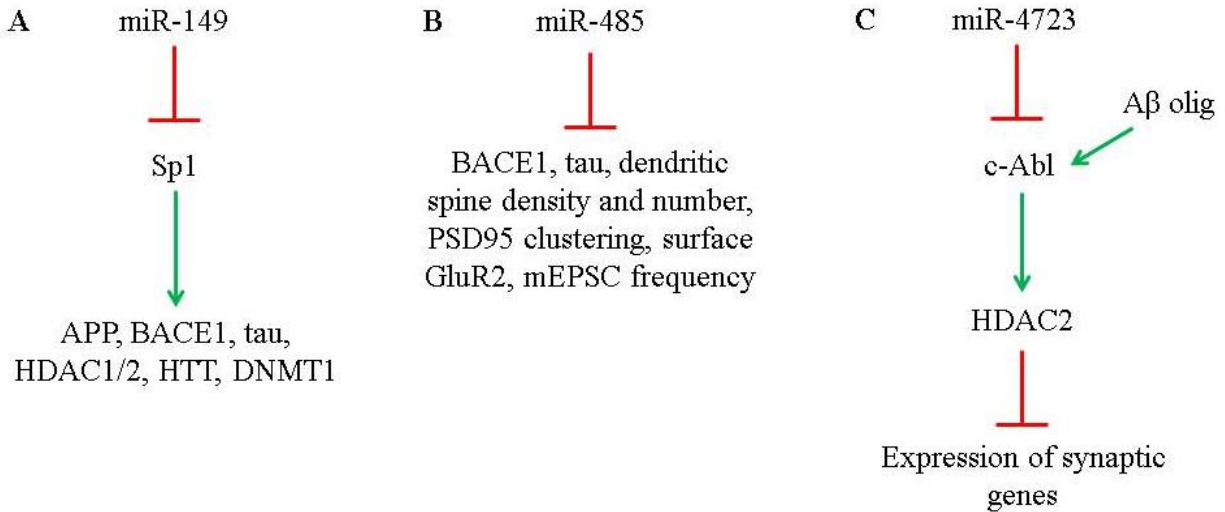
Figure 4.1. Functions of miR-149, -485 and -4723

MiR-149 (A), -485 (B) and -4723 (C) are involved in regulation of synaptic genes. Sp1 – specificity protein 1, APP – amyloid precursor protein, BACE1 – beta-secretase 1, HDAC1/2 – histone deacetylase 1/2, HTT – huntingtin, DNMT1 – DNA methyltransferase, PSD95 – postsynaptic density protein 95, GluR2 – glutamate receptor 2, mEPSC – miniature excitatory postsynaptic currents, c-Abl - Abelson tyrosine-protein kinase 1. References are provided in text.

Next, we isolated RNA from post-mortem hippocampi and frontal cortices of control, AD and NDAN to determine the levels of these three miRs (case subject data is provided in Table 4.1). We found that, as predicted by the IPA, the three miRs are indeed differentially regulated in both hippocampus and frontal cortex of AD and NDAN when compared to control subjects (Fig. 4.2). Interestingly, in AD hippocampus miR-4723 was significantly decreased (Fig. 4.2A), while in the frontal cortex it was below detection limit when compared to control (Fig. 4.2B). In the frontal cortex, miR-149 and miR-485 were significantly upregulated in AD when compared to control (Fig. 4.2B). NDAN, on the other hand, had a non-significant trend towards reduction of the three miRs in hippocampus and frontal cortex when compared to control (Fig. 4.2). These results suggest that the three miRs may play a role in the progression of AD and can potentially

be one of the mechanisms providing resistance to clinical manifestation of the disease for some individuals.
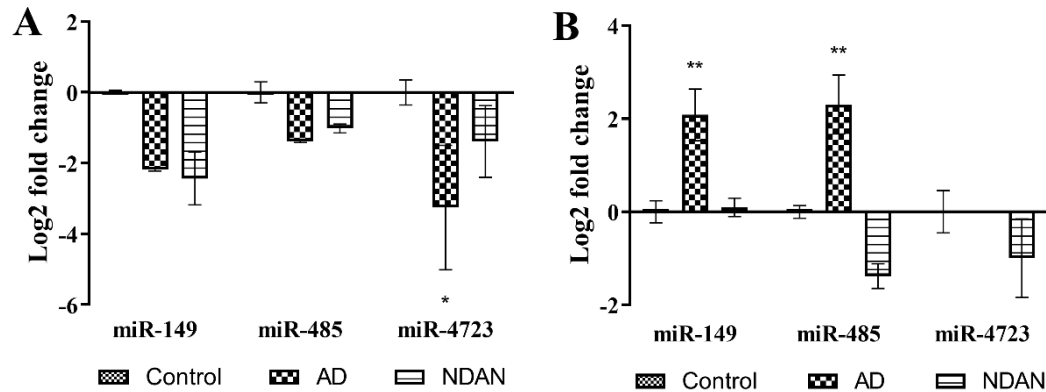
Figure 4.2. MiR levels in hippocampus of control, AD and NDAN

IPA-predicted miR-149, -485 and -4723 are differentially regulated in post-mortem hippocampi (A) and frontal cortices (B) of AD and NDAN when compared to control, which is set at zero. MiR-4723 was below detection limit in AD frontal cortex. Measured miR values were normalized to the expression level of U6. Values represent the means ± SEM. n=4 frontal cortex, n=3 hippocampus. *, $p < 0.05$ and **, $p < 0.01$ vs. control, Two-way ANOVA, followed by Dunnett's multiple comparisons test.

Table 4.1:   Demographic data of the cases used to validate IPA predictions

PMI – post-mortem interval, FC – frontal cortex, H – hippocampus.

Case number	Diagnosis	Brain region analyzed	Age, years	Sex	PMI, hours	Braak stage
767	Control	FC	86	F	8	2
785	Control	FC	83	M	14	1
1957	Control	H	>89	F	8	4
1965	Control	H	>89	F	5.5	2
1977	Control	FC	>89	F	4	4
2229	Control	FC, H	71	F	14.5	2
1969	AD	FC, H	67	F	13	6
2010	AD	FC, H	87	F	6	3
2305	AD	FC, H	85	F	5	6
2318	AD	FC	74	F	2	6
697	NDAN	FC, H	>89	M	5	5
1016	NDAN	FC	>89	F	8	6

Case number	Diagnosis	Brain region analyzed	Age, years	Sex	PMI, hours	Braak stage
1179	NDAN	FC, H	89	F	2.5	5
1284	NDAN	FC	>89	M	72	5
1362	NDAN	H	>89	F	48	4

Aβ OLIGOMER BINDING TO THE SURFACE OF SH-SY5Y

We then tested whether these three miRs had an effect on Aβ oligomer binding to neuronal cells *in vitro*. We utilized SH-SY5Y cells, a human neuroblastoma cell line, which expresses immature neuronal markers [306]. Cells were transfected with the miRs and 48 hours later collected with 10 mM EDTA (to preserve membrane proteins) and then challenged with 2 μM HiLyteTM Fluor 647-labeled Aβ oligomers *ex vivo*. The cells were also co-transfected with FAM-labeled control siRNA to allow for measurement of Aβ binding only in miR-transfected cells (Suppl. fig. 4.1D-F). The Aβ oligomer binding to the cellular surface was assessed by flow cytometry analysis (Fig. 4.3). Representative flow cytometry acquisitions are provided in Suppl. fig. 4.1. Treatment with miR-485 and miR-4723 resulted in a significantly decreased amount of Aβ oligomers associated with the SH-SY5Y surface, while the transfection with miR-149 had no effect on sensitivity to Aβ oligomers. These results suggest that miR-485 and miR-4723 promote resilience to Aβ oligomer binding in SH-SY5Y.
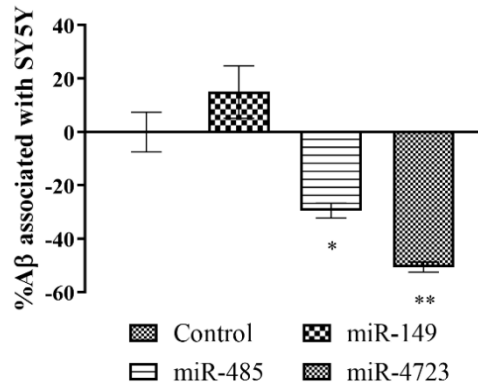
Figure 4.3. HiLyteTM Fluor 647-labeled Aβ oligomers interact with the surface of SH-SY5Y cells transfected with miR-149, -485 and -4723

MiR-transfected SH-SY5Y were incubated with 2 μM tagged Aβ oligomers and analyzed using flow cytometry. SH-SY5Y cells were transfected with scrambled miR as a control; levels of Aβ binding to the scrambled-transfected cells were set at zero. Values represent the means ± SEM. n=3. *, $p < 0.05$ and **, $p < 0.01$ vs. control, One-way ANOVA, followed by Dunnett's multiple comparisons test.

EFFECT OF MIRS ON Aβ AND TAU OLIGOMER BINDING TO SYNAPTOSOMES

The results of our experiments in SH-SY5Y human neuroblastoma cells suggested that miRs are capable of providing resistance to Aβ oligomers *in vitro*, therefore, we aimed to test their effect *in vivo*. In addition to Aβ oligomers, we have also determined binding of tau oligomers to synaptic terminals since recent reports suggest that also tau oligomers bind to synapses where they play a critical role in synaptic dysfunction [51]. In order to determine if the *in vivo* administration of these miRs had an effect on Aβ and tau oligomer binding to the synapses, wild-type C57BL/6 male and female mice received a single ICV injection of the selected miRs. Scrambled miR was injected as a control. At 24 hours post-injection, the hippocampi and frontal cortices were collected for analysis, and synaptosomes were isolated. Synaptosomes were challenged *ex vivo* with either 2.5 μm Aβ or 2 μm tau oligomers as described

in the Methods section. Flow cytometry was used to assess the Aβ binding and ELISA was used for tau oligomers.

In order to analyze synaptosomes using flow cytometry, the 2, 3, 5 and 7 μm standard size beads were used to set up the flow gates. Representative acquisitions are provided in the Suppl. fig. 4.2. The gate was set up to include ~1-5 μm particles, which is the typical size of synaptosomes, as previously described by others [307,308]. When we analyzed the Aβ binding to the synaptosomes isolated from female hippocampi and frontal cortices (Fig. 4.4A), we observed that injection of the selected miRs *in vivo* resulted in significantly decreased binding after treatment with miR-149 and miR-4723 only in the hippocampus. Synaptosomes isolated from the frontal cortex of females, on the other hand, had unaltered Aβ oligomer binding after treatment with miR-149 or miR-4723 when compared to scrambled miR (Fig. 4.4A). MiR-485 had no effect on Aβ binding in neither region analyzed. In contrast to females, males responded to treatments with miR-149 and miR-485 by significantly lower amounts of Aβ bound to the synaptosomes isolated from frontal cortex (Fig. 4.4B). A significant decrease in binding to hippocampal synaptosomes was seen only for miR-149 (Fig. 4.4B). MiR-4723 had no significant effect on the ability of male synaptosomes to bind Aβ oligomers.

When we analyzed tau oligomer binding to the synaptosomes, isolated from male and female frontal cortex and hippocampus, we observed a decreased binding in female hippocampi after treatment with miR-485 (Fig. 4.4C). In frontal cortex of males, miR-4723 increased the sensitivity of synaptosomes to tau (Fig. 4.4D) resulting in more binding. Other miRs had no significant effect on the amount of tau oligomers bounds to the synaptosomes (Fig. 4.4C, D). Collectively, our results suggest that these selected miRs are more potent at modulating Aβ, but not tau, oligomer binding to the synaptosomes.
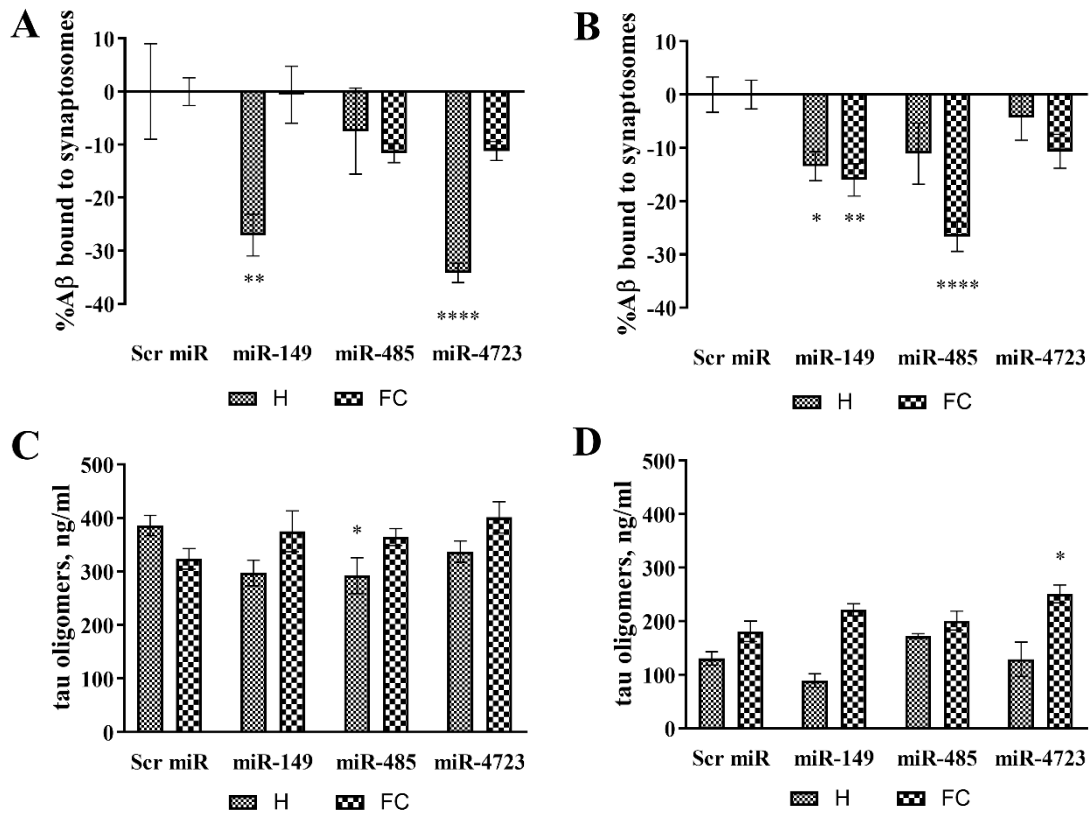
Figure 4.4. Aβ and tau oligomer binding to synaptosomes in mice after ICV treatment with miR-149, -485 and -4723

Female (A, C) and male (B, D) mice were injected ICV with the selected miRs, scrambled miR was used as control. (A, B) Synaptosomes were isolated from hippocampi and frontal cortices and incubated *ex vivo* with 2.5 μM tagged Aβ oligomers and analyzed using flow cytometry. Levels of binding to scrambled-injected mice were set at zero. n=7. (C, D) Synaptosomes were incubated *ex vivo* with 2 μM tau oligomers and analyzed using ELISA. n=4. Values represent the means ± SEM. *, $p<0.05$; **, $p<0.01$ and ****, $p<0.0001$ vs. scrambled miR, Two-way ANOVA, followed by Dunnett's multiple comparisons test.

HIPPOCAMPAL TRANSCRIPTOME CHANGES IN RESPONSE TO MIRS

Since we observed significant changes in Aβ binding to the synaptosomes isolated from hippocampi of miR-treated female mice (Fig. 4.4A), we decided to perform RNA-Seq to determine potential mechanisms providing resistance to Aβ oligomer binding in these mice. RNA-Seq was performed on three samples from each group and all readings were normalized to the scrambled miR-injected group. For the analysis, mRNAs were selected using the following

criteria: log2 fold change ≥ ±1, p-value < 0.05, FDR < 0.05. When we analyzed the hippocampal transcriptome of miR-treated female mice, we noticed small degree of overlap in the mRNA changes evoked by treatment with the different miRs (Fig. 4.5). Only seven genes were modified by all three miRs, additional 59 were common to miR-149 and miR-485, 98 – shared by miR-149 and miR-4723. Interestingly, miR-4723 altered only 110 genes, while miR-149 engaged 1020 genes, and miR-485 – 738 genes total (Suppl. table 4.1).
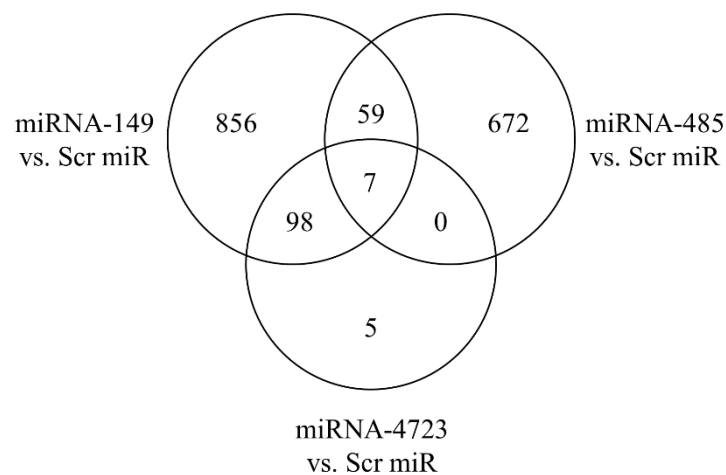
Figure 4.5. Changes in the female hippocampal transcriptome after treament with miR-149, miR-485 and miR-4723

mRNA changes in the hippocampi of miR-treated females were normalized to mice injected with scrambled miR. The Venn diagram shows an overlap in mRNA changes between three miR treatments. n=3 mice/group. The Venn diagram was built using the online Venny tool [309].

When the hippocampal transcriptome was evaluated using PANTHER, we noticed that even though the exact genes modified by the individual miRs were mostly different (Fig. 4.5), overall, the three treatments had some similarities when the mRNA changes were analyzed by the biological process and molecular function (Fig. 4.6A and B, respectively). The number of genes in each category is provided in Suppl. table 4.2 and 4.3. According to this analysis, mRNAs that changed in response to each miR treatment represent several biological processes

(Fig. 4.6A), however, four major categories shared by all miRs can be appreciated: biological regulation, cellular process, metabolic process, and response to stimulus. Binding and catalytic activity were the most common functional categories identified by those mRNAs as can be seen in Fig. 4.6B, followed by receptor activity and transporter activity.
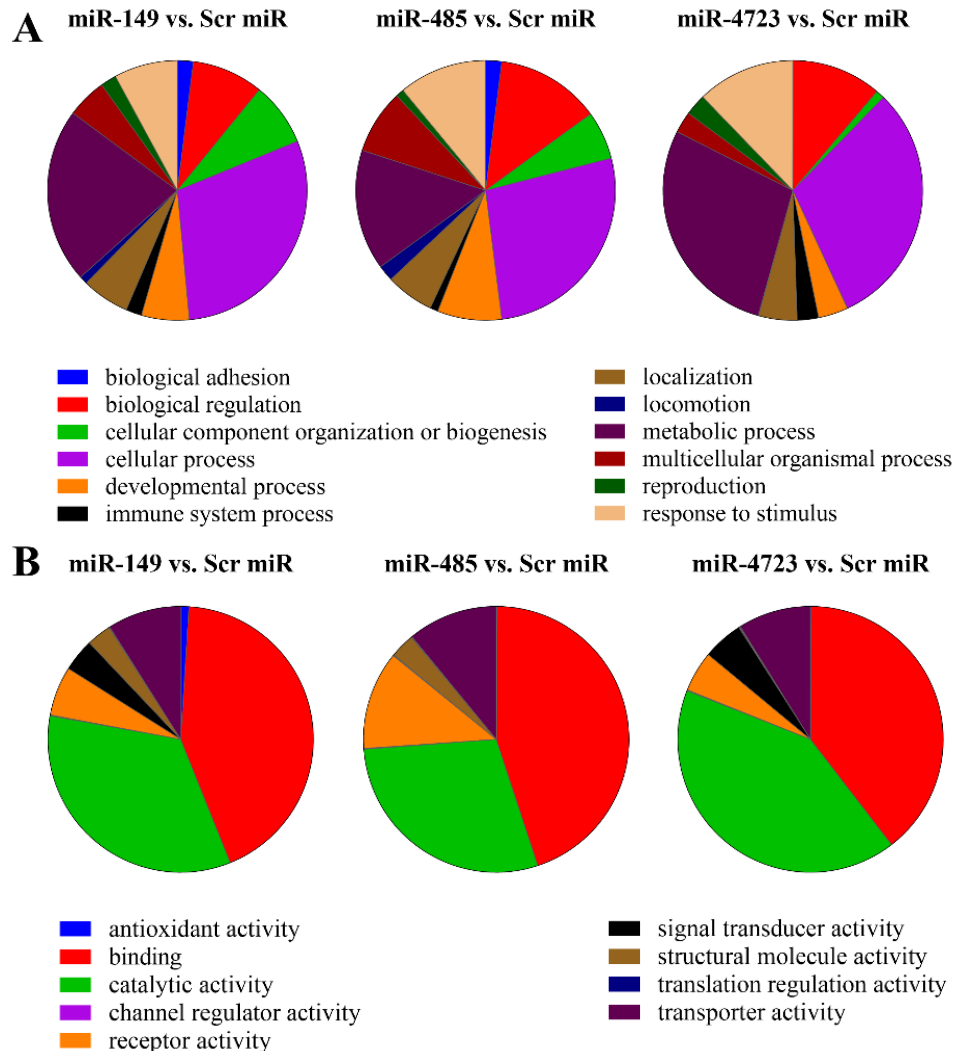
Figure 4.6. Female hippocampal transcriptome analyzed with PANTHER

PANTHER [186,187] was used to analyze the biological processes (A) and molecular functions (B) of mRNAs changed after female mice were treated ICV with miR-149, miR-485 and miR-4723. Changes in miR-treated animals were normalized to mice injected with scrambled miR. Three miR treatments activate similar biological processes and perform analogous molecular functions.

In order to validate the RNA-Seq results, several mRNAs were selected (Table 4.2). The validation was performed on an independent set of animals that were not used in the RNA-Seq experiment. Three mRNAs per treatment were selected to include at least one upregulated and one downregulated gene in each treatment. Clic6 was significantly upregulated after miR-149 and miR-485 treatment in the RNA-Seq dataset (4.59 and 4.2 log2 fold, respectively), while Snhg11 was downregulated by miR-149 and miR-4723 (-2.8 and -1.32 log2 fold, respectively). Rreb1 was downregulated by miR-149 (-2.4), Pcdh20 and Syt17 were downregulated by miR-485 (-1.7 and -1.54, respectively), and miR-4723 treatment resulted in upregulation of Ttr (5.53) and downregulation of Meg3 (-1.52).

Table 4.2:   mRNAs selected for validation from the RNA-Seq dataset
mRNA descriptions were obtained from the NCBI Gene database.

miR	mRNA	Log2 fold change in RNA-Seq	Brief description of mRNA
149	Snhg11	-2.8	Small nucleolar RNA host gene 11, non-coding RNA
	Rreb1	-2.4	Ras responsive element binding protein 1, protein coding
	Clic6	4.59	Chloride intracellular channel 6, protein coding
485	Clic6	4.2	Chloride intracellular channel 6, protein coding
	Pcdh20	-1.7	Protocadherin 20, protein coding
	Syt17	-1.54	Synaptotagmin XVII, protein coding
4723	Snhg11	-1.32	Small nucleolar RNA host gene 11, non-coding RNA
	Ttr	5.53	Transthyretin, protein coding
	Meg3	-1.52	Maternally expressed 3, non-coding RNA

The validation of the RNA-Seq results was done using qRT-PCR (Fig. 4.7). All mRNAs measured had the same direction of change in the qRT-PCR validation as they did in the RNA-

Seq, however, only the increase in Clic6 reached statistical significance (as measured by qRT-PCR) after treatment with miR-149 and miR-485 (Fig. 4.7A, B). Snhg11 and Rreb1 had a trend of decrease after miR-149 treatment (Fig.4.7A), and Pcdh20 and Syt17 demonstrated a trend to decrease in response to miR-485 (Fig.4.7B). Three selected targets of miR-4723 reached statistical significance during validation, Ttr was significantly upregulated, while Snhg11 and Meg3 were significantly downregulated (Fig.4.7C).
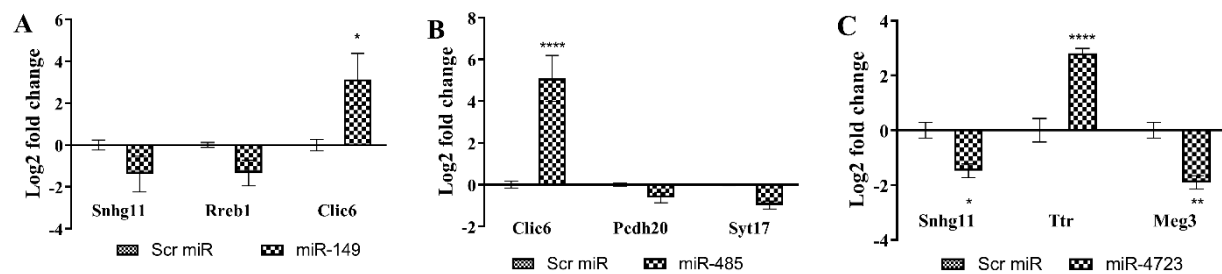
Figure 4.7. Real-time PCR of selected mRNAs to validate the RNA-Seq results

Three genes per miR treatment were selected from the RNA-Seq dataset to be validated using real-time qPCR in hippocampi obtained from female mice treated with miR-149 (A), miR-485 (B) and miR-4723 (C). The validation was performed on a different set of mice that were not used in RNA-Seq. Mice treated with scrambled miR were used as a control and set at zero. Measured mRNA levels were normalized to the expression level of actin. Values represent the means ± SEM. n=3. *, $p<0.05$; **, $p<0.01$; ****, $p<0.0001$ vs. scrambled miR, Two-way ANOVA, followed by Sidak's multiple comparisons test.

In summary, hippocampal transcriptome changes observed in female mice suggest that although each miR treatment engages a different set of mRNAs, overall the changes could be classified into four main biological processes (biological regulation, cellular process, metabolic process, and response to stimulus). Additionally, most of the mRNAs affected by the three miR examined here are involved in binding and catalytic activity.

EXPRESSION LEVELS OF SYNAPTIC GENES AFTER MIR TREATMENT

While the RNA-Seq experiment for male hippocampi is in progress, we decided to use qRT-PCR to determine the levels of several synaptic genes. It is well-documented that Aβ oligomers cause synaptic dysfunction (reviewed by [34]), moreover, Aβ oligomers have multiple docking partners at synaptic terminals [29]. In the present study we have observed decreased Aβ oligomer binding to the synapses after administration of miRs, which then led us to question if these miRs modify genes related to the synaptic function. In order to determine whether this was indeed the case, we measured the levels of several synaptic genes in the hippocampus of mice injected ICV with miR-149, miR-485 and miR-4723 as compared to control mice injected with the scrambled RNA (Suppl. table 4.4). Twelve genes were selected and quantified using qRT-PCR in male hippocampi (Fig. 4.8). Interestingly, miR-485 upregulated the levels of selected genes, in particular, App, Syn1, Ppp3ca, Mapt, Snap25 and Snca, which were significantly increased compared to control. MiR-4723 had an inhibitory effect overall, which can be seen in Fig. 4.8 by the decreased expression of Vamp2, Syn1, Bace1, Dnm1, Mapt, Snap25 and Snca. App was the only gene that was significantly upregulated by miR-4723. Treatment with miR-149 did not result in any significant changes in the levels of selected mRNAs with the exception of Creb1 upregulation. These results indicate that the three miRs in our study target different genes, which could potentially translate into different degree of protection against Aβ oligomer binding.
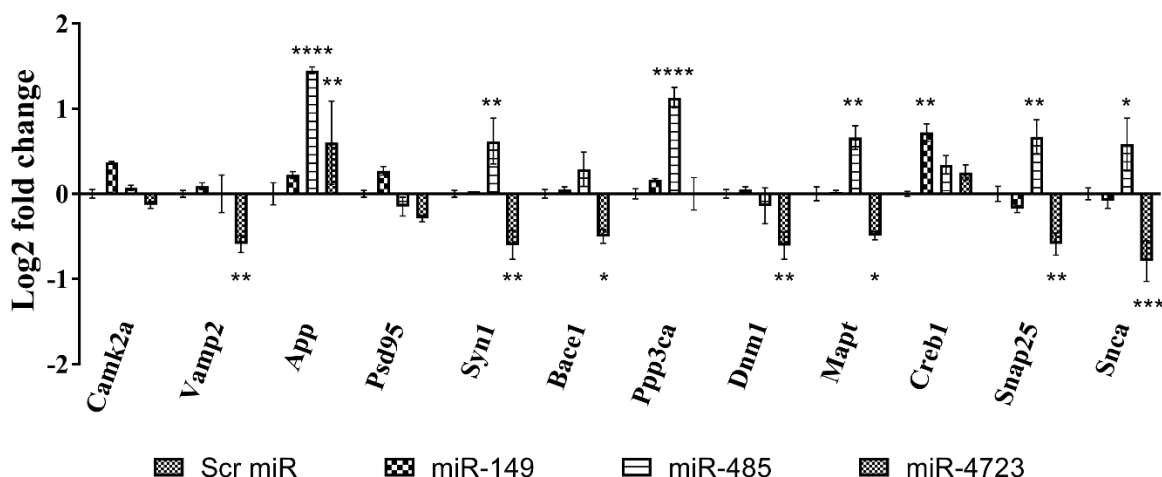
Figure 4.8. Expression of synaptic genes in male hippocampi after treatment with miR-149, miR-485 and miR-4723

Several genes involved in synaptic function were assessed using qRT-PCR in hippocampi obtained from male mice treated with miRs. Mice treated with scrambled miR were used as a control and set at zero. Measured mRNA levels were normalized to the expression level of actin. Values represent the means ± SEM. n=3. *, $p<0.05$; **, $p<0.01$; ***, $p<0.001$; ****, $p<0.0001$ vs. scrambled miR, Two-way ANOVA, followed by Dunnett's multiple comparisons test.

Discussion

MiRs are extremely potent molecules, regulating thousands of genes and hundreds of networks, known to be involved in multiple stages of AD pathogenesis ([159–163], reviewed by [164–167]). Here, we focused on three miRs that were selected based on the analysis of the postsynaptic density proteome of NDAN vs. AD and healthy age-matched control individuals [130]. MiR-149, miR-485 and miR-4723 were identified by IPA as the drivers of differential protein expression at the PSDs of NDAN vs. AD, previously reported by our group [130]. Interestingly, these miRs predicted by IPA are all involved in the regulation of synaptic genes [299–302,305].

We show that while all these miRs were decreased in the hippocampus of AD patients, in frontal cortex from the same patients miR-149 and miR-485 were increased, whereas miR-4723 was found below detection limit. On the other hand, in NDAN all three miRs were decreased in both the hippocampus and frontal cortex as compared to control subjects. Hence, the IPA-predicted miRs, involved in regulation of synaptic genes, are differentially expressed in post-mortem human frontal cortices and hippocampi of control, AD and NDAN, thus suggesting that these miRs could potentially be involved in providing synaptic resilience against Aβ oligomers as seen in NDAN individuals [66].

Aβ oligomers are known to disrupt integrity of synapses [32,310], and multiple miRs have been reported to play key roles in synaptic function and plasticity (*i.e.* miR-9, -132, -134, -138, -125 and other) (reviewed by [311–314]). MiRs are capable of regulating both functional and structural plasticity at the synapse, thus impacting neural development, physiological function, and possibly disease pathogenesis. Moreover, an interplay between Aβ oligomers and miRs has been described; for instance, Schonrock *et al*. showed that 47% of all miRs they have tested were rapidly downregulated after treatment with Aβ oligomers [315]. Similar to this published evidence, in our study we observed a downregulation of endogenous miR-149, miR-485 and miR-4723 after treatment with Aβ oligomers in SH-SY5Y cells (data not shown). It is then tempting to speculate that the balance and fine regulation of miR levels are important factors that can provide resistance or increased sensitivity of synapses to Aβ oligomers. Consistent with this view, we found reduced binding of Aβ oligomers to the cellular surface of cultured human SH-SY5Y neuroblastoma when the cells were treated with miR-485 and miR-4723, although miR-149 was not effective.

Most importantly, we observed a similar resilience to Aβ oligomers when wild-type mice received these miRs ICV. A significant reduction of Aβ oligomer binding to synaptosomes isolated from hippocampi and frontal cortices of miR-treated mice was detected, and such effects appeared to be sex-dependent. MiR-485 was more potent at providing protection against Aβ oligomers in males, while miR-4723 treatment resulted in less binding in females. Surprisingly, despite miR-149 effectiveness in male hippocampus and frontal cortex, in females it provided protection against Aβ oligomers only in the hippocampus. Furthermore, in females, the hippocampus appeared to be more responsive/sensitive to alterations in miRs, while in males this was true for the frontal cortex. On the other hand, treatment with miR-485 in females and miR-4723 in males did not cause any significant changes in Aβ oligomer synaptic binding when compared to control.

Our data show that all three miRs were more efficient in providing protection of synapses against Aβ vs. tau oligomers. Only miR-485 treatment resulted in decreased tau oligomer binding in female hippocampi, while other miRs did not cause any significant changes. Males, on the other hand, did not benefit from the selected miRs, whereas in the frontal cortex miR-4723 even resulted in significantly increased tau oligomer binding to the synaptic terminals, and for other miRs a trend towards increased binding was observed.

In order to understand the mechanisms behind the protection against Aβ oligomers provided by these miRs, we performed deep RNA sequencing to determine overall mRNA network changes after treatments with miR-149, miR-485 or miR-4723. We elected to perform this experiment in female hippocampi since stronger responses to miRs were observed in females when compared to males (reduction in binding up to 34% vs. 13%, respectively). Using this approach we found that each of these miRs modifies a distinct set of mRNAs and, as a result,

there was a very small overlap between the three miRs – only seven protein coding genes. Nevertheless, when each miR treatment was analyzed individually using PANTHER, we noticed that each of three miRs evoked similar biological processes. Specifically, the transcription changes induced by each miR fell into the following categories: biological regulation, cellular process, metabolic process and response to stimulus. Surprisingly, when the same transcriptome changes were analyzed on the basis of the molecular function, the majority of the mRNAs collectively modified by the miR treatments converged onto binding and catalytic functions in addition to a small fraction of receptor activity-related mRNAs.

It is important to emphasize here that the miR-149, miR-485 and miR-4723 engage mRNAs involved in binding, catalytic function and receptor activity in hippocampus, as discussed above, since these miRs were identified based on the unique hippocampal postsynaptic proteome of NDAN individuals [130] as potential upstream modifiers of synaptic resilience to amyloid oligomers. In fact, when applied *in vivo*, these three miRs can provide protection against Aβ oligomers, which could then suggest that the resistance to Aβ oligomers is in tight relationship with the miR homeostasis. Thus, Aβ oligomers, miR levels and synaptic plasticity appear to be intimately interconnected and possibly dependent on each other. While synaptic activity stimulates the production of Aβ (reviewed by [310]), Aβ oligomers can affect miR homeostasis. In turn, while miRs are known to be also regulated by neuronal activity (reviewed by [311]), synaptic plasticity is highly dependent on proper levels of critical miRs.

We have performed RNA-Seq only on female hippocampi. It would be interesting to determine whether or not similar pathways and processes are modulated in response to miR treatments in males. While the RNA-Seq for male hippocampi is awaiting, qRT-PCR was used to measure a limited set of mRNAs that are either relevant to synaptic function [310,316–318], are

known docking sites of Aβ oligomers [29], or are predicted targets of our miRs (miRWalk database [319,320]). We found that overall miR-485 upregulated the synaptic genes measured, including App, Syn1, Ppp3ca, Mapt, Snap25 and Snca. MiR-4723 downregulated Vamp2, Syn1, Bace1, Dnm1, Mapt, Snap25 and Snca, however, App was increased after treatment with this miR. MiR-149 did not significantly alter the levels of selected genes with the exception of Creb1. Thus, two out of the three miRs engaged with the selected synaptic mRNA in the male hippocampus, resulting either in their up- or downregulation. In fact, it has been previously documented that the effect of individual miR on its target mRNA can be quite small (up to two fold, as seen in our results), but network misregulation in response to miR treatment could reveal effects of greater magnitude (reviewed by [165]). This suggests that analysis of global network responses to miRs can provide more insights into the mechanisms behind a particular functional phenomenon, as shown above for RNA-Seq analysis of female hippocampi. Additionally, more information could be obtained if individual cellular compartments are analyzed since miRs were shown to play distinct roles in cytoplasm vs. nucleus where they can inhibit or activate their target genes (reviewed by [321]). Importantly, miR:mRNA interaction, as well as miR homeostasis, have multiple levels of regulation. Thus, most frequently miR binds to mRNA in the 3'UTR or coding region, but interactions in non-canonical sites are often observed as well resulting in varying degree of up- or downregulation of mRNA [322]. Additionally, the half-life of miRs, as well as their turnover, varies from 1 to more than 24 hours [311,323], which indicates that miRs are very carefully regulated potent molecules that can profoundly alter gene expression.

The complexity of miR-driven gene regulation in various cellular compartments in addition to different degree of up- or downregulation provided by these small potent molecules

infers that even modest alterations in miR homeostasis could be detrimental to the organism. However, it remains unclear if dysregulation of miR levels is a cause or a consequence of the disease state. Nonetheless, while more research needs to be done to determine the exact miR targets and study pathways evoked by application of miRs, in this work we presented strong evidence of reduced Aβ oligomer binding to the synaptic terminals in response to treatment with selected miRs that could be involved in modulation of synaptic resilience to AD neuropathology in NDAN individuals.

Conclusion

In the present work, we focused on three miRs that were predicted to be upstream drivers of the changes of the postsynaptic proteome that we previously reported in non-demented individuals with AD-like neuropathology who have synapses resilient to the detrimental binding of amyloid oligomers. We found that, although with varying efficiency, all three miRs (miR-149, -485 and -4723) were capable of increasing synapse resilience to Aβ oligomers and, to a much lesser extent, tau oligomers, when delivered *in vivo* ICV in adult mice, possibly via modulating the expression of key synaptic mRNAs. Interestingly, we found these protective effects to be brain region- and sex-dependent. While to the best of our knowledge this is the first evidence of synaptic resilience to oligomers regulated by selected miRs, these results further emphasize the importance of studying the role of miRs in the AD pathology with due attention to the sex-specific differences.

CHAPTER 5. SUMMARY AND CONCLUSIONS

Alzheimer's Disease affects millions of Americans, which includes over 5.7 million currently living with this detrimental disease, but also over 16 million people who are providing care for the people diagnosed with AD or other dementia [1]. Despite the discovery of this "peculiar severe disease process of the cerebral cortex" by Alois Alzheimer over a century ago [324], there are more questions than answers.

While there is no question that a significant progress has been made in our understanding of the clinical and pathological features of AD, there is still no effective cure. Many clinical trials have been conducted, but they have all failed. The failure of these trials may be due, at least in part, to how little we still know about the disease, thus strongly pointing towards a need of deeper understanding of the molecular aspects of AD.

Since the first AD clinical trial by Pfizer in 1987 [325], over 400 clinical trials have been attempted and many are currently ongoing. From some of the clinical trials, it was concluded that plaques and tangles are not the best therapeutic targets, and in fact, targeting plaques and tangles might actually make the disease worse. Additionally, clinicians and researchers have also concluded that the therapeutic timing was not ideal, and that most of the attempts to treat AD were made when it's already too late, when the irreversible damage had already taken place and the therapeutic window opportunity might have already passed. One of the main remaining questions is how can AD be diagnosed early enough for the therapies to be effective or at least have a chance at success?

The research effort to identify reliable and clinically valuable AD biomarkers is very active with more than 11,000 articles currently published [PubMed assessed 10/10/18

"biomarker   Alzheimer's",   11062   articles.   Retrieved   from www.ncbi.nlm.nih.gov/pubmed/?term=biomarker+alzheimer%27s]. Nevertheless, there are still no proven biomarkers that have been identified to early diagnose or predict later development of AD. Some individuals (~5% of all AD cases) do have a genetic predisposition to AD and this can be predicted through family history or by genetic testing. However, knowledge of genetic risk factors in familial AD has not translated into understanding of the mechanisms, thus allowing to effectively treat or even slow down the progression to the diseased state. In fact, the genetic risk factors result in an even earlier age of onset of the disease (~50 years of age for familial AD compared to ~65 years for sporadic AD). Despite such knowledge, there are still no effective treatments for familial or sporadic AD.

Furthermore, imaging approaches presently used to measure the load of pathologic proteins in humans cannot be used to predict the progression of the disease in the absence of clinical symptoms (*i.e.* cognitive impairments), since, as extensively discussed in the present dissertation, a huge percentage of people (up to 60% according to some studies) accumulate amyloid plaques and NFTs without developing cognitive decline. To some extent, these observations have hampered the advancement of our understanding due to the ongoing debate of their importance in the progression of the cognitive decline. It is therefore important to investigate what are the early events or the upstream factors that contribute to the disease onset and define the progression to neurodegenerative state. These questions can be addressed using a group of individuals that show cognitive resilience to the amyloidogenic protein loads.

Since these pathology-resistant individuals were first described, they have been referred to by a variety of names including "high pathology controls", "cognitively successful aging", "pathological aging", "asymptomatic AD", "resilient AD", etc. As a result, the lack of consistent

nomenclature, unfortunately, created difficulties assessing the results of multiple studies involving these dementia-resistant individuals. Additionally, a school of thought proposes that NDAN (as we refer to them), could have developed dementia if they had lived long enough. Nevertheless, a fact that cannot be overlooked is that the onset of the sporadic disease at ~65 years of age does not occur among these individuals since they demonstrate no cognitive decline during their life (average age at death being around 90 years old in our sample set). Even if NDAN individuals might have developed dementia if they had lived longer than 90 years of age, we can still investigate which compensatory processes or factors are responsible for this delay of disease onset. Furthermore, if the mechanism of resilience to dementia present in NDAN is elucidated, this could lead to the development of an effective therapy that could potentially provide protection against cognitive decline in anyone manifesting AD neuropathology. Thus, our approach has a potential to contribute towards the development of therapies that could save billions of dollars in health care related costs and improve the quality of life for millions of people.

For my dissertation work, I studied the NDAN individuals who are naturally resistant to cognitive impairments, aiming to understand what makes them resilient to AD neuropathology in order to aid the future development of effective therapeutics for AD. Multiple protective mechanisms allowing NDAN individuals to escape dementia have been proposed (some are discussed in Chapter 2). Several years ago, our laboratory was among the first to describe that the synapses of NDAN are capable of rejecting the attack of Aβ oligomers [66] and, therefore, I hypothesized that the postsynaptic density of NDAN subjects has a unique protein signature that protects synapses from detrimental binding of amyloid oligomers. To test this hypothesis, I took a proteomic approach to compare the postsynaptic density proteins of NDAN, AD, and healthy

age-matched controls (Chapter 3). I discovered that NDAN PSDs have 15 unique proteins that set them apart from AD. Furthermore, I determined that this unique proteomic signature was driven by three specific miRs (miR-149, miR-485 and miR-4723), which, according to the literature, are involved in the regulation of synaptic genes. This was exciting since it opened additional avenues for research in the previously uncharted field of miR-driven resistance to amyloid toxicity, and thus allowed me to design essential experiments to test the role of these miRs *in vitro* and *in vivo*.

Hence, I further proposed that the global action of selected miRs allows NDAN synapses to acquire resistance to Aβ oligomer binding and toxicity via modulation of the PSD proteome. When I tested these miRs *in vitro* (SH-SY5Y neuroblastoma cells) and *in vivo* (wild-type mice), I observed protection against Aβ oligomer binding (Chapter 4). Importantly, *in vivo* I found brain region and sex-specific effects driven by these miRs. The brain-region differences that I described here are consistent with what has been found by others (reviewed by [165]); however, the sex-specific sensitivity to Aβ oligomer binding and miR treatments are novel observations. Thus, as a result of treatment with the three miRs, synaptic terminals of female hippocampi were more resistant to Aβ oligomers than male hippocampi, while male frontal cortices were more resilient vs. female frontal cortices. Surprisingly, there was not much improvement in tau binding overall, and in males it was quite the opposite – tau sensitivity had a trend towards increased binding, although this was not statistically significant. Overall, these results suggest that miR-149, miR-485 and miR-4723 are more efficient at protecting against Aβ oligomer binding rather than tau binding. Thus, my work is pioneering the use of miRs as potential therapeutic targets to provide resistance to Aβ oligomers at the synaptic terminals. Furthermore, the sex-specific differences described in this dissertation highlight the importance of including (whenever

possible) both males and females in the preclinical research, since determining the inherent differences between two sexes could help guide the development of clinical trials. Below I provide some additional thoughts on potential future directions for continuation of the work described in this dissertation, and at the end of discussion – more on sex-dependent responses in AD.

In Chapter 4, I have shown that in response to miR-149, miR-485 or miR-4723 the hippocampal transcriptome of female mice is significantly changed. It would be interesting to compare those changes to males, and potentially look at different brain regions. Since each miR can target hundreds of genes, thus engaging multiple networks simultaneously, it might be risky to use miRs directly as a therapy due to potential side effects. Consequently, more specialized targets will need to be elucidated in order to develop novel therapeutic approaches. One approach to identify such targets would be to investigate transcriptional changes among the Aβ resilient groups to identify molecular "hubs" that are engaged in response to miRs and could play a role in the Aβ resistance.

Furthermore, the testing of the three miRs can be performed in a transgenic mouse model of AD, where the effects of the three miRs (individually or in combination) could be evaluated at different pathologic states to potentially determine the optimal intervention window. Moreover, using an animal model of AD could potentially help determine if the misregulation of the miRs is driving the AD pathology, or if the levels of miRs are altered as a consequence of the disease onset. This information would be critical as it could guide future studies pursuing the development of therapeutic approaches, but also serve as a possible avenue for biomarker development utilizing miRs.

Further work is necessary to fully understand the molecular mechanisms of resilience to amyloid pathology. My research has opened new possibilities for future studies of resilience to AD-like pathology that could help determine important molecules and potentially identify specific gene networks targeted by these miRs. One of these research possibilities would be to determine the PSD proteome changes evoked by the three miRs in an animal model and compare those to the unique protein signature of NDAN. Additionally, since NDAN PSDs are capable of rejecting amyloid oligomers, it would be informative to determine if membrane proteins are differentially expressed in NDAN vs. AD, as it could provide additional targets and improve our understanding of the protective mechanisms in NDAN.

As described above, one of the most intriguing observations of this dissertation is the sex-dependent response to miR treatments, suggesting that female hippocampi are more sensitive to the alterations in miR levels when compared to males. Overwhelming literature evidence has ultimately established that females have higher risk for AD development, in addition to greater cognitive impairment and severity of the disease (reviewed by [326]). Most frequently this is attributed to the post-menopausal loss of estrogen as well as longer life span (reviewed by [326,327]). Moreover, the number of estrogen receptor-positive neurons decreases with age and some polymorphisms in the estrogen receptor are associated with increased risk for AD [327,328]. Additionally, whereas the levels of estrogen in the brain decrease after the reproductive years, some females enhance local synthesis of estrogen in the brain as a compensatory mechanism during menopause [329–331]. This local estrogen availability positively modifies the density of dendritic spines and synapses [332,333], and allows for regulation of synaptic genes via the estrogen receptor (which is a sequence-specific DNA-binding transcription factor) (reviewed by [326,327,334]). An interesting fact in the scope of the

present discussion is that estrogen receptors, in turn, can promote the expression and maturation of miRs (reviewed by [327,334]), including the regulation of miR-218 which was shown to increase tau phosphorylation via PTPα (protein tyrosine phosphatase alpha) [328]. Additionally, it was shown that estrogen-replacement therapy promotes the shift of APP processing towards the non-amyloidogenic pathway via BACE1 downregulation ([331], reviewed by [326,335]).

Overall, there is ample literature consensus in the field concerning the significance of estrogen receptor/miR connection with the Aβ and tau production, toxicity, degradation, and elimination. MiRs, in turn, have sex-dependent effects on synaptic resilience to Aβ, as described in this dissertation. It is then tempting to speculate that the estrogen receptor might be mediating some of these differences. Further research is needed to determine if there is a direct link between estrogen receptor and miR-149, miR-485 or miR-4723, or if there are other factors contributing towards greater sensitivity to AD in females.

Concluding remarks

Currently available medications do not change the underlying disease processes and people affected by AD are in desperate need for novel disease-modifying drugs. This dissertation identified and validated three miRs as potential therapeutic targets against Aβ toxicity based on the study of unique postsynaptic proteome in dementia-resistant NDAN individuals. Stemming from the work described here, several future directions can be undertaken to further develop and expand our understanding of the complex mechanisms modulating and/or promoting brain resilience to overt AD neuropathology. I hope that my small contribution to the big science one day will become something greater and stimulate new thoughts, hypotheses, and of course discoveries and inventions.

Appendix A. Supplemental Information for Chapter 3

S<small>UPPLEMENTARY TABLE</small> 3.1: A <small>LIST OF PROTEINS IDENTIFIED USING</small> MS/MS <small>OR LIQUID CHROMATOGRAPHY</small> (LC)

Proteins included in the table have ±1.5 fold change in NDAN vs. AD and p-value ≤ 0.05. Ten additional proteins that do not meet the abovementioned criteria but are relevant to the discussion are included.

Protein name	Accession No.	pI	MW (kDa)	MS ID Protein Score	AD vs. Control	p - value	NDAN vs. AD	p - value	NDAN vs. Control	p - value
Glial fibrillary acidic protein, GFAP	E9PAX3	5	20	LC 400	-1.12	0.366	-4.32	0.006	-4.84	0.004
Isoform Non-brain of Clathrin light chain A, CLTA	P09496-2	4.69	30	62	-1.01	0.933	-3.31	0.005	-3.34	0.004
Keratin, type II cytoskeletal 1, KRT1	P04264	5.54	17	130	1.33	0.811	-3.10	0.370	-2.33	0.022
Tubulin alpha-1B chain (Fragment), TUBA1B	F8VVB9	5.23	33	128	-1.32	0.050	-2.97	0.041	-3.93	0.021
Calreticulin, CALR	P27797	4.65	71	70	-1.15	0.335	-2.85	0.001	-3.27	0.000
Creatine kinase B-type (Fragment), CKB	G3V4N7	5	20	116	1.09	0.415	-2.80	0.003	-2.57	0.004
Tubulin beta-6 chain (Fragment), TUBB6	K7ESM5	5.26	12	LC 123	-1.59	0.298	-2.51	0.098	-4.01	0.036

Protein name	Accession No.	pI	MW (kDa)	MS ID Protein Score	AD vs. Control	p - value	NDAN vs. AD	p - value	NDAN vs. Control	p - value
Ubiquitin carboxyl-terminal hydrolase isozyme L1, UCHL1	D6R974	5.15	20	133	1.04	0.877	-2.47	0.022	-2.37	0.019
Isoform Cytoplasmic+peroxisomal of Peroxiredoxin-5, mitochondrial, PRDX5	P30044-2	7.75	16	LC 143	1.31	0.335	-2.27	0.088	-1.73	0.123
Profilin-2, PFN2	C9J0J7	5.06	13	78	1.01	0.929	-2.08	0.047	-2.06	0.026
Glial fibrillary acidic protein, GFAP	P14136	5.06	34	850	-1.44	0.030	-2.07	0.079	-2.97	0.027
Isoform IB of Synapsin-1, SYN1	P17600-2	8.87	74	290	1.17	0.376	-2.00	0.032	-1.71	0.056
Glial fibrillary acidic protein, GFAP	E9PAX3	4.98	18	LC 374	1.27	0.234	-1.98	0.022	-1.56	0.192
Creatine kinase B-type, CKB	P12277	6.93	17	70	1.05	0.596	-1.98	0.001	-1.88	0.003
Spectrin alpha chain, non-erythrocytic 1, SPTAN1	Q13813	5.38	134	439	1.22	0.465	-1.91	0.039	-1.56	0.202
Tubulin beta-2A chain, TUBB2A	Q13885	5.45	34	139	1.19	0.490	-1.84	0.184	-1.55	0.421
Tubulin beta-4A chain, TUBB4A	P04350	4.81	16	62	-1.20	0.137	-1.84	0.004	-2.20	0.001

Protein name	Accession No.	pI	MW (kDa)	MS ID Protein Score	AD vs. Control	p - value	NDAN vs. AD	p - value	NDAN vs. Control	p - value
Keratin, type II cytoskeletal 1, KRT1	P04264	4.66	35	63	-1.14	0.118	-1.81	0.001	-2.07	0.000
Keratin, type I cytoskeletal 10, KRT10	P13645	5.33	102	78	-1.04	0.794	-1.80	0.019	-1.87	0.018
Rho GDP-dissociation inhibitor 1 (Fragment), ARHGDIA	J3KTF8	5.02	20	185	1.18	0.094	-1.77	0.009	-1.50	0.033
Isoform 3 of Peroxiredoxin-5, mitochondrial, PRDX5	P30044-3	7.7	15	154	1.29	0.081	-1.77	0.009	-1.37	0.005
Isoform IB of Synapsin-1, SYN1	P17600-2	9.17	75	271	1.16	0.173	-1.72	0.001	-1.48	0.005
Tubulin alpha-1B chain (Fragment), TUBA1B	F8VVB9	5.29	33	342	-1.26	0.377	-1.66	0.110	-2.09	0.020
Septin-7, SEPT7	F5GZE5	8.68	45	84	1.48	0.336	-1.66	0.075	-1.12	0.908
Isoform 2 of Glial fibrillary acidic protein, GFAP	P14136-2	5.74	48	284	2.04	0.041	-1.60	0.157	1.27	0.292
Isoform 3 of Dynamin-1, DNM1	Q05193-3	4.88	19	LC 300	-1.35	0.015	-1.60	0.016	-2.16	0.001
Pyruvate carboxylase, mitochondrial, PC	P11498	6.28	119	96	1.12	0.577	-1.59	0.048	-1.42	0.042

Protein name	Accession No.	pI	MW (kDa)	MS ID Protein Score	AD vs. Control	p - value	NDAN vs. AD	p - value	NDAN vs. Control	p - value
Keratin, type I cytoskeletal 9, KRT9	P35527	4.82	13	213	-1.21	0.405	-1.56	0.179	-1.89	0.046
Profilin-2, PFN2	C9J0J7	5.76	14	126	1.80	0.523	-1.54	0.684	1.17	0.554
Keratin, type II cytoskeletal 1, KRT1	P04264	7.55	12	181	1.32	0.067	-1.54	0.105	-1.17	0.447
Actin, cytoplasmic 2, ACTG1	P63261	6.31	15	78	-1.50	0.170	-1.49	0.351	-2.23	0.029
NADH dehydrogenase [ubiquinone] flavoprotein 1, mitochondrial (Fragment), NDUFV1	E9PQP1	8.26	46	105	2.77	0.003	-1.47	0.208	1.88	0.195
NADH dehydrogenase [ubiquinone] 1 alpha subcomplex subunit 5, NDUFA5	F8WAS3	5.5	13	LC 237	-3.21	0.134	-1.44	0.869	-4.62	0.040
Neurofilament medium polypeptide, NEFM	E7EMV2	5.4	50	210	-1.28	0.321	1.50	0.241	1.17	0.635
Glial fibrillary acidic protein, GFAP	P14136	5.07	37	915	-1.48	0.001	1.53	0.001	1.03	0.587
Isoform 2 of Glial fibrillary acidic protein, GFAP	P14136-2	5.16	49	828	-1.19	0.337	1.53	0.040	1.28	0.139

Protein name	Accession No.	pI	MW (kDa)	MS ID Protein Score	AD vs. Control	p - value	NDAN vs. AD	p - value	NDAN vs. Control	p - value
Keratin, type I cytoskeletal 9, KRT9	P35527	6.14	17	95	-1.37	0.076	1.55	0.072	1.13	0.469
Isoform 2 of Glial fibrillary acidic protein, GFAP	P14136-2	5.07	37	790	-1.53	0.009	1.56	0.006	1.02	0.726
Tubulin alpha-1A chain (Fragment), TUBA1A	F8VRZ4	5.09	22	67	-2.13	0.032	1.56	0.233	-1.37	0.299
Isoform 2 of Glial fibrillary acidic protein, GFAP	P14136-2	5.5	46	974	-1.08	0.550	1.60	0.047	1.48	0.029
Isoform 2 of Glial fibrillary acidic protein, GFAP	P14136-2	5.23	46	945	1.02	0.856	1.63	0.017	1.66	0.033
Isoform 2 of Glial fibrillary acidic protein, GFAP	P14136-2	5.17	38	885	-1.12	0.100	1.63	0.016	1.46	0.045
Hemoglobin subunit beta, HBB	P68871	7.34	14	212	1.75	0.092	1.67	0.212	2.92	0.034
Isoform 3 of Dynamin-1, DNM1	Q05193-3	4.93	20	LC 346	-1.23	0.257	1.69	0.016	1.38	0.094
Isoform 2 of Glial fibrillary acidic protein, GFAP	P14136-2	5.16	35	92	-1.91	0.002	1.70	0.002	-1.12	0.175

| Protein name	Accession No.	pI	MW (kDa)	MS ID Protein Score	AD vs. Control	p - value	NDAN vs. AD	p - value	NDAN vs. Control	p - value
Malate dehydrogenase, mitochondrial, MDH2	P40926	8.94	30	228	1.67	0.005	1.77	0.102	2.97	0.016
Isoform CNPI of 2',3'-cyclic-nucleotide 3'-phosphodiesterase, CNP	P09543-2	9.11	40	97	-1.66	0.127	1.82	0.293	1.10	0.970
Annexin (Fragment), ANXA2	H0YN42	8.03	30	141	1.55	0.404	1.83	0.358	2.85	0.099
Hemoglobin subunit beta, HBB	P68871	7	14	70	1.68	0.071	1.84	0.182	3.09	0.043
Isoform 3 of Ras-related protein Rap-1b, RAP1B	P61224-3	6.37	19	112	-1.19	0.034	1.92	0.006	1.62	0.015
Isoform 1 of Vinculin, VCL	P18206-2	5.88	118	LC 322	1.03	0.864	1.92	0.124	1.97	0.020
Calcium/calmodulin-dependent protein kinase type II subunit alpha, CAMK2A	Q9UQM7	5.84	17	LC 115	1.43	0.452	1.98	0.143	2.83	0.041
Glial fibrillary acidic protein (Fragment), GFAP	K7EJU1	5.61	21	LC 339	-4.13	0.009	2.00	0.196	-2.07	0.073
Syntaxin-binding protein 1, STXBP1	P61764	5.52	31	LC 171	1.12	0.359	2.00	0.001	2.24	0.001

Protein name	Accession No.	pI	MW (kDa)	MS ID Protein Score	AD vs. Control	p - value	NDAN vs. AD	p - value	NDAN vs. Control	p - value
Tubulin alpha-1B chain (Fragment), TUBA1B	F8VVB9	5.54	46	91	-1.31	0.006	2.04	0.004	1.55	0.021
Glial fibrillary acidic protein, GFAP	P14136	5.18	46	863	-1.02	0.925	2.06	0.006	2.02	0.007
Glial fibrillary acidic protein, GFAP	P14136	5.43	46	1050	-1.25	0.175	2.12	0.004	1.69	0.024
Glial fibrillary acidic protein, GFAP	P14136	5.28	46	969	-1.32	0.440	2.15	0.010	1.63	0.108
Glial fibrillary acidic protein, GFAP	P14136	5.34	46	950	-1.23	0.145	2.18	0.001	1.77	0.003
Isoform 2 of Glial fibrillary acidic protein, GFAP	P14136-2	5.09	36	223	-2.19	0.036	2.42	0.027	1.10	0.639
Glial fibrillary acidic protein, GFAP	P14136	5.39	46	1010	-1.44	0.013	2.58	0.001	1.79	0.000
Hemoglobin subunit beta, HBB	P68871	7.35	13	170	1.26	0.506	2.90	0.016	3.66	0.001
Glyceraldehyde-3-phosphate dehydrogenase, GAPDH	E7EUT4	9.17	32	88	-6.19	0.141	6.55	0.149	1.06	0.990

Appendix B. Supplemental Information for Chapter 4

SUPPLEMENTARY FIGURE 4.1: Aβ OLIGOMER ASSOCIATION WITH SH-SY5Y CELLS

(A) A representative acquisition of SH-SY5Y cells using flow cytometry. (B) The quadrants are set up using non-transfected SH-SY5Y cells. SH-SY5Y cells transfected with FAM labeled siRNA (C) and miR-149 (D), -485 (E) or -4723 (F) were incubated with 2 μM HiLyteTM Fluor 647-labeled Aβ oligomers. (C-F) Transfected cells that are bound with Aβ oligomers are in the top left quadrant.
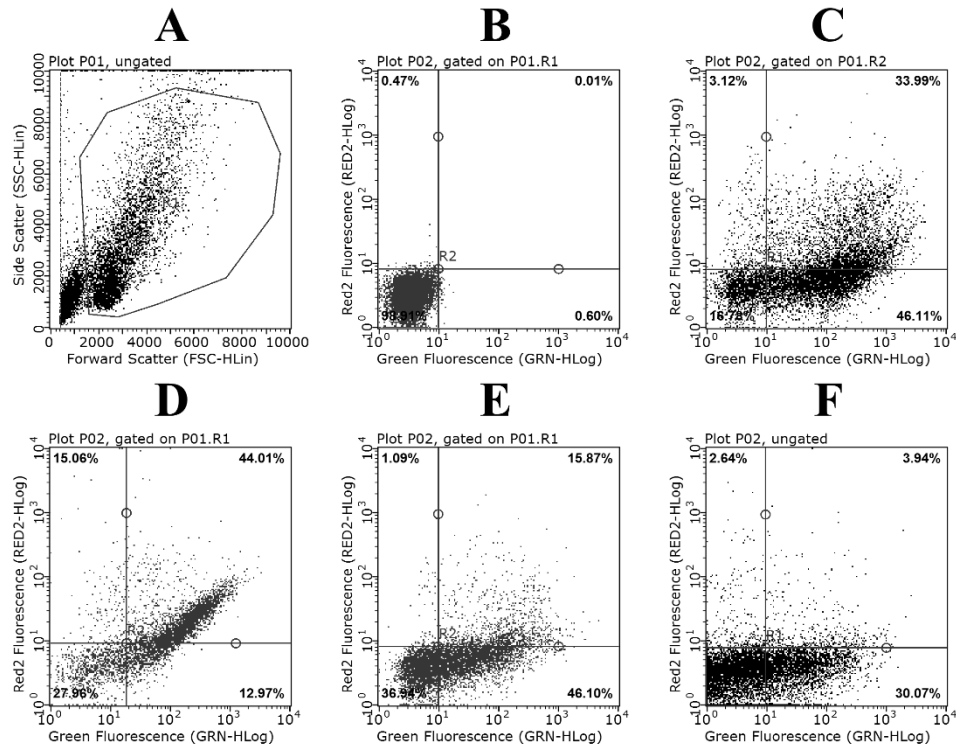
(A) The size beads were used to set up the gate for particles ~1-5 μm in diameter. (B) A
representative acquisition of synaptosomes using the size gate (in red) set up in (A). (C)
The quadrants are set up using synaptosomes that were not incubated with the HiLyteTM
Fluor 647-labeled Aβ oligomers. (D) A representative acquisition of synaptosomes
incubated with labeled Aβ oligomers. Synaptosomes that are bound with Aβ oligomers
are in the top left quadrant.
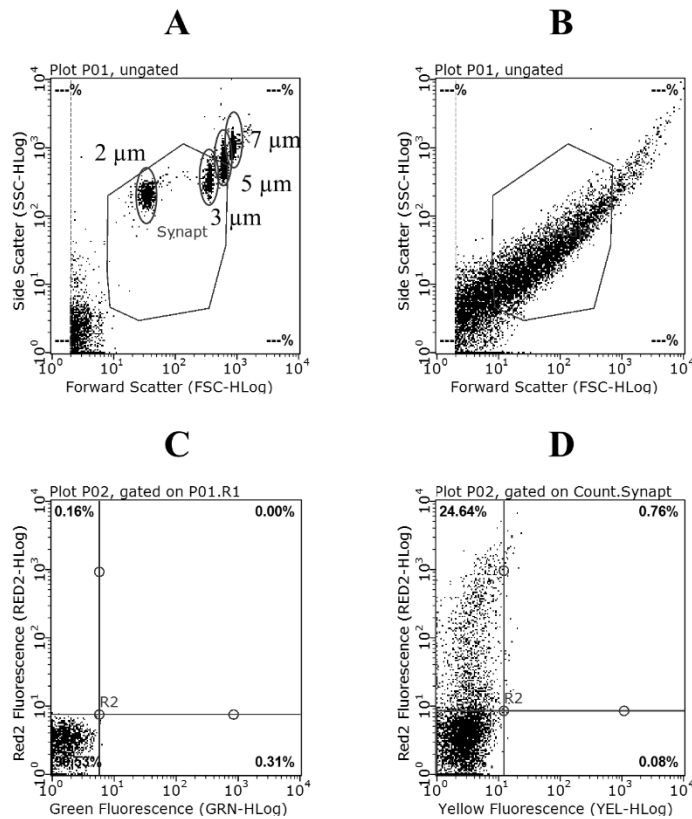
SUPPLEMENTARY TABLE 4.1: NUMBER OF GENES MODIFIED IN RESPONSE TO MIR
TREATMENTS IN THE HIPPOCAMPAL TRANSCRIPTOME IN FEMALES

The number in the table represents the number of genes modified by each miR treatment
vs. Scrambled miR.

miR treatment vs. Scr miR	Total	Upregulated	Downregulated
miR-149	1020	81	939
miR-485	738	477	261
miR-4723	110	3	107

SUPPLEMENTARY TABLE 4.2: NUMBER OF MRNAS BY CATEGORY FROM THE PANTHER
BIOLOGICAL PROCESS ANALYSIS OF THE HIPPOCAMPAL TRANSCRIPTOME IN FEMALES

Number provided in this table represent the number of mRNAs falling into each category.

Biological process	miR-149	miR-485	miR-4723
biological adhesion	18	25	0
biological regulation	85	168	9
cellular component organization or biogenesis	70	72	1
cellular process	271	346	25
developmental process	50	99	3
immune system process	21	16	2
localization	55	74	4
locomotion	7	20	0
metabolic process	197	187	23
multicellular organismal process	41	107	2
reproduction	15	12	2
response to stimulus	73	140	10

Number provided in this table represent the number of mRNAs falling into each category.

Molecular function	miR-149	miR-485	miR-4723
antioxidant activity	3	1	0
binding	176	215	17
catalytic activity	136	139	18
channel regulator activity	0	1	0
receptor activity	23	60	2
signal transducer activity	17	0	2
structural molecule activity	11	14	0
translation regulation activity	1	0	0
transporter activity	38	53	4

SUPPLEMENTARY TABLE 4.4: SYNAPTIC GENES MEASURED IN MALE MICE TREATED WITH MIR-149, MIR-485 AND MIR-4723

mRNA descriptions were obtained from the NCBI Gene database.

mRNA	Brief description
App	amyloid precursor protein
Bace1	beta-secretase 1
Camk2a	calcium/calmodulin-dependent protein kinase II alpha
Creb1	cAMP responsive element binding protein 1
Dnm1	dynamin 1
Mapt	microtubule-associated protein tau
Ppp3ca	protein phosphatase 3, catalytic subunit, alpha isoform
Psd95	postsynaptic density protein 95
Snap25	synaptosomal-associated protein 25
Snca	synuclein, alpha
Syn1	synapsin I
Vamp2	vesicle-associated membrane protein 2

Bibliography

[1]   Alzheimer's Association (2018) 2018 Alzheimer's Disease Facts and Figures. *Alzheimers Dement* **14**, 367–429.

[2]   Dorszewska J, Prendecki M, Oczkowska A, Dezor M, Kozubski W (2016) Molecular Basis of Familial and Sporadic Alzheimer's Disease. *Curr. Alzheimer Res.* **13**, 952–63.

[3]   Matrone C, Djelloul M, Taglialatela G, Perrone L (2015) Inflammatory risk factors and pathologies promoting Alzheimer's disease progression: is RAGE the key? *Histol Histopathol* **30**, 125–139.

[4]   Markesbery WR (1997) Oxidative stress hypothesis in Alzheimer's disease. *Free Radic Biol Med* **23**, 134–147.

[5]   Chakrabarti S, Khemka VK, Banerjee A, Chatterjee G, Ganguly A, Biswas A (2015) Metabolic Risk Factors of Sporadic Alzheimer's Disease: Implications in the Pathology, Pathogenesis and Treatment. *Aging Dis.* **6**, 282–99.

[6]   Philipps V, Amieva H, Andrieu S, Dufouil C, Berr C, Dartigues JF, Jacqmin-Gadda H, Proust-Lima C (2014) Normalized Mini-Mental State Examination for Assessing Cognitive Change in Population-Based Brain Aging Studies. *Neuroepidemiology* **43**, 15–25.

[7]   (1997) Consensus recommendations for the postmortem diagnosis of Alzheimer's disease. The National Institute on Aging, and Reagan Institute Working Group on Diagnostic Criteria for the Neuropathological Assessment of Alzheimer's Disease. *Neurobiol Aging* **18**, S1-2.

[8]   Braak H, Braak E (1991) Neuropathological stageing of Alzheimer-related changes. *Acta Neuropathol* **82**, 239–259.

[9]   Yaari R, Corey-Bloom J (2007) Alzheimer's disease. *Semin Neurol* **27**, 32–41.

[10]   Nixon RA (2007) Autophagy, amyloidogenesis and Alzheimer disease. *J Cell Sci* **120**, 4081–4091.

[11]   Kim GH, Jeon S, Seo SW, Kim MJ, Kim JH, Roh JH, Shin JS, Kim CH, Im K, Lee JM, Qiu A, Kim ST, Na DL (2012) Topography of cortical thinning areas associated with hippocampal atrophy (HA) in patients with Alzheimer's disease

(AD). *Arch Gerontol Geriatr* **54**, e122-9.

[12] Vandenberghe R (2014) The Relationship between Amyloid Deposition, Neurodegeneration, and Cognitive Decline in Dementia. *Curr Neurol Neurosci Rep* **14**, 498.

[13] Selkoe DJ (2002) Alzheimer's disease is a synaptic failure. *Science* **298**, 789–91.

[14] Coleman PD, Yao PJ (2003) Synaptic slaughter in Alzheimer's disease. *Neurobiol. Aging* **24**, 1023–7.

[15] Henstridge CM, Pickett E, Spires-Jones TL (2016) Synaptic pathology: A shared mechanism in neurological disease. *Ageing Res. Rev.* **28**, 72–84.

[16] Dahms SO, Hoefgen S, Roeser D, Schlott B, Gührs KH, Than ME (2010) Structure and biochemical analysis of the heparin-induced E1 dimer of the amyloid precursor protein. *Proc Natl Acad Sci U S A* **107**, 5381–5386.

[17] Del Prete D, Lombino F, Liu X, D'Adamio L (2014) APP Is Cleaved by Bace1 in Pre-Synaptic Vesicles and Establishes a Pre-Synaptic Interactome, via Its Intracellular Domain, with Molecular Complexes that Regulate Pre-Synaptic Vesicles Functions. *PLoS One* **9**, e108576.

[18] Maarouf CL, Daugs ID, Kokjohn TA, Walker DG, Hunter JM, Kruchowsky JC, Woltjer R, Kaye J, Castaño EM, Sabbagh MN, Beach TG, Roher AE (2011) Alzheimer's disease and non-demented high pathology control nonagenarians: comparing and contrasting the biochemistry of cognitively successful aging. *PLoS One* **6**, e27291.

[19] Jonsson T, Atwal JK, Steinberg S, Snaedal J, Jonsson P V, Bjornsson S, Stefansson H, Sulem P, Gudbjartsson D, Maloney J, Hoyte K, Gustafson A, Liu Y, Lu Y, Bhangale T, Graham RR, Huttenlocher J, Bjornsdottir G, Andreassen OA, Jönsson EG, Palotie A, Behrens TW, Magnusson OT, Kong A, Thorsteinsdottir U, Watts RJ, Stefansson K (2012) A mutation in APP protects against Alzheimer's disease and age-related cognitive decline. *Nature* **488**, 96–99.

[20] Lazarov O, Demars MP (2012) All in the Family: How the APPs Regulate Neurogenesis. *Front Neurosci* **6**, 81.

[21] Nunan J, Small DH (2000) Regulation of APP cleavage by alpha-, beta- and gamma-secretases. *FEBS Lett* **483**, 6–10.

[22] Cole SL, Vassar R (2007) The Alzheimer's disease beta-secretase enzyme,

BACE1. *Mol Neurodegener* **2**, 22.

[23] Polanco JC, Li C, Bodea L-G, Martinez-Marmol R, Meunier FA, Götz J (2018) Amyloid-β and tau complexity - towards improved biomarkers and targeted therapies. *Nat. Rev. Neurol.* **14**, 22–39.

[24] Stains CI, Mondal K, Ghosh I (2007) Molecules that target beta-amyloid. *ChemMedChem* **2**, 1674–1692.

[25] Aisenbrey C, Borowik T, Byström R, Bokvist M, Lindström F, Misiak H, Sani MA, Gröbner G (2008) How is protein aggregation in amyloidogenic diseases modulated by biological membranes? *Eur Biophys J* **37**, 247–255.

[26] Koffie RM, Meyer-Luehmann M, Hashimoto T, Adams KW, Mielke ML, Garcia-Alloza M, Micheva KD, Smith SJ, Kim ML, Lee VM, Hyman BT, Spires-Jones TL (2009) Oligomeric amyloid beta associates with postsynaptic densities and correlates with excitatory synapse loss near senile plaques. *Proc Natl Acad Sci U S A* **106**, 4012–4017.

[27] Lacor PN, Buniel MC, Chang L, Fernandez SJ, Gong Y, Viola KL, Lambert MP, Velasco PT, Bigio EH, Finch CE, Krafft GA, Klein WL (2004) Synaptic targeting by Alzheimer's-related amyloid beta oligomers. *J Neurosci* **24**, 10191–10200.

[28] Reese LC, Zhang W, Dineley KT, Kayed R, Taglialatela G (2008) Selective induction of calcineurin activity and signaling by oligomeric amyloid beta. *Aging Cell* **7**, 824–835.

[29] Dinamarca MC, Ríos JA, Inestrosa NC (2012) Postsynaptic Receptors for Amyloid-β Oligomers as Mediators of Neuronal Damage in Alzheimer's Disease. *Front Physiol* **3**, 464.

[30] Sengupta U, Nilson AN, Kayed R (2016) The Role of Amyloid-β Oligomers in Toxicity, Propagation, and Immunotherapy. *EBioMedicine* **6**, 42–49.

[31] Reese LC, Laezza F, Woltjer R, Taglialatela G (2011) Dysregulated phosphorylation of Ca(2+) /calmodulin-dependent protein kinase II-α in the hippocampus of subjects with mild cognitive impairment and Alzheimer's disease. *J Neurochem* **119**, 791–804.

[32] Dineley KT, Kayed R, Neugebauer V, Fu Y, Zhang W, Reese LC, Taglialatela G (2010) Amyloid-beta oligomers impair fear conditioned memory in a calcineurin-dependent fashion in mice. *J Neurosci Res* **88**, 2923–2932.

[33] Kayed R, Lasagna-Reeves CA (2013) Molecular mechanisms of amyloid oligomers toxicity. *J Alzheimers Dis* **33 Suppl 1**, S67-78.

[34] Spires-Jones TL, Hyman BT (2014) The intersection of amyloid beta and tau at synapses in Alzheimer's disease. *Neuron* **82**, 756–771.

[35] Aizenstein HJ, Nebes RD, Saxton JA, Price JC, Mathis CA, Tsopelas ND, Ziolko SK, James JA, Snitz BE, Houck PR, Bi W, Cohen AD, Lopresti BJ, DeKosky ST, Halligan EM, Klunk WE (2008) Frequent amyloid deposition without significant cognitive impairment among the elderly. *Arch Neurol* **65**, 1509–1517.

[36] Gomez-Isla T, Hollister R, West H, Mui S, Growdon JH, Petersen RC, Parisi JE, Hyman BT (1997) Neuronal loss correlates with but exceeds neurofibrillary tangles in Alzheimer's disease. *Ann Neurol* **41**, 17–24.

[37] Karran E, Mercken M, De Strooper B (2011) The amyloid cascade hypothesis for Alzheimer's disease: an appraisal for the development of therapeutics. *Nat Rev Drug Discov* **10**, 698–712.

[38] Gendron TF, Petrucelli L (2009) The role of tau in neurodegeneration. *Mol. Neurodegener.* **4**, 13.

[39] Goedert M, Spillantini MG, Jakes R, Rutherford D, Crowther RA (1989) Multiple isoforms of human microtubule-associated protein tau: sequences and localization in neurofibrillary tangles of Alzheimer's disease. *Neuron* **3**, 519–26.

[40] Iqbal K, Grundke-Iqbal I, Zaidi T, Merz PA, Wen GY, Shaikh SS, Wisniewski HM, Alafuzoff I, Winblad B (1986) Defective brain microtubule assembly in Alzheimer's disease. *Lancet (London, England)* **2**, 421–6.

[41] Spires-Jones TL, Hyman BT (2014) The Intersection of Amyloid Beta and Tau at Synapses in Alzheimer's Disease. *Neuron* **82**, 756–771.

[42] Iqbal K, Gong C-X, Liu F (2013) Hyperphosphorylation-induced tau oligomers. *Front. Neurol.* **4**, 112.

[43] Köpke E, Tung YC, Shaikh S, Alonso AC, Iqbal K, Grundke-Iqbal I (1993) Microtubule-associated protein tau. Abnormal phosphorylation of a non-paired helical filament pool in Alzheimer disease. *J. Biol. Chem.* **268**, 24374–84.

[44] Hoover BR, Reed MN, Su J, Penrod RD, Kotilinek LA, Grant MK, Pitstick R, Carlson GA, Lanier LM, Yuan L-L, Ashe KH, Liao D (2010) Tau mislocalization to dendritic spines mediates synaptic dysfunction independently of

neurodegeneration. *Neuron* **68**, 1067–81.

[45]   Fein JA, Sokolow S, Miller CA, Vinters H V., Yang F, Cole GM, Gylys KH
        (2008) Co-Localization of Amyloid Beta and Tau Pathology in Alzheimer's
        Disease Synaptosomes. *Am. J. Pathol.* **172**, 1683–1692.

[46]   Tai H-C, Wang BY, Serrano-Pozo A, Frosch MP, Spires-Jones TL, Hyman BT
        (2014) Frequent and symmetric deposition of misfolded tau oligomers within
        presynaptic and postsynaptic terminals in Alzheimer's disease. *Acta Neuropathol.
        Commun.* **2**, 146.

[47]   Zhou L, McInnes J, Wierda K, Holt M, Herrmann AG, Jackson RJ, Wang Y-C,
        Swerts J, Beyens J, Miskiewicz K, Vilain S, Dewachter I, Moechars D, De
        Strooper B, Spires-Jones TL, De Wit J, Verstreken P (2017) Tau association with
        synaptic vesicles causes presynaptic dysfunction. *Nat. Commun.* **8**, 15295.

[48]   Lasagna-Reeves CA, Castillo-Carranza DL, Sengupta U, Clos AL, Jackson GR,
        Kayed R (2011) Tau oligomers impair memory and induce synaptic and
        mitochondrial dysfunction in wild-type mice. *Mol. Neurodegener.* **6**, 39.

[49]   Chabrier MA, Cheng D, Castello NA, Green KN, LaFerla FM (2014) Synergistic
        effects of amyloid-beta and wild-type human tau on dendritic spine loss in a floxed
        double transgenic model of Alzheimer's disease. *Neurobiol Dis* **64**, 107–117.

[50]   Lasagna-Reeves CA, Castillo-Carranza DL, Sengupta U, Clos AL, Jackson GR,
        Kayed R (2011) Tau oligomers impair memory and induce synaptic and
        mitochondrial dysfunction in wild-type mice. *Mol Neurodegener* **6**, 39.

[51]   Fá M, Puzzo D, Piacentini R, Staniszewski A, Zhang H, Baltrons MA, Li Puma
        DD, Chatterjee I, Li J, Saeed F, Berman HL, Ripoli C, Gulisano W, Gonzalez J,
        Tian H, Costa JA, Lopez P, Davidowitz E, Yu WH, Haroutunian V, Brown LM,
        Palmeri A, Sigurdsson EM, Duff KE, Teich AF, Honig LS, Sierks M, Moe JG,
        D'Adamio L, Grassi C, Kanaan NM, Fraser PE, Arancio O (2016) Extracellular
        Tau Oligomers Produce An Immediate Impairment of LTP and Memory. *Sci Rep*
        6, 19393.

[52]   Talantova M, Sanz-Blasco S, Zhang X, Xia P, Akhtar MW, Okamoto S,
        Dziewczapolski G, Nakamura T, Cao G, Pratt AE, Kang Y-J, Tu S, Molokanova
        E, McKercher SR, Hires SA, Sason H, Stouffer DG, Buczynski MW, Solomon JP,
        Michael S, Powers ET, Kelly JW, Roberts A, Tong G, Fang-Newmeyer T, Parker
        J, Holland EA, Zhang D, Nakanishi N, Chen H-SV, Wolosker H, Wang Y, Parsons
        LH, Ambasudhan R, Masliah E, Heinemann SF, Piña-Crespo JC, Lipton SA
        (2013) Aβ induces astrocytic glutamate release, extrasynaptic NMDA receptor
        activation, and synaptic loss. *Proc. Natl. Acad. Sci. U. S. A.* **110**, E2518-27.

[53]   Guerrero-Muñoz MJ, Gerson J, Castillo-Carranza DL (2015) Tau Oligomers: The Toxic Player at Synapses in Alzheimer's Disease. *Front Cell Neurosci* **9**, 464.

[54]   Rhein V, Song X, Wiesner A, Ittner LM, Baysang G, Meier F, Ozmen L, Bluethmann H, Drose S, Brandt U, Savaskan E, Czech C, Gotz J, Eckert A (2009) Amyloid- and tau synergistically impair the oxidative phosphorylation system in triple transgenic Alzheimer's disease mice. *Proc. Natl. Acad. Sci.* **106**, 20057–20062.

[55]   Reese LC, Taglialatela G (2010) Neuroimmunomodulation by calcineurin in aging and Alzheimer's disease. *Aging Dis* **1**, 245–253.

[56]   Yin Y, Gao D, Wang Y, Wang Z-H, Wang X, Ye J, Wu D, Fang L, Pi G, Yang Y, Wang X-C, Lu C, Ye K, Wang J-Z (2016) Tau accumulation induces synaptic impairment and memory deficit by calcineurin-mediated inactivation of nuclear CaMKIV/CREB signaling. *Proc. Natl. Acad. Sci. U. S. A.* **113**, E3773-81.

[57]   Kayed R, Head E, Thompson JL, McIntire TM, Milton SC, Cotman CW, Glabel CG (2003) Common structure of soluble amyloid oligomers implies common mechanism of pathogenesis. *Science (80-.)*. **300**, 486–489.

[58]   Glabe CG, Kayed R (2006) Common structure and toxic function of amyloid oligomers implies a common mechanism of pathogenesis. *Neurology* **66**, S74–S78.

[59]   Martin ZS, Neugebauer V, Dineley KT, Kayed R, Zhang W, Reese LC, Taglialatela G (2012) α-Synuclein oligomers oppose long-term potentiation and impair memory through a calcineurin-dependent mechanism: relevance to human synucleopathic diseases. *J Neurochem* **120**, 440–452.

[60]   Lasagna-Reeves CA, Castillo-Carranza DL, Sengupta U, Sarmiento J, Troncoso J, Jackson GR, Kayed R (2012) Identification of oligomers at early stages of tau aggregation in Alzheimer's disease. *FASEB J* **26**, 1946–1959.

[61]   Sperling RA, Aisen PS, Beckett LA, Bennett DA, Craft S, Fagan AM, Iwatsubo T, Jack CR, Kaye J, Montine TJ, Park DC, Reiman EM, Rowe CC, Siemers E, Stern Y, Yaffe K, Carrillo MC, Thies B, Morrison-Bogorad M, Wagster M V, Phelps CH (2011) Toward defining the preclinical stages of Alzheimer's disease: recommendations from the National Institute on Aging-Alzheimer's Association workgroups on diagnostic guidelines for Alzheimer's disease. *Alzheimers Dement* **7**, 280–292.

[62]   The Nun Study, [Internet] https://www.psychiatry.umn.edu/research/research-labs-and-programs/nun-study Last updated 2018, Accessed on 2018.

[63]   Snowdon DA, Greiner LH, Mortimer JA, Riley KP, Greiner PA, Markesbery WR (1997) Brain infarction and the clinical expression of Alzheimer disease. The Nun Study. *JAMA* **277**, 813–7.

[64]   Rothschild D, Trainor MA (1937) PATHOLOGIC CHANGES IN SENILE PSYCHOSES AND THEIR PSYCHOBIOLOGIC SIGNIFICANCE. *Am. J. Psychiatry* **93**, 757–788.

[65]   Katzman R, Terry R, DeTeresa R, Brown T, Davies P, Fuld P, Renbing X, Peck A (1988) Clinical, pathological, and neurochemical changes in dementia: a subgroup with preserved mental status and numerous neocortical plaques. *Ann Neurol* **23**, 138–144.

[66]   Bjorklund NL, Reese LC, Sadagoparamanujam VM, Ghirardi V, Woltjer RL, Taglialatela G (2012) Absence of amyloid β oligomers at the postsynapse and regulated synaptic Zn2+ in cognitively intact aged individuals with Alzheimer's disease neuropathology. *Mol Neurodegener* **7**, 23.

[67]   Briley D, Ghirardi V, Woltjer R, Renck A, Zolochevska O, Taglialatela G, Micci M-A (2016) Preserved neurogenesis in non-demented individuals with AD neuropathology. *Sci. Rep.* **6**,.

[68]   Price JL, McKeel DW, Buckles VD, Roe CM, Xiong C, Grundman M, Hansen LA, Petersen RC, Parisi JE, Dickson DW, Smith CD, Davis DG, Schmitt FA, Markesbery WR, Kaye J, Kurlan R, Hulette C, Kurland BF, Higdon R, Kukull W, Morris JC (2009) Neuropathology of nondemented aging: presumptive evidence for preclinical Alzheimer disease. *Neurobiol Aging* **30**, 1026–1036.

[69]   Riudavets MA, Iacono D, Resnick SM, O'Brien R, Zonderman AB, Martin LJ, Rudow G, Pletnikova O, Troncoso JC (2007) Resistance to Alzheimer's pathology is associated with nuclear hypertrophy in neurons. *Neurobiol Aging* **28**, 1484–1492.

[70]   Erten-Lyons D, Woltjer RL, Dodge H, Nixon R, Vorobik R, Calvert JF, Leahy M, Montine T, Kaye J (2009) Factors associated with resistance to dementia despite high Alzheimer disease pathology. *Neurology* **72**, 354–360.

[71]   Gefen T, Peterson M, Papastefan ST, Martersteck A, Whitney K, Rademaker A, Bigio EH, Weintraub S, Rogalski E, Mesulam MM, Geula C (2015) Morphometric and histologic substrates of cingulate integrity in elders with exceptional memory capacity. *J Neurosci* **35**, 1781–1791.

[72]   Iacono D, O'Brien R, Resnick SM, Zonderman AB, Pletnikova O, Rudow G, An Y, West MJ, Crain B, Troncoso JC (2008) Neuronal hypertrophy in asymptomatic

Alzheimer disease. *J Neuropathol Exp Neurol* **67**, 578–589.

[73] Kramer PL, Xu H, Woltjer RL, Westaway SK, Clark D, Erten-Lyons D, Kaye JA, Welsh-Bohmer KA, Troncoso JC, Markesbery WR, Petersen RC, Turner RS, Kukull WA, Bennett DA, Galasko D, Morris JC, Ott J (2011) Alzheimer disease pathology in cognitively healthy elderly: a genome-wide study. *Neurobiol Aging* **32**, 2113–2122.

[74] Liang WS, Dunckley T, Beach TG, Grover A, Mastroeni D, Ramsey K, Caselli RJ, Kukull WA, McKeel D, Morris JC, Hulette CM, Schmechel D, Reiman EM, Rogers J, Stephan DA (2010) Neuronal gene expression in non-demented individuals with intermediate Alzheimer's Disease neuropathology. *Neurobiol Aging* **31**, 549–566.

[75] Bilousova T, Miller CA, Poon WW, Vinters H V, Corrada M, Kawas C, Hayden EY, Teplow DB, Glabe C, Albay R, Cole GM, Teng E, Gylys KH (2016) Synaptic Amyloid-β Oligomers Precede p-Tau and Differentiate High Pathology Control Cases. *Am. J. Pathol.* **186**, 185–98.

[76] Arnold SE, Louneva N, Cao K, Wang LS, Han LY, Wolk DA, Negash S, Leurgans SE, Schneider JA, Buchman AS, Wilson RS, Bennett DA (2013) Cellular, synaptic, and biochemical features of resilient cognition in Alzheimer's disease. *Neurobiol Aging* **34**, 157–168.

[77] Schmitt FA, Davis DG, Wekstein DR, Smith CD, Ashford JW, Markesbery WR (2000) "Preclinical" AD revisited: neuropathology of cognitively normal older adults. *Neurology* **55**, 370–376.

[78] Silva AR, Grinberg LT, Farfel JM, Diniz BS, Lima LA, Silva PJ, Ferretti RE, Rocha RM, Filho WJ, Carraro DM, Brentani H (2012) Transcriptional alterations related to neuropathology and clinical manifestation of Alzheimer's disease. *PLoS One* **7**, e48751.

[79] Arriagada P V, Marzloff K, Hyman BT (1992) Distribution of Alzheimer-type pathologic changes in nondemented elderly individuals matches the pattern in Alzheimer's disease. *Neurology* **42**, 1681–1688.

[80] De Meyer G, Shapiro F, Vanderstichele H, Vanmechelen E, Engelborghs S, De Deyn PP, Coart E, Hansson O, Minthon L, Zetterberg H, Blennow K, Shaw L, Trojanowski JQ, Initiative ADN (2010) Diagnosis-independent Alzheimer disease biomarker signature in cognitively normal elderly people. *Arch Neurol* **67**, 949–956.

[81] Gomperts SN, Rentz DM, Moran E, Becker JA, Locascio JJ, Klunk WE, Mathis

CA, Elmaleh DR, Shoup T, Fischman AJ, Hyman BT, Growdon JH, Johnson KA (2008) Imaging amyloid deposition in Lewy body diseases. *Neurology* **71**, 903–910.

[82]   Jack CR, Lowe VJ, Senjem ML, Weigand SD, Kemp BJ, Shiung MM, Knopman DS, Boeve BF, Klunk WE, Mathis CA, Petersen RC (2008) 11C PiB and structural MRI provide complementary information in imaging of Alzheimer's disease and amnestic mild cognitive impairment. *Brain* **131**, 665–680.

[83]   Mintun MA, Larossa GN, Sheline YI, Dence CS, Lee SY, Mach RH, Klunk WE, Mathis CA, DeKosky ST, Morris JC (2006) [11C]PIB in a nondemented population: potential antecedent marker of Alzheimer disease. *Neurology* **67**, 446–452.

[84]   Montine TJ, Peskind ER, Quinn JF, Wilson AM, Montine KS, Galasko D (2011) Increased cerebrospinal fluid F2-isoprostanes are associated with aging and latent Alzheimer's disease as identified by biomarkers. *Neuromolecular Med* **13**, 37–43.

[85]   Morris JC, Storandt M, McKeel DW, Rubin EH, Price JL, Grant EA, Berg L (1996) Cerebral amyloid deposition and diffuse plaques in "normal" aging: Evidence for presymptomatic and very mild Alzheimer's disease. *Neurology* **46**, 707–719.

[86]   Rowe CC, Ellis KA, Rimajova M, Bourgeat P, Pike KE, Jones G, Fripp J, Tochon-Danguy H, Morandeau L, O'Keefe G, Price R, Raniga P, Robins P, Acosta O, Lenzo N, Szoeke C, Salvado O, Head R, Martins R, Masters CL, Ames D, Villemagne VL (2010) Amyloid imaging results from the Australian Imaging, Biomarkers and Lifestyle (AIBL) study of aging. *Neurobiol Aging* **31**, 1275–1283.

[87]   Hedden T, Van Dijk KR, Becker JA, Mehta A, Sperling RA, Johnson KA, Buckner RL (2009) Disruption of functional connectivity in clinically normal older adults harboring amyloid burden. *J Neurosci* **29**, 12686–12694.

[88]   Sheline YI, Raichle ME, Snyder AZ, Morris JC, Head D, Wang S, Mintun MA (2010) Amyloid plaques disrupt resting state default mode network connectivity in cognitively normal elderly. *Biol Psychiatry* **67**, 584–587.

[89]   Sperling RA, Laviolette PS, O'Keefe K, O'Brien J, Rentz DM, Pihlajamaki M, Marshall G, Hyman BT, Selkoe DJ, Hedden T, Buckner RL, Becker JA, Johnson KA (2009) Amyloid deposition is associated with impaired default network function in older persons without dementia. *Neuron* **63**, 178–188.

[90]   Schott JM, Bartlett JW, Fox NC, Barnes J, Investigators ADNI (2010) Increased brain atrophy rates in cognitively normal older adults with low cerebrospinal fluid

138

Aβ1-42. *Ann Neurol* **68**, 825–834.

[91]   Gosche KM, Mortimer JA, Smith CD, Markesbery WR, Snowdon DA (2002) Hippocampal volume as an index of Alzheimer neuropathology: findings from the Nun Study. *Neurology* **58**, 1476–1482.

[92]   Chételat G, Villemagne VL, Pike KE, Baron JC, Bourgeat P, Jones G, Faux NG, Ellis KA, Salvado O, Szoeke C, Martins RN, Ames D, Masters CL, Rowe CC, Group AIB, of Ageing (AIBL) Research LS (2010) Larger temporal volume in elderly with high versus low beta-amyloid deposition. *Brain* **133**, 3349–3358.

[93]   Silva AR, Santos AC, Farfel JM, Grinberg LT, Ferretti RE, Campos AH, Cunha IW, Begnami MD, Rocha RM, Carraro DM, de Bragança Pereira CA, Jacob-Filho W, Brentani H (2014) Repair of oxidative DNA damage, cell-cycle regulation and neuronal death may influence the clinical manifestation of Alzheimer's disease. *PLoS One* **9**, e99897.

[94]   Dickerson BC, Bakkour A, Salat DH, Feczko E, Pacheco J, Greve DN, Grodstein F, Wright CI, Blacker D, Rosas HD, Sperling RA, Atri A, Growdon JH, Hyman BT, Morris JC, Fischl B, Buckner RL (2009) The cortical signature of Alzheimer's disease: regionally specific cortical thinning relates to symptom severity in very mild to mild AD dementia and is detectable in asymptomatic amyloid-positive individuals. *Cereb Cortex* **19**, 497–510.

[95]   Bennett DA, Wilson RS, Schneider JA, Evans DA, de Leon CF, Arnold SE, Barnes LL, Bienias JL (2003) Education modifies the relation of AD pathology to level of cognitive function in older persons. *Neurology* **60**, 1909–1915.

[96]   Coffey CE, Saxton JA, Ratcliff G, Bryan RN, Lucke JF (1999) Relation of education to brain size in normal aging: implications for the reserve hypothesis. *Neurology* **53**, 189–196.

[97]   Roe CM, Xiong C, Miller JP, Morris JC (2007) Education and Alzheimer disease without dementia: support for the cognitive reserve hypothesis. *Neurology* **68**, 223–228.

[98]   Wilson RS, Li Y, Aggarwal NT, Barnes LL, McCann JJ, Gilley DW, Evans DA (2004) Education and the course of cognitive decline in Alzheimer disease. *Neurology* **63**, 1198–1202.

[99]   Mufson EJ, Malek-Ahmadi M, Perez SE, Chen K (2016) Braak staging, plaque pathology, and APOE status in elderly persons without cognitive impairment. *Neurobiol Aging* **37**, 147–153.

[100] Fotenos AF, Mintun MA, Snyder AZ, Morris JC, Buckner RL (2008) Brain volume decline in aging: evidence for a relation between socioeconomic status, preclinical Alzheimer disease, and reserve. *Arch Neurol* **65**, 113–120.

[101] Ngandu T, von Strauss E, Helkala EL, Winblad B, Nissinen A, Tuomilehto J, Soininen H, Kivipelto M (2007) Education and dementia: what lies behind the association? *Neurology* **69**, 1442–1450.

[102] Valenzuela MJ, Sachdev P (2006) Brain reserve and dementia: a systematic review. *Psychol Med* **36**, 441–454.

[103] SantaCruz KS, Sonnen JA, Pezhouh MK, Desrosiers MF, Nelson PT, Tyas SL (2011) Alzheimer disease pathology in subjects without dementia in 2 studies of aging: the Nun Study and the Adult Changes in Thought Study. *J Neuropathol Exp Neurol* **70**, 832–840.

[104] Mortimer JA, Borenstein AR, Gosche KM, Snowdon DA (2005) Very early detection of Alzheimer neuropathology and the role of brain reserve in modifying its clinical expression. *J Geriatr Psychiatry Neurol* **18**, 218–223.

[105] Hall CB, Derby C, LeValley A, Katz MJ, Verghese J, Lipton RB (2007) Education delays accelerated decline on a memory test in persons who develop dementia. *Neurology* **69**, 1657–1664.

[106] Tucker AM, Stern Y (2011) Cognitive reserve in aging. *Curr Alzheimer Res* **8**, 354–360.

[107] Stern Y, Tang MX, Denaro J, Mayeux R (1995) Increased risk of mortality in Alzheimer's disease patients with more advanced educational and occupational attainment. *Ann Neurol* **37**, 590–595.

[108] Scarmeas N, Albert SM, Manly JJ, Stern Y (2006) Education and rates of cognitive decline in incident Alzheimer's disease. *J Neurol Neurosurg Psychiatry* **77**, 308–316.

[109] Stern Y, Albert S, Tang MX, Tsai WY (1999) Rate of memory decline in AD is related to education and occupation: cognitive reserve? *Neurology* **53**, 1942–1947.

[110] Teri L, McCurry SM, Edland SD, Kukull WA, Larson EB (1995) Cognitive decline in Alzheimer's disease: a longitudinal investigation of risk factors for accelerated decline. *J Gerontol A Biol Sci Med Sci* **50A**, M49-55.

[111] Helzner EP, Scarmeas N, Cosentino S, Portet F, Stern Y (2007) Leisure activity

and cognitive decline in incident Alzheimer disease. *Arch Neurol* **64**, 1749–1754.

[112] Craft S (2007) Insulin resistance and Alzheimer's disease pathogenesis: potential mechanisms and implications for treatment. *Curr Alzheimer Res* **4**, 147–152.

[113] de la Monte SM (2009) Insulin resistance and Alzheimer's disease. *BMB Rep* **42**, 475–481.

[114] Zhao WQ, Townsend M (2009) Insulin resistance and amyloidogenesis as common molecular foundation for type 2 diabetes and Alzheimer's disease. *Biochim Biophys Acta* **1792**, 482–496.

[115] De Felice FG, Vieira MN, Bomfim TR, Decker H, Velasco PT, Lambert MP, Viola KL, Zhao WQ, Ferreira ST, Klein WL (2009) Protection of synapses against Alzheimer's-linked toxins: insulin signaling prevents the pathogenic binding of Abeta oligomers. *Proc Natl Acad Sci U S A* **106**, 1971–1976.

[116] Freiherr J, Hallschmid M, Frey WH, Brünner YF, Chapman CD, Hölscher C, Craft S, De Felice FG, Benedict C (2013) Intranasal insulin as a treatment for Alzheimer's disease: a review of basic research and clinical evidence. *CNS Drugs* **27**, 505–514.

[117] Pedersen WA, McMillan PJ, Kulstad JJ, Leverenz JB, Craft S, Haynatzki GR (2006) Rosiglitazone attenuates learning and memory deficits in Tg2576 Alzheimer mice. *Exp Neurol* **199**, 265–273.

[118] Reger MA, Watson GS, Green PS, Wilkinson CW, Baker LD, Cholerton B, Fishel MA, Plymate SR, Breitner JC, DeGroodt W, Mehta P, Craft S (2008) Intranasal insulin improves cognition and modulates beta-amyloid in early AD. *Neurology* **70**, 440–448.

[119] Watson GS, Cholerton BA, Reger MA, Baker LD, Plymate SR, Asthana S, Fishel MA, Kulstad JJ, Green PS, Cook DG, Kahn SE, Keeling ML, Craft S (2005) Preserved cognition in patients with early Alzheimer disease and amnestic mild cognitive impairment during treatment with rosiglitazone: a preliminary study. *Am J Geriatr Psychiatry* **13**, 950–958.

[120] Gold M, Alderton C, Zvartau-Hind M, Egginton S, Saunders AM, Irizarry M, Craft S, Landreth G, Linnamägi U, Sawchak S (2010) Rosiglitazone monotherapy in mild-to-moderate Alzheimer's disease: results from a randomized, double-blind, placebo-controlled phase III study. *Dement Geriatr Cogn Disord* **30**, 131–146.

[121] Tzimopoulou S, Cunningham VJ, Nichols TE, Searle G, Bird NP, Mistry P, Dixon

IJ, Hallett WA, Whitcher B, Brown AP, Zvartau-Hind M, Lotay N, Lai RY, Castiglia M, Jeter B, Matthews JC, Chen K, Bandy D, Reiman EM, Gold M, Rabiner EA, Matthews PM (2010) A multi-center randomized proof-of-concept clinical trial applying [^{18}F]FDG-PET for evaluation of metabolic therapy with rosiglitazone XR in mild to moderate Alzheimer's disease. *J Alzheimers Dis* **22**, 1241–1256.

[122] Selkoe DJ (2001) Clearing the brain's amyloid cobwebs. *Neuron* **32**, 177–180.

[123] Zhao L, Teter B, Morihara T, Lim GP, Ambegaokar SS, Ubeda OJ, Frautschy SA, Cole GM (2004) Insulin-degrading enzyme as a downstream target of insulin receptor signaling cascade: implications for Alzheimer's disease intervention. *J Neurosci* **24**, 11120–11126.

[124] Moloney AM, Griffin RJ, Timmons S, O'Connor R, Ravid R, O'Neill C (2010) Defects in IGF-1 receptor, insulin receptor and IRS-1/2 in Alzheimer's disease indicate possible resistance to IGF-1 and insulin signalling. *Neurobiol Aging* **31**, 224–243.

[125] Scheff SW, Price DA, Ansari MA, Roberts KN, Schmitt FA, Ikonomovic MD, Mufson EJ (2015) Synaptic change in the posterior cingulate gyrus in the progression of Alzheimer's disease. *J Alzheimers Dis* **43**, 1073–1090.

[126] Lue LF, Brachova L, Civin WH, Rogers J (1996) Inflammation, A beta deposition, and neurofibrillary tangle formation as correlates of Alzheimer's disease neurodegeneration. *J Neuropathol Exp Neurol* **55**, 1083–1088.

[127] Scheff SW, Price DA, Schmitt FA, DeKosky ST, Mufson EJ (2007) Synaptic alterations in CA1 in mild Alzheimer disease and mild cognitive impairment. *Neurology* **68**, 1501–1508.

[128] Bjorklund NL, Sadagoparamanujam VM, Taglialatela G (2012) Selective, quantitative measurement of releasable synaptic zinc in human autopsy hippocampal brain tissue from Alzheimer's disease patients. *J Neurosci Methods* **203**, 146–151.

[129] Deshpande A, Kawai H, Metherate R, Glabe CG, Busciglio J (2009) A role for synaptic zinc in activity-dependent Abeta oligomer formation and accumulation at excitatory synapses. *J Neurosci* **29**, 4004–4015.

[130] Zolochevska O, Bjorklund N, Woltjer R, Wiktorowicz JE, Taglialatela G (2018) Postsynaptic Proteome of Non-Demented Individuals with Alzheimer's Disease Neuropathology. *J. Alzheimer's Dis.* **65**, 659–682.

[131] Eriksson PS, Perfilieva E, Björk-Eriksson T, Alborn AM, Nordborg C, Peterson DA, Gage FH (1998) Neurogenesis in the adult human hippocampus. *Nat Med* **4**, 1313–1317.

[132] Ge S, Sailor KA, Ming GL, Song H (2008) Synaptic integration and plasticity of new neurons in the adult hippocampus. *J Physiol* **586**, 3759–3765.

[133] Farin A, Liu CY, Langmoen IA, Apuzzo ML (2009) The biological restoration of central nervous system architecture and function: part 2-emergence of the realization of adult neurogenesis. *Neurosurgery* **64**, 581.

[134] Mufson EJ, He B, Nadeem M, Perez SE, Counts SE, Leurgans S, Fritz J, Lah J, Ginsberg SD, Wuu J, Scheff SW (2012) Hippocampal proNGF signaling pathways and β-amyloid levels in mild cognitive impairment and Alzheimer disease. *J Neuropathol Exp Neurol* **71**, 1018–1029.

[135] Song JH, Yu JT, Tan L (2014) Brain-Derived Neurotrophic Factor in Alzheimer's Disease: Risk, Mechanisms, and Therapy. *Mol Neurobiol*.

[136] Lee J, Duan W, Mattson MP (2002) Evidence that brain-derived neurotrophic factor is required for basal neurogenesis and mediates, in part, the enhancement of neurogenesis by dietary restriction in the hippocampus of adult mice. *J Neurochem* **82**, 1367–1375.

[137] Ansari MA, Scheff SW (2010) Oxidative stress in the progression of Alzheimer disease in the frontal cortex. *J Neuropathol Exp Neurol* **69**, 155–167.

[138] Choi BH (1995) Oxidative stress and Alzheimer's disease. *Neurobiol Aging* **16**, 675–678.

[139] Markesbery WR (1999) The role of oxidative stress in Alzheimer disease. *Arch Neurol* **56**, 1449–1452.

[140] Simpson JE, Ince PG, Minett T, Matthews FE, Heath PR, Shaw PJ, Goodall E, Garwood CJ, Ratcliffe LE, Brayne C, Rattray M, Wharton SB, Group MRCCF, Study AN (2015) Neuronal DNA damage response-associated dysregulation of signalling pathways and cholesterol metabolism at the earliest stages of Alzheimer-type pathology. *Neuropathol Appl Neurobiol*.

[141] Eng LF, Ghirnikar RS, Lee YL (2000) Glial fibrillary acidic protein: GFAP-thirty-one years (1969-2000). *Neurochem Res* **25**, 1439–1451.

[142] Kashon ML, Ross GW, O'Callaghan JP, Miller DB, Petrovitch H, Burchfiel CM,

Sharp DS, Markesbery WR, Davis DG, Hardman J, Nelson J, White LR (2004) Associations of cortical astrogliosis with cognitive performance and dementia status. *J Alzheimers Dis* **6**, 581–595.

[143] Norenberg MD (1994) Astrocyte responses to CNS injury. *J Neuropathol Exp Neurol* **53**, 213–220.

[144] Donato R, Sorci G, Riuzzi F, Arcuri C, Bianchi R, Brozzi F, Tubaro C, Giambanco I (2009) S100B's double life: intracellular regulator and extracellular signal. *Biochim Biophys Acta* **1793**, 1008–1022.

[145] Esposito G, Scuderi C, Lu J, Savani C, De Filippis D, Iuvone T, Steardo L, Sheen V (2008) S100B induces tau protein hyperphosphorylation via Dickopff-1 up-regulation and disrupts the Wnt pathway in human neural stem cells. *J Cell Mol Med* **12**, 914–927.

[146] Rothermundt M, Peters M, Prehn JH, Arolt V (2003) S100B in brain damage and neurodegeneration. *Microsc Res Tech* **60**, 614–632.

[147] Serbinek D, Ullrich C, Pirchl M, Hochstrasser T, Schmidt-Kastner R, Humpel C (2010) S100b counteracts neurodegeneration of rat cholinergic neurons in brain slices after oxygen-glucose deprivation. *Cardiovasc Psychiatry Neurol* **2010**, 106123.

[148] Perez-Nievas BG, Stein TD, Tai HC, Dols-Icardo O, Scotton TC, Barroeta-Espar I, Fernandez-Carballo L, de Munain EL, Perez J, Marquie M, Serrano-Pozo A, Frosch MP, Lowe V, Parisi JE, Petersen RC, Ikonomovic MD, López OL, Klunk W, Hyman BT, Gómez-Isla T (2013) Dissecting phenotypic traits linked to human resilience to Alzheimer's pathology. *Brain* **136**, 2510–2526.

[149] Hiesberger T, Trommsdorff M, Howell BW, Goffinet A, Mumby MC, Cooper JA, Herz J (1999) Direct binding of Reelin to VLDL receptor and ApoE receptor 2 induces tyrosine phosphorylation of disabled-1 and modulates tau phosphorylation. *Neuron* **24**, 481–489.

[150] Ohkubo N, Lee YD, Morishima A, Terashima T, Kikkawa S, Tohyama M, Sakanaka M, Tanaka J, Maeda N, Vitek MP, Mitsuda N (2003) Apolipoprotein E and Reelin ligands modulate tau phosphorylation through an apolipoprotein E receptor/disabled-1/glycogen synthase kinase-3beta cascade. *FASEB J* **17**, 295–297.

[151] Trommsdorff M, Gotthardt M, Hiesberger T, Shelton J, Stockinger W, Nimpf J, Hammer RE, Richardson JA, Herz J (1999) Reeler/Disabled-like disruption of neuronal migration in knockout mice lacking the VLDL receptor and ApoE

receptor 2. *Cell* **97**, 689–701.

[152] Durakoglugil MS, Chen Y, White CL, Kavalali ET, Herz J (2009) Reelin signaling antagonizes beta-amyloid at the synapse. *Proc Natl Acad Sci U S A* **106**, 15938–15943.

[153] Adwan L, Zawia NH (2013) Epigenetics: a novel therapeutic approach for the treatment of Alzheimer's disease. *Pharmacol Ther* **139**, 41–50.

[154] Yao B, Jin P (2014) Cytosine modifications in neurodevelopment and diseases. *Cell Mol Life Sci* **71**, 405–418.

[155] Chouliaras L, Rutten BP, Kenis G, Peerbooms O, Visser PJ, Verhey F, van Os J, Steinbusch HW, van den Hove DL (2010) Epigenetic regulation in the pathophysiology of Alzheimer's disease. *Prog Neurobiol* **90**, 498–510.

[156] Coppieters N, Dieriks B V, Lill C, Faull RL, Curtis MA, Dragunow M (2014) Global changes in DNA methylation and hydroxymethylation in Alzheimer's disease human brain. *Neurobiol Aging* **35**, 1334–1344.

[157] Mill J (2011) Toward an integrated genetic and epigenetic approach to Alzheimer's disease. *Neurobiol Aging* **32**, 1188–1191.

[158] Lord J, Cruchaga C (2014) The epigenetic landscape of Alzheimer's disease. *Nat Neurosci* **17**, 1138–1140.

[159] Cogswell JP, Ward J, Taylor IA, Waters M, Shi Y, Cannon B, Kelnar K, Kemppainen J, Brown D, Chen C, Prinjha RK, Richardson JC, Saunders AM, Roses AD, Richards CA (2008) Identification of miRNA changes in Alzheimer's disease brain and CSF yields putative biomarkers and insights into disease pathways. *J Alzheimers Dis* **14**, 27–41.

[160] Lukiw WJ (2007) Micro-RNA speciation in fetal, adult and Alzheimer's disease hippocampus. *Neuroreport* **18**, 297–300.

[161] Schipper HM, Maes OC, Chertkow HM, Wang E (2007) MicroRNA expression in Alzheimer blood mononuclear cells. *Gene Regul Syst Bio* **1**, 263–274.

[162] Szafranski K, Abraham KJ, Mekhail K (2015) Non-coding RNA in neural function, disease, and aging. *Front Genet* **6**, 87.

[163] Li W, Chen L, Qu X, He W, He Y, Feng C, Jia X, Zhou Y, Lv J, Liang B, Chen B, Jiang J (2013) Unraveling the characteristics of microRNA regulation in the

145

developmental and aging process of the human brain. *BMC Med Genomics* **6**, 55.

[164] Dehghani R, Rahmani F, Rezaei N (2018) MicroRNA in Alzheimer's disease revisited: implications for major neuropathological mechanisms. *Rev. Neurosci.* **29**, 161–182.

[165] Millan MJ (2017) Linking deregulation of non-coding RNA to the core pathophysiology of Alzheimer's disease: An integrative review. *Prog. Neurobiol.* **156**, 1–68.

[166] Zhao J, Yue D, Zhou Y, Jia L, Wang H, Guo M, Xu H, Chen C, Zhang J, Xu L (2017) The Role of MicroRNAs in Aβ Deposition and Tau Phosphorylation in Alzheimer's Disease. *Front. Neurol.* **8**, 342.

[167] Nelson PT, Wang W-X, Rajeev BW (2008) MicroRNAs (miRNAs) in neurodegenerative diseases. *Brain Pathol.* **18**, 130–8.

[168] Wang W-X, Rajeev BW, Stromberg AJ, Ren N, Tang G, Huang Q, Rigoutsos I, Nelson PT (2008) The expression of microRNA miR-107 decreases early in Alzheimer's disease and may accelerate disease progression through regulation of beta-site amyloid precursor protein-cleaving enzyme 1. *J. Neurosci.* **28**, 1213–23.

[169] Llorens F, Thüne K, Andrés-Benito P, Tahir W, Ansoleaga B, Hernández-Ortega K, Martí E, Zerr I, Ferrer I (2017) MicroRNA Expression in the Locus Coeruleus, Entorhinal Cortex, and Hippocampus at Early and Middle Stages of Braak Neurofibrillary Tangle Pathology. *J. Mol. Neurosci.* **63**, 206–215.

[170] Reese LC, Taglialatela G (2011) A role for calcineurin in Alzheimer's disease. *Curr Neuropharmacol* **9**, 685–692.

[171] Folstein MF, Folstein SE, McHugh PR (1975) "Mini-mental state". A practical method for grading the cognitive state of patients for the clinician. *J Psychiatr Res* **12**, 189–198.

[172] Franklin W, Taglialatela G (2016) A method to determine insulin responsiveness in synaptosomes isolated from frozen brain tissue. *J. Neurosci. Methods* **261**, 128–134.

[173] Comerota MM, Krishnan B, Taglialatela G (2017) Near infrared light decreases synaptic vulnerability to amyloid beta oligomers. *Sci. Rep.* **7**, 15012.

[174] Wiktorowicz JE, Stafford S, Rea H, Urvil P, Soman K, Kurosky A, Perez-Polo JR, Savidge TC (2011) Quantification of cysteinyl S-nitrosylation by fluorescence in

unbiased proteomic studies. *Biochemistry* **50**, 5601–5614.

[175] Wiktorowicz JE, Stafford SJ, Garg NJ (2017) Protein Cysteinyl-S-Nitrosylation: Analysis and Quantification. *Methods Enzym.* **586**, 1–14.

[176] Pretzer E, Wiktorowicz JE (2008) Saturation fluorescence labeling of proteins for proteomic analyses. *Anal Biochem* **374**, 250–262.

[177] Straub C, Pazdrak K, Young TW, Stafford SJ, Wu Z, Wiktorowicz JE, Haag AM, English RD, Soman K V, Kurosky A (2009) Toward the Proteome of the Human Peripheral Blood Eosinophil. *Proteomics Clin Appl* **3**, 1151–1173.

[178] Hochberg B (1995) Controlling the False Discovery Rate: a Practical and Powerful Approach to Multiple Testing. *J. R. Stat. Soc.* **57**, 289–300.

[179] Allen M, Kachadoorian M, Quicksall Z, Zou F, Chai HS, Younkin C, Crook JE, Pankratz VS, Carrasquillo MM, Krishnan S, Nguyen T, Ma L, Malphrus K, Lincoln S, Bisceglio G, Kolbert CP, Jen J, Mukherjee S, Kauwe JK, Crane PK, Haines JL, Mayeux R, Pericak-Vance MA, Farrer LA, Schellenberg GD, Parisi JE, Petersen RC, Graff-Radford NR, Dickson DW, Younkin SG, Ertekin-Taner N (2014) Association of MAPT haplotypes with Alzheimer's disease risk and MAPT brain gene expression levels. *Alzheimers Res Ther* **6**, 39.

[180] Singhrao SK, Thomas P, Wood JD, MacMillan JC, Neal JW, Harper PS, Jones AL (1998) Huntingtin protein colocalizes with lesions of neurodegenerative diseases: An investigation in Huntington's, Alzheimer's, and Pick's diseases. *Exp Neurol* **150**, 213–222.

[181] Kelleher RJ, Shen J (2017) Presenilin-1 mutations and Alzheimer's disease. *Proc Natl Acad Sci U S A* **114**, 629–631.

[182] O'Brien RJ, Wong PC (2011) Amyloid precursor protein processing and Alzheimer's disease. *Annu Rev Neurosci* **34**, 185–204.

[183] Van Cauwenberghe C, Van Broeckhoven C, Sleegers K (2016) The genetic landscape of Alzheimer disease: clinical implications and perspectives. *Genet Med* **18**, 421–430.

[184] Chen Z, Zhong C (2013) Decoding Alzheimer's disease from perturbed cerebral glucose metabolism: implications for diagnostic and therapeutic strategies. *Prog Neurobiol* **108**, 21–43.

[185] Huang da W, Sherman BT, Lempicki RA (2009) Systematic and integrative

analysis of large gene lists using DAVID bioinformatics resources. *Nat Protoc* **4**, 44–57.

[186] Mi H, Lazareva-Ulitsky B, Loo R, Kejariwal A, Vandergriff J, Rabkin S, Guo N, Muruganujan A, Doremieux O, Campbell MJ, Kitano H, Thomas PD (2005) The PANTHER database of protein families, subfamilies, functions and pathways. *Nucleic Acids Res* **33**, D284-8.

[187] Thomas PD, Campbell MJ, Kejariwal A, Mi H, Karlak B, Daverman R, Diemer K, Muruganujan A, Narechania A (2003) PANTHER: a library of protein families and subfamilies indexed by function. *Genome Res* **13**, 2129–2141.

[188] Gerke V, Moss SE (2002) Annexins: from structure to function. *Physiol Rev* **82**, 331–371.

[189] Bamburg JR, Bernstein BW (2016) Actin dynamics and cofilin-actin rods in alzheimer disease. *Cytoskelet.* **73**, 477–497.

[190] Rescher U, Gerke V (2004) Annexins--unique membrane binding proteins with diverse functions. *J Cell Sci* **117**, 2631–2639.

[191] Gauthier-Kemper A, Weissmann C, Golovyashkina N, Sebö-Lemke Z, Drewes G, Gerke V, Heinisch JJ, Brandt R (2011) The frontotemporal dementia mutation R406W blocks tau's interaction with the membrane in an annexin A2-dependent manner. *J. Cell Biol.* **192**, 647–661.

[192] Ghosh A, Giese KP (2015) Calcium/calmodulin-dependent kinase II and Alzheimer's disease. *Mol Brain* **8**, 78.

[193] Gu Z, Liu W, Yan Z (2009) {beta}-Amyloid impairs AMPA receptor trafficking and function by reducing Ca2+/calmodulin-dependent protein kinase II synaptic distribution. *J Biol Chem* **284**, 10639–10649.

[194] Wang YJ, Chen GH, Hu XY, Lu YP, Zhou JN, Liu RY (2005) The expression of calcium/calmodulin-dependent protein kinase II-alpha in the hippocampus of patients with Alzheimer's disease and its links with AD-related pathology. *Brain Res* **1031**, 101–108.

[195] Lisman J, Schulman H, Cline H (2002) The molecular basis of CaMKII function in synaptic and behavioural memory. *Nat Rev Neurosci* **3**, 175–190.

[196] Kennedy M (2000) Signal-Processing Machines at the Postsynaptic Density: Science (New York, N.Y.). *Science (80-.).* **290**, 750–755.

[197] Ferrer I, Gómez A, Carmona M, Huesa G, Porta S, Riera-Codina M, Biagioli M, Gustincich S, Aso E (2011) Neuronal hemoglobin is reduced in Alzheimer's disease, argyrophilic grain disease, Parkinson's disease, and dementia with Lewy bodies. *J Alzheimers Dis* **23**, 537–550.

[198] Wilson MT, Reeder BJ (2008) Oxygen-binding haem proteins. *Exp Physiol* **93**, 128–132.

[199] Chuang JY, Lee CW, Shih YH, Yang T, Yu L, Kuo YM (2012) Interactions between amyloid-β and hemoglobin: implications for amyloid plaque formation in Alzheimer's disease. *PLoS One* **7**, e33120.

[200] Ryu JK, McLarnon JG (2009) A leaky blood-brain barrier, fibrinogen infiltration and microglial reactivity in inflamed Alzheimer's disease brain. *J Cell Mol Med* **13**, 2911–2925.

[201] van de Haar HJ, Burgmans S, Jansen JF, van Osch MJ, van Buchem MA, Muller M, Hofman PA, Verhey FR, Backes WH (2017) Blood-Brain Barrier Leakage in Patients with Early Alzheimer Disease. *Radiology* **282**, 615.

[202] Ueno M, Chiba Y, Murakami R, Matsumoto K, Kawauchi M, Fujihara R (2016) Blood-brain barrier and blood-cerebrospinal fluid barrier in normal and pathological conditions. *Brain Tumor Pathol* **33**, 89–96.

[203] Richter F, Meurers BH, Zhu C, Medvedeva VP, Chesselet MF (2009) Neurons express hemoglobin alpha- and beta-chains in rat and human brains. *J Comp Neurol* **515**, 538–547.

[204] Schelshorn DW, Schneider A, Kuschinsky W, Weber D, Krüger C, Dittgen T, Bürgers HF, Sabouri F, Gassler N, Bach A, Maurer MH (2009) Expression of hemoglobin in rodent neurons. *J Cereb Blood Flow Metab* **29**, 585–595.

[205] Shephard F, Greville-Heygate O, Marsh O, Anderson S, Chakrabarti L (2014) A mitochondrial location for haemoglobins--dynamic distribution in ageing and Parkinson's disease. *Mitochondrion* **14**, 64–72.

[206] Shi Q, Xu H, Kleinman WA, Gibson GE (2008) Novel functions of the alpha-ketoglutarate dehydrogenase complex may mediate diverse oxidant-induced changes in mitochondrial enzymes associated with Alzheimer's disease. *Biochim Biophys Acta* **1782**, 229–238.

[207] Shi Q, Gibson GE (2011) Up-regulation of the mitochondrial malate dehydrogenase by oxidative stress is mediated by miR-743a. *J Neurochem* **118**,

440–448.

[208] Balasubramanian P, Howell PR, Anderson RM (2017) Aging and Caloric Restriction Research: A Biological Perspective With Translational Potential. *EBioMedicine* **21**, 37–44.

[209] Ntsapi C, Loos B (2016) Caloric restriction and the precision-control of autophagy: A strategy for delaying neurodegenerative disease progression. *Exp Gerontol* **83**, 97–111.

[210] Janke C, Bulinski JC (2011) Post-translational regulation of the microtubule cytoskeleton: mechanisms and functions. *Nat Rev Mol Cell Biol* **12**, 773–786.

[211] Reinikainen KJ, Pitkänen A, Riekkinen PJ (1989) 2′,3′-Cyclic nucleotide-3′-phosphodiesterase activity as an index of myelin in the post-mortem brains of patients with Alzheimer's disease. *Neurosci. Lett.* **106**, 229–232.

[212] Vlkolinský R, Cairns N, Fountoulakis M, Lubec G (2001) Decreased brain levels of 2′,3′-cyclic nucleotide-3′-phosphodiesterase in Down syndrome and Alzheimer's disease. *Neurobiol. Aging* **22**, 547–553.

[213] Thompson RJ (1992) 2',3'-cyclic nucleotide-3'-phosphohydrolase and signal transduction in central nervous system myelin. *Biochem Soc Trans* **20**, 621–626.

[214] Lee J, Gravel M, Zhang R, Thibault P, Braun PE (2005) Process outgrowth in oligodendrocytes is mediated by CNP, a novel microtubule assembly myelin protein. *J Cell Biol* **170**, 661–673.

[215] Butterfield DA, Hardas SS, Lange ML (2010) Oxidatively modified glyceraldehyde-3-phosphate dehydrogenase (GAPDH) and Alzheimer's disease: many pathways to neurodegeneration. *J Alzheimers Dis* **20**, 369–393.

[216] Schulze H, Schuler A, Stüber D, Döbeli H, Langen H, Huber G (1993) Rat Brain Glyceraldehyde-3-Phosphate Dehydrogenase Interacts with the Recombinant Cytoplasmic Domain of Alzheimer's β-Amyloid Precursor Protein. *J. Neurochem.* **60**, 1915–1922.

[217] Mazzola JL, Sirover MA (2001) Reduction of glyceraldehyde-3-phosphate dehydrogenase activity in Alzheimer's disease and in Huntington's disease fibroblasts. *J Neurochem* **76**, 442–449.

[218] Garcia ML, Lobsiger CS, Shah SB, Deerinck TJ, Crum J, Young D, Ward CM, Crawford TO, Gotow T, Uchiyama Y, Ellisman MH, Calcutt NA, Cleveland DW

(2003) NF-M is an essential target for the myelin-directed "outside-in" signaling cascade that mediates radial axonal growth. *J Cell Biol* **163**, 1011–1020.

[219] Elder GA, Friedrich VL, Bosco P, Kang C, Gourov A, Tu PH, Lee VM, Lazzarini RA (1998) Absence of the mid-sized neurofilament subunit decreases axonal calibers, levels of light neurofilament (NF-L), and neurofilament content. *J Cell Biol* **141**, 727–739.

[220] Yuan A, Rao M V, Veeranna, Nixon RA (2012) Neurofilaments at a glance. *J Cell Sci* **125**, 3257–3263.

[221] Kinoshita A, Kinoshita M, Akiyama H, Tomimoto H, Akiguchi I, Kumar S, Noda M, Kimura J (1998) Identification of septins in neurofibrillary tangles in Alzheimer's disease. *Am J Pathol* **153**, 1551–1560.

[222] Mostowy S, Cossart P (2012) Septins: the fourth component of the cytoskeleton. *Nat Rev Mol Cell Biol* **13**, 183–194.

[223] Kinoshita A, Noda M, Kinoshita M (2000) Differential localization of septins in the mouse brain. *J Comp Neurol* **428**, 223–239.

[224] Groenendyk J, Lynch J, Michalak M (2004) Calreticulin, Ca2+, and calcineurin - signaling from the endoplasmic reticulum. *Mol Cells* **17**, 383–389.

[225] Taguchi J, Fujii A, Fujino Y, Tsujioka Y, Takahashi M, Tsuboi Y, Wada I, Yamada T (2000) Different expression of calreticulin and immunoglobulin binding protein in Alzheimer's disease brain. *Acta Neuropathol* **100**, 153–160.

[226] Duus K, Hansen PR, Houen G (2008) Interaction of calreticulin with amyloid beta peptide 1-42. *Protein Pept Lett* **15**, 103–107.

[227] Johnson RJ, Xiao G, Shanmugaratnam J, Fine RE (2001) Calreticulin functions as a molecular chaperone for the beta-amyloid precursor protein. *Neurobiol Aging* **22**, 387–395.

[228] Michalak M, Corbett EF, Mesaeli N, Nakamura K, Opas M (1999) Calreticulin: one protein, one gene, many functions. *Biochem J* **344 Pt 2**, 281–292.

[229] Stemmer N, Strekalova E, Djogo N, Plöger F, Loers G, Lutz D, Buck F, Michalak M, Schachner M, Kleene R (2013) Generation of amyloid-β is reduced by the interaction of calreticulin with amyloid precursor protein, presenilin and nicastrin. *PLoS One* **8**, e61299.

[230] Vattemi G, Engel WK, McFerrin J, Askanas V (2004) Endoplasmic reticulum stress and unfolded protein response in inclusion body myositis muscle. *Am J Pathol* **164**, 1–7.

[231] Lynch J, Guo L, Gelebart P, Chilibeck K, Xu J, Molkentin JD, Agellon LB, Michalak M (2005) Calreticulin signals upstream of calcineurin and MEF2C in a critical Ca(2+)-dependent signaling cascade. *J Cell Biol* **170**, 37–47.

[232] Lynch J, Michalak M (2003) Calreticulin is an upstream regulator of calcineurin. *Biochem Biophys Res Commun* **311**, 1173–1179.

[233] Abdul HM, Sama MA, Furman JL, Mathis DM, Beckett TL, Weidner AM, Patel ES, Baig I, Murphy MP, LeVine H, Kraner SD, Norris CM (2009) Cognitive decline in Alzheimer's disease is associated with selective changes in calcineurin/NFAT signaling. *J Neurosci* **29**, 12957–12969.

[234] Norris CM, Kadish I, Blalock EM, Chen KC, Thibault V, Porter NM, Landfield PW, Kraner SD (2005) Calcineurin triggers reactive/inflammatory processes in astrocytes and is upregulated in aging and Alzheimer's models. *J Neurosci* **25**, 4649–4658.

[235] Dineley KT, Hogan D, Zhang WR, Taglialatela G (2007) Acute inhibition of calcineurin restores associative learning and memory in Tg2576 APP transgenic mice. *Neurobiol Learn Mem* **88**, 217–224.

[236] Taglialatela G, Hogan D, Zhang WR, Dineley KT (2009) Intermediate- and long-term recognition memory deficits in Tg2576 mice are reversed with acute calcineurin inhibition. *Behav Brain Res* **200**, 95–99.

[237] Taglialatela G, Rastellini C, Cicalese L (2015) Reduced Incidence of Dementia in Solid Organ Transplant Patients Treated with Calcineurin Inhibitors. *J Alzheimers Dis* **47**, 329–333.

[238] Nakamura Y, Takeda M, Yoshimi K, Hattori H, Hariguchi S, Kitajima S, Hashimoto S, Nishimura T (1994) Involvement of clathrin light chains in the pathology of Alzheimer's disease. *Acta Neuropathol* **87**, 23–31.

[239] Tojima T, Itofusa R, Kamiguchi H (2010) Asymmetric clathrin-mediated endocytosis drives repulsive growth cone guidance. *Neuron* **66**, 370–377.

[240] Kuboyama T, Lee YA, Nishiko H, Tohda C (2015) Inhibition of clathrin-mediated endocytosis prevents amyloid β-induced axonal damage. *Neurobiol Aging* **36**, 1808–1819.

[241] Kuiper JW, Oerlemans FT, Fransen JA, Wieringa B (2008) Creatine kinase B deficient neurons exhibit an increased fraction of motile mitochondria. *BMC Neurosci* **9**, 73.

[242] Schlattner U, Tokarska-Schlattner M, Wallimann T (2006) Mitochondrial creatine kinase in human health and disease. *Biochim Biophys Acta* **1762**, 164–180.

[243] Brady ST, Lasek RJ (1981) Nerve-specific enolase and creatine phosphokinase in axonal transport: soluble proteins and the axoplasmic matrix. *Cell* **23**, 515–523.

[244] Moreira PI, Carvalho C, Zhu X, Smith MA, Perry G (2010) Mitochondrial dysfunction is a trigger of Alzheimer's disease pathophysiology. *Biochim Biophys Acta* **1802**, 2–10.

[245] Swerdlow RH, Burns JM, Khan SM (2010) The Alzheimer's disease mitochondrial cascade hypothesis. *J Alzheimers Dis* **20 Suppl 2**, S265-79.

[246] Gray LR, Tompkins SC, Taylor EB (2014) Regulation of pyruvate metabolism and human disease. *Cell Mol Life Sci* **71**, 2577–2604.

[247] Tiwari V, Patel AB (2014) Pyruvate carboxylase and pentose phosphate fluxes are reduced in AβPP-PS1 mouse model of Alzheimer's disease: a ^{13}C NMR study. *J Alzheimers Dis* **41**, 387–399.

[248] Nestler EJ, Greengard P (1982) Distribution of protein I and regulation of its state of phosphorylation in the rabbit superior cervical ganglion. *J Neurosci* **2**, 1011–1023.

[249] Qin S, Hu XY, Xu H, Zhou JN (2004) Regional alteration of synapsin I in the hippocampal formation of Alzheimer's disease patients. *Acta Neuropathol* **107**, 209–215.

[250] Pevsner J, Hsu SC, Scheller RH (1994) n-Sec1: a neural-specific syntaxin-binding protein. *Proc Natl Acad Sci U S A* **91**, 1445–1449.

[251] Misura KM, Scheller RH, Weis WI (2000) Three-dimensional structure of the neuronal-Sec1-syntaxin 1a complex. *Nature* **404**, 355–362.

[252] Donovan LE, Higginbotham L, Dammer EB, Gearing M, Rees HD, Xia Q, Duong DM, Seyfried NT, Lah JJ, Levey AI (2012) Analysis of a membrane-enriched proteome from postmortem human brain tissue in Alzheimer's disease. *Proteomics Clin Appl* **6**, 201–211.

[253] Liu Y, Fallon L, Lashuel HA, Liu Z, Lansbury PT (2002) The UCH-L1 gene encodes two opposing enzymatic activities that affect alpha-synuclein degradation and Parkinson's disease susceptibility. *Cell* **111**, 209–218.

[254] Osaka H, Wang YL, Takada K, Takizawa S, Setsuie R, Li H, Sato Y, Nishikawa K, Sun YJ, Sakurai M, Harada T, Hara Y, Kimura I, Chiba S, Namikawa K, Kiyama H, Noda M, Aoki S, Wada K (2003) Ubiquitin carboxy-terminal hydrolase L1 binds to and stabilizes monoubiquitin in neuron. *Hum Mol Genet* **12**, 1945–1958.

[255] Satoh JI, Kuroda Y (2001) Ubiquitin C-terminal hydrolase-L1 (PGP9.5) expression in human neural cell lines following induction of neuronal differentiation and exposure to cytokines, neurotrophic factors or heat stress. *Neuropathol Appl Neurobiol* **27**, 95–104.

[256] Choi J, Levey AI, Weintraub ST, Rees HD, Gearing M, Chin LS, Li L (2004) Oxidative modifications and down-regulation of ubiquitin carboxyl-terminal hydrolase L1 associated with idiopathic Parkinson's and Alzheimer's diseases. *J Biol Chem* **279**, 13256–13264.

[257] Lombardino AJ, Li XC, Hertel M, Nottebohm F (2005) Replaceable neurons and neurodegenerative disease share depressed UCHL1 levels. *Proc Natl Acad Sci U S A* **102**, 8036–8041.

[258] Hotulainen P, Hoogenraad CC (2010) Actin in dendritic spines: connecting dynamics to function. *J Cell Biol* **189**, 619–629.

[259] Zolochevska O, Taglialatela G (2016) Non-demented individuals with Alzheimer's disease neuropathology: Resistance to cognitive decline may reveal new treatment strategies. *Curr. Pharm. Des.* **22**,.

[260] Pollard TD, Blanchoin L, Mullins RD (2000) Molecular mechanisms controlling actin filament dynamics in nonmuscle cells. *Annu Rev Biophys Biomol Struct* **29**, 545–576.

[261] Thievessen I, Thompson PM, Berlemont S, Plevock KM, Plotnikov S V, Zemljic-Harpf A, Ross RS, Davidson MW, Danuser G, Campbell SL, Waterman CM (2013) Vinculin-actin interaction couples actin retrograde flow to focal adhesions, but is dispensable for focal adhesion growth. *J Cell Biol* **202**, 163–177.

[262] Quinlan MP (2004) Vinculin, VASP, and profilin are coordinately regulated during actin remodeling in epithelial cells, which requires de novo protein synthesis and protein kinase signal transduction pathways. *J Cell Physiol* **200**, 277–290.

[263] Kalló G, Emri M, Varga Z, Ujhelyi B, Tőzsér J, Csutak A, Csősz É (2016) Changes in the Chemical Barrier Composition of Tears in Alzheimer's Disease Reveal Potential Tear Diagnostic Biomarkers. *PLoS One* **11**, e0158000.

[264] Ohtsuka T, Shimizu K, Yamamori B, Kuroda S, Takai Y (1996) Activation of brain B-Raf protein kinase by Rap1B small GTP-binding protein. *J Biol Chem* **271**, 1258–1261.

[265] Schwamborn JC, Püschel AW (2004) The sequential activity of the GTPases Rap1B and Cdc42 determines neuronal polarity. *Nat. Neurosci.* **7**, 923–929.

[266] Melendez J, Grogg M, Zheng Y (2011) Signaling role of Cdc42 in regulating mammalian physiology. *J Biol Chem* **286**, 2375–2381.

[267] Boulter E, Garcia-Mata R, Guilluy C, Dubash A, Rossi G, Brennwald PJ, Burridge K (2010) Regulation of Rho GTPase crosstalk, degradation and activity by RhoGDI1. *Nat Cell Biol* **12**, 477–483.

[268] Nobes CD, Hall A (1995) Rho, rac, and cdc42 GTPases regulate the assembly of multimolecular focal complexes associated with actin stress fibers, lamellipodia, and filopodia. *Cell* **81**, 53–62.

[269] Tapon N, Hall A (1997) Rho, Rac and Cdc42 GTPases regulate the organization of the actin cytoskeleton. *Curr Opin Cell Biol* **9**, 86–92.

[270] Yan XX, Jeromin A (2012) Spectrin Breakdown Products (SBDPs) as Potential Biomarkers for Neurodegenerative Diseases. *Curr Transl Geriatr Exp Gerontol Rep* **1**, 85–93.

[271] Fernández-Shaw C, Marina A, Cazorla P, Valdivieso F, Vázquez J (1997) Anti-brain spectrin immunoreactivity in Alzheimer's disease: Degradation of spectrin in an animal model of cholinergic degeneration. *J. Neuroimmunol.* **77**, 91–98.

[272] Masliah E, Iimoto DS, Saitoh T, Hansen LA, Terry RD (1990) Increased immunoreactivity of brain spectrin in Alzheimer disease: a marker for synapse loss? *Brain Res* **531**, 36–44.

[273] Wechsler A, Teichberg VI (1998) Brain spectrin binding to the NMDA receptor is regulated by phosphorylation, calcium and calmodulin. *EMBO J* **17**, 3931–3939.

[274] Steiner JP, Walke HT, Bennett V (1989) Calcium/calmodulin inhibits direct binding of spectrin to synaptosomal membranes. *J Biol Chem* **264**, 2783–2791.

[275] Lue LF, Kuo YM, Roher AE, Brachova L, Shen Y, Sue L, Beach T, Kurth JH, Rydel RE, Rogers J (1999) Soluble amyloid beta peptide concentration as a predictor of synaptic change in Alzheimer's disease. *Am J Pathol* **155**, 853–862.

[276] Kelly BL, Vassar R, Ferreira A (2005) Beta-amyloid-induced dynamin 1 depletion in hippocampal neurons. A potential mechanism for early cognitive decline in Alzheimer disease. *J Biol Chem* **280**, 31746–31753.

[277] Guo CH, Senzel A, Li K, Feng ZP (2010) De novo protein synthesis of syntaxin-1 and dynamin-1 in long-term memory formation requires CREB1 gene transcription in Lymnaea stagnalis. *Behav Genet* **40**, 680–693.

[278] Fa M, Staniszewski A, Saeed F, Francis YI, Arancio O (2014) Dynamin 1 is required for memory formation. *PLoS One* **9**, e91954.

[279] Zhu L, Su M, Lucast L, Liu L, Netzer WJ, Gandy SE, Cai D (2012) Dynamin 1 regulates amyloid generation through modulation of BACE-1. *PLoS One* **7**, e45033.

[280] Hol EM, Roelofs RF, Moraal E, Sonnemans MA, Sluijs JA, Proper EA, de Graan PN, Fischer DF, van Leeuwen FW (2003) Neuronal expression of GFAP in patients with Alzheimer pathology and identification of novel GFAP splice forms. *Mol Psychiatry* **8**, 786–796.

[281] Shiozaki A, Tsuji T, Kohno R, Kawamata J, Uemura K, Teraoka H, Shimohama S (2004) Proteome analysis of brain proteins in Alzheimer's disease: subproteomics following sequentially extracted protein preparation. *J Alzheimers Dis* **6**, 257–268.

[282] Korolainen MA, Auriola S, Nyman TA, Alafuzoff I, Pirttilä T (2005) Proteomic analysis of glial fibrillary acidic protein in Alzheimer's disease and aging brain. *Neurobiol. Dis.* **20**, 858–870.

[283] Richens JL, Spencer HL, Butler M, Cantlay F, Vere KA, Bajaj N, Morgan K, O'Shea P (2016) Rationalising the role of Keratin 9 as a biomarker for Alzheimer's disease. *Sci Rep* **6**, 22962.

[284] Richens JL, Vere KA, Light RA, Soria D, Garibaldi J, Smith AD, Warden D, Wilcock G, Bajaj N, Morgan K, O'Shea P (2014) Practical detection of a definitive biomarker panel for Alzheimer's disease; comparisons between matched plasma and cerebrospinal fluid. *Int J Mol Epidemiol Genet* **5**, 53–70.

[285] Vafadar-Isfahani B, Ball G, Coveney C, Lemetre C, Boocock D, Minthon L, Hansson O, Miles AK, Janciauskiene SM, Warden D, Smith AD, Wilcock G,

Kalsheker N, Rees R, Matharoo-Ball B, Morgan K (2012) Identification of SPARC-like 1 protein as part of a biomarker panel for Alzheimer's disease in cerebrospinal fluid. *J Alzheimers Dis* **28**, 625–636.

[286] Neuner SM, Wilmott LA, Hoffmann BR, Mozhui K, Kaczorowski CC (2017) Hippocampal proteomics defines pathways associated with memory decline and resilience in normal aging and Alzheimer's disease mouse models. *Behav Brain Res* **322**, 288–298.

[287] Jiang S, Wu J, Yang Y, Liu J, Ding Y, Ding M (2012) Proteomic analysis of the cerebrospinal fluid in multiple sclerosis and neuromyelitis optica patients. *Mol Med Rep* **6**, 1081–1086.

[288] Knoops B, Clippe A, Bogard C, Arsalane K, Wattiez R, Hermans C, Duconseille E, Falmagne P, Bernard A (1999) Cloning and characterization of AOEB166, a novel mammalian antioxidant enzyme of the peroxiredoxin family. *J Biol Chem* **274**, 30451–30458.

[289] Davey GP, Bolaños JP (2013) Peroxiredoxin 5 links mitochondrial redox signalling with calcium dynamics: Impact on Parkinson's disease. *J. Neurochem.* **125**, 332–333.

[290] Dubuisson M, Vander Stricht D, Clippe A, Etienne F, Nauser T, Kissner R, Koppenol WH, Rees JF, Knoops B (2004) Human peroxiredoxin 5 is a peroxynitrite reductase. *FEBS Lett* **571**, 161–165.

[291] Trujillo M, Clippe A, Manta B, Ferrer-Sueta G, Smeets A, Declercq JP, Knoops B, Radi R (2007) Pre-steady state kinetic characterization of human peroxiredoxin 5: taking advantage of Trp84 fluorescence increase upon oxidation. *Arch Biochem Biophys* **467**, 95–106.

[292] Femminella GD, Ferrara N, Rengo G (2015) The emerging role of microRNAs in Alzheimer's disease. *Front Physiol* **6**, 40.

[293] Eacker SM, Dawson TM, Dawson VL (2009) Understanding microRNAs in neurodegeneration. *Nat Rev Neurosci* **10**, 837–841.

[294] Clark WG, Vivonia CA, Baxter CF (1968) Accurate freehand injection into the lateral brain ventricle of the conscious mouse. *J Appl Physiol* **25**, 319–321.

[295] Lasagna-Reeves CA, Castillo-Carranza DL, Guerrero-Muñoz MJ, Jackson GR, Kayed R (2010) Preparation and Characterization of Neurotoxic Tau Oligomers. *Biochemistry* **49**, 10039–10041.

[296] Dobin A, Davis CA, Schlesinger F, Drenkow J, Zaleski C, Jha S, Batut P, Chaisson M, Gingeras TR (2013) STAR: ultrafast universal RNA-seq aligner. *Bioinformatics* **29**, 15–21.

[297] Love MI, Huber W, Anders S (2014) Moderated estimation of fold change and dispersion for RNA-seq data with DESeq2. *Genome Biol.* **15**, 550.

[298] Wang F, Ma YL, Zhang P, Shen TY, Shi CZ, Yang YZ, Moyer MP, Zhang HZ, Chen HQ, Liang Y, Qin HL (2013) SP1 mediates the link between methylation of the tumour suppressor miR-149 and outcome in colorectal cancer. *J Pathol* **229**, 12–24.

[299] Pevida M, Lastra A, Hidalgo A, Baamonde A, Menéndez L (2013) Spinal CCL2 and microglial activation are involved in paclitaxel-evoked cold hyperalgesia. *Brain Res Bull* **95**, 21–27.

[300] Cohen JE, Lee PR, Chen S, Li W, Fields RD (2011) MicroRNA regulation of homeostatic synaptic plasticity. *Proc Natl Acad Sci U S A* **108**, 11650–11655.

[301] Cohen JE, Lee PR, Fields RD (2014) Systematic identification of 3'-UTR regulatory elements in activity-dependent mRNA stability in hippocampal neurons. *Philos Trans R Soc L. B Biol Sci* **369**,.

[302] Faghihi MA, Zhang M, Huang J, Modarresi F, der Brug MP, Nalls MA, Cookson MR, St-Laurent G, Wahlestedt C (2010) Evidence for natural antisense transcript-mediated inhibition of microRNA function. *Genome Biol* **11**, R56.

[303] Arora S, Saini S, Fukuhara S, Majid S, Shahryari V, Yamamura S, Chiyomaru T, Deng G, Tanaka Y, Dahiya R (2013) MicroRNA-4723 inhibits prostate cancer growth through inactivation of the Abelson family of nonreceptor protein tyrosine kinases. *PLoS One* **8**, e78023.

[304] Alvarez AR, Sandoval PC, Leal NR, Castro PU, Kosik KS (2004) Activation of the neuronal c-Abl tyrosine kinase by amyloid-beta-peptide and reactive oxygen species. *Neurobiol Dis* **17**, 326–336.

[305] Gonzalez-Zuñiga M, Contreras PS, Estrada LD, Chamorro D, Villagra A, Zanlungo S, Seto E, Alvarez AR (2014) c-Abl stabilizes HDAC2 levels by tyrosine phosphorylation repressing neuronal gene expression in Alzheimer's disease. *Mol Cell* **56**, 163–173.

[306] Kovalevich J, Langford D (2013) Considerations for the use of SH-SY5Y neuroblastoma cells in neurobiology. *Methods Mol. Biol.* **1078**, 9–21.

[307] Gylys KH, Fein JA, Yang F, Cole GM (2004) Enrichment of presynaptic and postsynaptic markers by size-based gating analysis of synaptosome preparations from rat and human cortex. *Cytometry* **60A**, 90–96.

[308] Gylys KH, Fein JA, Cole GM (2000) Quantitative characterization of crude synaptosomal fraction (P-2) components by flow cytometry. *J. Neurosci. Res.* **61**, 186–192.

[309] Oliveros JC (2015) Venny. An interactive tool for comparing lists with Venn's diagrams. bioinfogp.cnb.csic.es/tools/venny/

[310] Parihar MS, Brewer GJ (2010) Amyloid-β as a modulator of synaptic plasticity. *J Alzheimers Dis* **22**, 741–763.

[311] Aksoy-Aksel A, Zampa F, Schratt G (2014) MicroRNAs and synaptic plasticity--a mutual relationship. *Philos Trans R Soc L. B Biol Sci* **369**,.

[312] Eacker SM, Dawson TM, Dawson VL (2013) The interplay of microRNA and neuronal activity in health and disease. *Front Cell Neurosci* **7**, 136.

[313] Ye Y, Xu H, Su X, He X (2016) Role of MicroRNA in Governing Synaptic Plasticity. *Neural Plast* **2016**, 4959523.

[314] Nadim WD, Simion V, Benedetti H, Pichon C, Baril P, Morisset-Lopez S (2017) MicroRNAs in Neurocognitive Dysfunctions: New Molecular Targets for Pharmacological Treatments? *Curr. Neuropharmacol.* **15**, 260–275.

[315] Schonrock N, Ke YD, Humphreys D, Staufenbiel M, Ittner LM, Preiss T, Götz J (2010) Neuronal microRNA deregulation in response to Alzheimer's disease amyloid-beta. *PLoS One* **5**, e11070.

[316] Biundo F, Del Prete D, Zhang H, Arancio O, D'Adamio L (2018) A role for tau in learning, memory and synaptic plasticity. *Sci. Rep.* **8**, 3184.

[317] Antonucci F, Corradini I, Fossati G, Tomasoni R, Menna E, Matteoli M (2016) SNAP-25, a Known Presynaptic Protein with Emerging Postsynaptic Functions. *Front. Synaptic Neurosci.* **8**, 7.

[318] Burré J (2015) The Synaptic Function of α-Synuclein. *J. Parkinsons. Dis.* **5**, 699–713.

[319] Dweep H, Sticht C, Pandey P, Gretz N (2011) miRWalk--database: prediction of possible miRNA binding sites by "walking" the genes of three

genomes. *J. Biomed. Inform.* **44**, 839–47.

[320] Dweep H, Gretz N (2015) miRWalk2.0: a comprehensive atlas of microRNA-target interactions. *Nat. Methods* **12**, 697–697.

[321] Catalanotto C, Cogoni C, Zardo G (2016) MicroRNA in Control of Gene Expression: An Overview of Nuclear Functions. *Int. J. Mol. Sci.* **17**,.

[322] Boudreau RL, Jiang P, Gilmore BL, Spengler RM, Tirabassi R, Nelson JA, Ross CA, Xing Y, Davidson BL (2014) Transcriptome-wide discovery of microRNA binding sites in human brain. *Neuron* **81**, 294–305.

[323] Marzi MJ, Ghini F, Cerruti B, de Pretis S, Bonetti P, Giacomelli C, Gorski MM, Kress T, Pelizzola M, Muller H, Amati B, Nicassio F (2016) Degradation dynamics of microRNAs revealed by a novel pulse-chase approach. *Genome Res* **26**, 554–565.

[324] Hippius H, Neundörfer G (2003) The discovery of Alzheimer's disease. *Dialogues Clin. Neurosci.* **5**, 101–8.

[325] Alzheimer's & Brain Research Milestones, [Internet] https://www.alz.org/research/science/major_milestones_in_alzheimers.asp Last updated 2010, Accessed on 2010.

[326] Merlo S, Spampinato SF, Sortino MA (2017) Estrogen and Alzheimer's disease: Still an attractive topic despite disappointment from early clinical results. *Eur. J. Pharmacol.* **817**, 51–58.

[327] Bean LA, Ianov L, Foster TC (2014) Estrogen receptors, the hippocampus, and memory. *Neuroscientist* **20**, 534–45.

[328] Xiong YS, Liu FF, Liu D, Huang HZ, Wei N, Tan L, Chen JG, Man HY, Gong CX, Lu Y, Wang JZ, Zhu LQ (2015) Opposite effects of two estrogen receptors on tau phosphorylation through disparate effects on the miR-218/PTPA pathway. *Aging Cell* **14**, 867–877.

[329] Butler HT, Warden DR, Hogervorst E, Ragoussis J, Smith AD, Lehmann DJ (2010) Association of the aromatase gene with Alzheimer's disease in women. *Neurosci. Lett.* **468**, 202–206.

[330] Hojo Y, Murakami G, Mukai H, Higo S, Hatanaka Y, Ogiue-Ikeda M, Ishii H, Kimoto T, Kawato S (2008) Estrogen synthesis in the brain--role in synaptic plasticity and memory. *Mol. Cell. Endocrinol.* **290**, 31–43.

[331] Li R, He P, Cui J, Staufenbiel M, Harada N, Shen Y (2013) Brain Endogenous Estrogen Levels Determine Responses to Estrogen Replacement Therapy via Regulation of BACE1 and NEP in Female Alzheimer's Transgenic Mice. *Mol. Neurobiol.* **47**, 857–867.

[332] Kretz O, Fester L, Wehrenberg U, Zhou L, Brauckmann S, Zhao S, Prange-Kiel J, Naumann T, Jarry H, Frotscher M, Rune GM (2004) Hippocampal Synapses Depend on Hippocampal Estrogen Synthesis. *J. Neurosci.* **24**, 5913–5921.

[333] Maki PM (2005) Estrogen effects on the hippocampus and frontal lobes. *Int. J. Fertil. Womens. Med.* **50**, 67–71.

[334] Gupta A, Caffrey E, Callagy G, Gupta S (2012) Oestrogen-dependent regulation of miRNA biogenesis: many ways to skin the cat. *Biochem. Soc. Trans.* **40**, 752–8.

[335] Amtul Z, Wang L, Westaway D, Rozmahel RF (2010) Neuroprotective mechanism conferred by 17beta-estradiol on the biochemical basis of Alzheimer's disease. *Neuroscience* **169**, 781–786.

<div align="center">**Curriculum Vita**</div>

PRESENT POSITION AND ADDRESS:

Ph.D. candidate
University of Texas Medical Branch at Galveston
Department of Neuroscience and Cell Biology
10.148 Medical Research Building
301 University Blvd.
Galveston, TX 77555-1045
Email: olzoloch@utmb.edu

BIOGRAPHICAL:

Birthplace: Kharkiv, Ukraine
Citizenship: United States

EDUCATION:

08/2013 to present   **Predoctoral Research Fellow**
Cell Biology Program
Department of Neuroscience, Cell Biology and Anatomy
The University of Texas Medical Branch, Galveston, TX

09/2006-07/2007   **Master of Science in Biophysics**, *summa cum laude*
V. Karazin Kharkiv National University, Kharkiv, Ukraine

09/2006-07/2007   **Master of Education in Biophysics**, *summa cum laude*
V. Karazin Kharkiv National University, Kharkiv, Ukraine

09/2002-07/2006   **Bachelor of Science in Applied Physics**, *magna cum laude*
V. Karazin Kharkiv National University, Kharkiv, Ukraine

CERTIFICATIONS:

2011 to present   Certified in Biosafety Level 2 (BSL2) and Animal Biosafety Level 2 (ASBL2), UTMB, TX

2011 to present   Certified in Laboratory Animal Science from the American Association, UTMB, TX

PROFESSIONAL AND TEACHING EXPERIENCE:

Professional Experience:

08/2013 to present	**Predoctoral Research Fellow**, Department of Neuroscience and Cell Biology, University of Texas Medical Branch, Galveston, TX Mentor: Giulio Taglialatela Project: Synaptic proteome of individuals with Alzheimer's Disease and Non-Demented with Alzheimer's Neuropathology.
08/2013-12/2013	**Predoctoral Research Fellow**, Department of Pharmacology and Toxicology, University of Texas Medical Branch, Galveston, TX Mentor: Marxa L. Figueiredo Project: Cloning of IL-27 receptors to perform split-luciferase assay.
03/2011-08/2013	**Research Associate II**, Department of Pharmacology and Toxicology, University of Texas Medical Branch, Galveston, TX P.I: Marxa L. Figueiredo Projects: 1) Cancer gene-therapy using adipose-derived stem cells. 2) Sonoporation delivery of cytokines to treat prostate cancer.
07/2009-02/2011	**Research Associate II**, Comparative Biomedical Sciences, School of Veterinary Medicine, Louisiana State University, Baton Rouge, LA P.I: Marxa L. Figueiredo Projects: 1) Oncogenic potential of XMRV in prostate cancer. 2) Development of tissue-targeted adenoviral vectors for squamous cell carcinoma.
07/2008-07/2009	**Research Associate I**, Comparative Biomedical Sciences, School of Veterinary Medicine, Louisiana State University, Baton Rouge, LA P.I: Marxa L. Figueiredo Projects: 1) Cell cycle regulation by Cdk2ap1 to inhibit tumor growth 2) *In vivo* prostate cancer treatment using p27 and MDA7 as tumor suppressor genes.
01/2008-06/2008	**Research Associate,** Mechanisms of Diabetes Complications Laboratory, Pennington Biomedical Research Center, Louisiana State University, Baton Rouge, LA P.I: Irina G. Obrosova

Teaching Experience:

06/2017 to present   **Adjunct Faculty, Biology**, San Jacinto College, Pasadena, TX

09/2014-12/2014   **Small Group Facilitator**, Teaching Biochemistry (BBSC 6401) University of Texas Medical Branch, Galveston, TX

09/2004-06/2006   **Teacher of Computer Science** Lyubotyn Interschool Educational-Manufacturing Center, Ukraine

RESEARCH ACTIVITIES:

Grant Support:

Current:

F31AG057217, NIA, NIH
"Epigenetic modulation of amyloid beta-resistant synapses in Non-Demented subjects with Alzheimer's Neuropathology" (PI: O. Zolochevska; 07/20/17-TBD)

Past:

T32ES007254, NIEHS Environmental Toxicology Training Grant, UTMB
"Characterization of synaptic proteome of Non-Demented subjects with Alzheimer's Neuropathology" (PI: B.T. Ameredes; 08/2015-06/2017)

TEACHING RESPONSIBILITIES AT UTMB:

Students/Mentees/Advisees/Trainees:

Ph.D. students:

03/2015-04/2015   Junaid Islam, Medical Student (3rd year), UTMB

03/2013-11/2013   Joseph Shearer, Predoctoral Research Fellow, GSBS, UTMB

01/2013-02/2013   Ches'Nique Phillips, Predoctoral Research Fellow, GSBS, UTMB

05/2012-06/2012   Yafang Zhang, Predoctoral Research Fellow, GSBS, UTMB

03/2012-04/2012   Valentina Fokina, Predoctoral Research Fellow, GSBS, UTMB

Undergraduate students:

06/2018-08/2018	Julianna Capece, Neuroscience Summer Undergraduate Research Program, UTMB
07/2017-08/2017	Tolulope Famuyiro, Neuroscience Summer Undergraduate Research Program, UTMB
09/2015-05/2016	Maria Quevedo, Bench Tutorials Program: Scientific Research and Design Program, UTMB-Ball High School

TEACHING RESPONSIBILITIES AT LSU:

Students/Mentees/Advisees/Trainees:

Ph.D. students:

09/2009-12/2009	Jie Zhu, Ph.D. student, Department of Comparative Biomedical Sciences, LSU

Undergraduate students:

07/2010-12/2010	Carlissa Wells, Student, Dept. of Comparative Biomedical Sciences, LSU
05/2010-08/2010	Brennen Comeaux (premed), Louisiana Biomedical Research Network (LBRN) Summer Program. Department of Comparative Biomedical Sciences, LSU
05/2010-08/2010	Richard Djapni (prepharmacy) BIOL 3999: Independent Research, Howard Hughes Medical Institute (HHMI) Summer Program. Department of Comparative Biomedical Sciences, LSU
2009-2010	Olivia Gioe (premed), Department of Comparative Biomedical Sciences, LSU

MEMBERSHIPS IN SCIENTIFIC SOCIETIES:

National:

08/2016 to present	Member, American Association for the Advancement of Science
04/2014 to present	Student Member, Society for Neuroscience
02/2011-12/2013	Member, American Association for Cancer Research

Local:

01/2014 to present	Student Member, Society for Neuroscience Galveston Chapter
01/2014 to present	Student Member, Society of Cell Biology at UTMB

10/2015-06/2017   Student Member, Lone Star and South Central Society of Toxicology

HONORS AND AWARDS:

12/2017   *The Arthur V. Simmang Scholarship Fund*, UTMB

07/2017   elected to the *Who's Who Among Students In American Universities & Colleges* for 2017

05/2017   *1st place in Oral Session 2: Pathophysiology, Injury, and Degeneration of the Neuron*, 4th Annual Cell Biology Student Symposium, UTMB, Galveston, TX

11/2016   *Shirley and Albert E. Sanders, M.D. Presidential Scholarship*, UTMB

10/2016   *Best poster presentation*, Lone Star and South Central SOT Joint 2016 Fall Meeting, Waco, TX

05/2016   *1st place in Oral Session 1: Neuronal Development and Pathophysiology, Outstanding Predoctoral Fellow*, 3rd Annual Cell Biology Student Symposium, UTMB

05/2016   *Outstanding Service Award, First Place,* 3rd Annual Cell Biology Student Symposium, UTMB

05/2016   *Sigma Xi Award for the Overall Best Presentation,* 3rd Annual Cell Biology Student Symposium, UTMB

11/2015   *Edith and Robert Zinn Presidential Scholarship,* UTMB

03/2015   *2nd place in Poster Session "Frontiers In Cell Biology". Poster title: "Synaptic proteome in individuals naturally resistant to Alzheimer's Disease".* 2nd Annual Cell Biology Student Symposium, UTMB

11/2014   *Dennis William Bowman Scholarship in Biomedical Research*, UTMB

04/2010   *Academic Support Award*, LSU School of Veterinary Medicine

ADDITIONAL INFORMATION:

__Journal Reviewer for__ Stem Cell and Development

Professional Development:

05/2016 and 08/2015   Certificate for attending UTMB Mini Medical School, UTMB, TX

04/2015   Certificate for attending The Hallmarks on Aging Lecture Series presented by Dr. John Papaconstantinou, UTMB, TX

COMMUNITY SERVICE AND ACTIVITIES:

03/2016 to present   Speaker's Bureau at the Alzheimer's Association Houston & Southeast Chapter

09/2014 to present   Volunteer at the Alzheimer's Association Houston & Southeast Chapter

08/2014 to present   Judge for the Summer Undergraduate Research Program, UTMB

01/2014 to present   Volunteer at the Society for Neuroscience Galveston Chapter

08/2013 to present   Member of the Committee for Career Development, UTMB

05/2015-07/2017   Vice-chair of the Committee for Career Development, UTMB

08/2013-05/2014,
05/2016-05/2017   Student Government Association Senator, UTMB

05/2015-05/2016   President of Society of Cell Biology, UTMB

06/2014-05/2016   Volunteer at the Galveston County Food Bank

PUBLISHED:

Articles in peer-reviewed journals:

1. **Zolochevska, O**, Bjorklund, N, Woltjer, R, Wiktorowicz, JE, Taglialatela, G. Postsynaptic proteome of non-demented individuals with Alzheimer's neuropathology. *Journal of Alzheimer's Disease*. 2018;65(2):659-682.
2. Briley, D, Ghirardi, V, Woltjer, R, Renck, A, **Zolochevska, O** and Taglialatela, G. Preserved neurogenesis in Non-Demented with AD Neuropathology. *Scientific Reports*. 2016 Jun 14; 6:27812.
3. Tran, TD, **Zolochevska, O,** Figueiredo, ML, Wang, H, Yang, LJ, Gimble, JM, Yao, S, Cheng H. Histamine-induced Ca2+ signaling is mediated by TRPM4 channels in human adipose-derived stem cells. *Biochemical Journal,* 2014 Jul 8. [Epub ahead of print]
4. Parelkar, SS, Letteri, R, Chan-Seng, D, **Zolochevska, O**, Ellis, J, Figueiredo, M, Emrick, T. Polymer-peptide delivery platforms effect of oligopeptide orientation on

polymer-based DNA delivery. *Biomacromolecules,* 2014 Apr 14;15(4):1328-36. Epub Mar 7.

5. **Zolochevska, O,** Shearer, J, Ellis, J, Fokina, V, Shah, F, Gimble, JM, Figueiredo, ML. Human adipose-derived mesenchymal stromal cell pigment epithelium-derived factor cytotherapy modifies genetic and epigenetic profiles of prostate cancer cells. *Cytotherapy,* 2014 Mar;16(3):346-56.

6. **Zolochevska, O**, Ellis J, Parelkar S, Chan-Seng, D, Emrick, T, Wei, J, Patrikeev, I, Motamedi, M, Figueiredo, ML. Interleukin-27 gene delivery for modifying malignant interactions between prostate tumor and bone. *Human Gene Therapy*, 2013 Dec;24(12):970-87.

7. **Zolochevska, O,** Diaz-Quinones, AO, Ellis, J, Figueiredo, ML. Interleukin-27 expression modifies prostate cancer crosstalk with bone and immune cells. *Journal of Cellular Physiology*, 2013 May;228(5): 1127-36.

8. Nelson, P, Tran, T, Zhang, H, **Zolochevska, O**, Figueiredo, M, Feng, JM, Gutierrez, D, Xiao, R, Yao, S, Penn, A, Yang, LJ, Cheng, H. Transient receptor potential melastatin 4 channel controls calcium signals and dental follicle stem cell differentiation. *Stem Cells,* 2013; 31:167-177.

9. **Zolochevska, O,** Bergstrom, SH, Comeaux, B, Emrick, T, Figueiredo, ML. Novel antitumor strategies using cytokine PEDF for prostate cancer therapy. *Current Angiogenesis,* 2012, 1.

10. **Zolochevska, O**, Figueiredo, ML. Advances in sonoporation strategies for cancer. *Frontiers in Bioscience,* 2012 Jan 1;S4, 988-1006.

11. **Zolochevska, O,** Xia, X, Williams, J, Ramsay, A, Li, S, Figueiredo, ML. Sonoporation delivery of Interleukin 27 gene therapy efficiently reduces prostate tumor cell growth in vivo. *Human Gene Therapy,* 2011 Dec 22(12): 1537-50.

12. **Zolochevska, O,** Yu G, Gimble, J, Figueiredo, ML. PEDF and MDA-7 cytokine gene therapies delivered by adipose-derived mesenchymal stem cells are effective in reducing prostate cancer cell growth. *Stem Cells and Development,* 2012 May 1; 21(7):1112-23.

13. Nelson, PL, **Zolochevska, O,** Figueiredo, ML, Soliman, A, Hsu, WH, Feng, JM, Zhang, H, Cheng, H. Regulation of Ca(2+)-entry in pancreatic α-cell line by transient receptor potential melastatin 4 plays a vital role in glucagon release. *Molecular and Cellular Endocrinology,* 2011 Mar 30;335(2):126-34.

14. **Zolochevska, O** and Figueiredo, ML. Cell cycle regulators cdk2ap1 and bicalutamide suppress malignant biological interactions between prostate cancer and bone cells. *The Prostate,* 2011 Mar 1;71(4):353-67.

15. **Zolochevska, O** and Figueiredo, ML. Novel tumor growth inhibition mechanism by cell cycle regulator cdk2ap1 involves anti-angiogenesis modulation. *Microvascular Research*, 2010 Dec;80(3):324-31.

16. **Zolochevska, O** and Figueiredo, ML. Cell cycle regulator cdk2ap1 inhibits prostate

cancer cell growth and modifies androgen-responsive pathway. *The Prostate. 2009.* Oct 1;69(14):1586-97.

17. **<u>Zolochevska, O</u>**, Figueiredo, ML. Expression of cell cycle regulator cdk2ap1 suppresses tumor cell phenotype by non-cell-autonomous mechanisms. *Oral Oncology.* 2009. Sep;45(9):e106-12.

Other:

Thesis/Dissertation:

1. **<u>Zolochevska, O</u>**. (2007) Molecular Dynamics of Proteins. M.S. thesis. V. Karazin Kharkiv National University, Kharkiv, Ukraine.
2. **<u>Zolochevska, O.</u>** (2006) Influence of Low-Intensive Laser Radiation of Various Range on Structural State of Liposome Membranes. B.S. thesis. V. Karazin Kharkiv National University, Kharkiv, Ukraine.

Reviews:

1. **<u>Zolochevska, O</u>** and Taglialatela, G. Non-demented individuals with Alzheimer's disease neuropathology: resistance to cognitive decline may reveal new treatment strategies. *Current Pharmaceutical Design.* 2016 May 18. [Epub ahead of print]

Book chapters:

1. **<u>Zolochevska, O</u>**, Watzel, R, Figueiredo, ML. Progress in gene therapy for oral cancer. *In:* Oral Cancer: Causes, Diagnosis and Treatment (2011). Ed. M.K. Harris. Nova publishers. pp 113-144.

ABSTRACTS:

1. **<u>Zolochevska, O</u>** and Taglialatela, G. Modulation of synaptic amyloid beta resistance by microRNAs. *Society for Neuroscience Annual Meeting.* November 3-7, 2018. San Diego, CA.

2. Micci, M-A, **<u>Zolochevska, O</u>**, Krishnan, B, Kayed, R, Zhang, W R, Bishop, E, Anacker, C, Taglialatela, G. Specific miRNAs enriched in neural stem cell-derived exosomes reduce vulnerability of hippocampal synapses to the dysfunctional impact of amyloid beta and tau oligomers. Society for Neuroscience Annual Meeting. November 3-7, 2018. San Diego, CA.

3. **Zolochevska, O** and Taglialatela, G. Epigenetic modulation of synaptic resilience in Alzheimer's Disease. *Gordon Conference: Neurobiology of Disease*. August 4-10, 2018. Castelldefels, Spain.

4. **Zolochevska, O** and Taglialatela, G. Modulation of synaptic amyloid beta resistance by microRNAs. *Gordon Conference: Cell Biology of the Neuron*. June 24-29, 2018. Waterville Valley, NH.

5. **Zolochevska, O** and Taglialatela, G. Modulation of synaptic amyloid beta resistance by microRNAs. *Cold Spring Harbor meeting: Regulatory and Non-Coding RNAs*. May 15-19, 2018. Cold Spring Harbor Laboratory, NY.

6. **Zolochevska, O** and Taglialatela, G. Modulation of synaptic amyloid beta resistance by microRNAs. *2018 Alzheimer's Association Research Symposium*. May 2, 2018. Houston, TX.

7. Famuyiro, T, **Zolochevska, O**, Comerota, M, Emmett, M, Taglialatela, G, Krishnan, B. Gamma radiation alters synaptosome size and amyloid beta oligomer susceptibility in C57BL/6 mice. *Neuroscience Summer Undergraduate Research Program Forum*. August 11, 2017. Galveston, TX.

8. **Zolochevska, O** and Taglialatela, G. MiRNA-4723 and -485 modulate synaptic resistance to amyloid beta in a cellular model. *The 4th Annual Cell Biology Student Symposium*. May 25, 2017. Galveston, TX.

9. **Zolochevska, O**, Woltjer, R and Taglialatela, G. Epigenetic modulation of synaptic resistance to amyloid-beta. *Society for Neuroscience Annual Meeting*. November 12-16, 2016. San Diego, CA.

10. Briley, D, **Zolochevska, O,** Woltjer, R, Micci, M-A, Taglialatela, G. Increased number of neural stem cells in the hippocampus correlates with maintenance of cognitive integrity in Non-Demented individuals with Alzheimer's Disease Neuropathology. *Society for Neuroscience Annual Meeting*. November 12-16, 2016. San Diego, CA.

11. **Zolochevska, O** and Taglialatela, G. MicroRNA-4723 and -485 modulate amyloid beta synaptotoxicity in a cellular model of Alzheimer's Disease. *Lone Star and South Central SOT Joint 2016 Fall Meeting*. October 21-22, 2016. Waco, TX.

12. **Zolochevska, O** and Taglialatela, G. Amyloid beta synaptotoxicity is regulated by miRNA-4723 and -485 in Alzheimer's Disease. *20th Annual Forum on Aging*. October 20, 2016. Galveston, TX.

13. **Zolochevska, O** and Taglialatela, G. Role of microRNA in modulation of synaptic amyloid-beta resistance in Non-Demented subjects with Alzheimer's Neuropathology. *The 3rd Annual Cell Biology Student Symposium.* May 4, 2016. Galveston, TX.

14. **Zolochevska, O,** Bjorklund, N, Woltjer, RL, Wiktorowicz, J, Taglialatela, G. Post-Synaptic Density S-Nitroso-Proteome in Individuals Naturally Resistant to Alzheimer's Disease. *Lone Star and South Central SOT Joint 2015 Fall Meeting.* October 22-24, 2015. Houston, TX.

15. **Zolochevska, O,** Bjorklund, N, Woltjer, RL, Wiktorowicz, J, Taglialatela, G. S-Nitroso-Proteome in Individuals Naturally Resistant to Alzheimer's Disease. *Society for Neuroscience Annual Meeting.* October 17-21, 2015. Chicago, IL.

16. Baymon, D, Chiesa, N, **Zolochevska, O,** Taglialatela, G. Increased BDNF levels in the central nervous system (CNS) in patients with non-dementing Alzheimer's neuropathology presentation. *The 9th Annual Research Symposium on Alzheimer's Disease and Related Dementias.* September 16, 2015. Houston, TX.

17. **Zolochevska, O,** Bjorklund, N, Woltjer, RL, Wiktorowicz, J, Taglialatela, G. S-Nitroso-Proteome in Individuals Naturally Resistant to Alzheimer's Disease. *The 9th Annual Research Symposium on Alzheimer's Disease and Related Dementias.* September 16, 2015. Houston, TX.

18. **Zolochevska, O,** Baymon, D, Woltjer, R, Taglialatela, G. Preserved BDNF levels in the CNS parallel cognitive integrity in Non-Demented Individuals with Alzheimer's Disease Neuropathology. *Alzheimer's Association International Conference.* July 17-23, 2015. Washington, DC.

19. **Zolochevska, O,** Bjorklund, N, Wiktorowicz, JE, Taglialatela, G. Synaptic proteome in individuals naturally resistant to Alzheimer's Disease. *2nd Annual Cell Biology Student Symposium.* March 19, 2015. Galveston, TX. - *2nd place in Poster Session "Frontiers In Cell Biology". Poster title: "Synaptic proteome in individuals naturally resistant to Alzheimer's Disease".*

20. Briley, DJ, **Zolochevska, O**, Micci, M-A, Taglialatela, G. Increased proportion of cells co-expressing Sox-2 and NeuN in dentate gyrus of Non-Demented patients with Alzheimer's Neuropathology. *18th Annual Forum on Aging.* December 2, 2014. Galveston, TX.

21. **Zolochevska, O,** Bjorklund, N, Wiktorowicz, JE, Taglialatela, G. Synaptic proteome in individuals naturally resistant to Alzheimer's Disease. *18th Annual Forum on Aging.* December 2, 2014. Galveston, TX.

22. **Zolochevska, O,** Ghirardi, V, Bjorklund, N, Micci, M-A, Taglialatela, G. Increased presence of cells co-expressing Sox2 and NeuN in the dentate gyrus of cognitively-intact individuals with substantial Alzheimer's Disease neuropathology. *Society for Neuroscience Annual Meeting.* November 15-19, 2014. Washington, DC.

23. **Zolochevska, O**, Figueiredo, ML. Sonoporation delivery of Interleukin-27 gene therapy efficiently reduces prostate tumor growth. *28th Southern Biomedical Engineering Conference.* May 4-6, 2012. Houston, TX.

24. **Zolochevska, O**, Figueiredo, ML. Efficient delivery of prostate cancer gene therapy via adipose-derived mesenchymal stem cells in vivo. *American Association for Cancer Research 103rd Annual Meeting*. April 31 – May 4, 2012. Chicago, IL.

25. Comeaux, BP, **Zolochevska, O**, Figueiredo, ML. A role for XMRV in prostate tumor promotion in vivo. *American Association for Cancer Research 103rd Annual Meeting*. April 31 – May 4, 2012. Chicago, IL.

26. **Zolochevska, O**, Figueiredo, ML. Novel tissue-targeted virogeneimaging system for squamous cell carcinoma therapy expressing cell cycle regulator cdk2ap1. *American Association for Cancer Research 103rd Annual Meeting*. April 31 – May 4, 2012. Chicago, IL.

27. **Zolochevska, O**, Figueiredo, ML. Novel tissue-targeted adenoviral vector for squamous cell carcinoma therapy expressing cell cycle regulator cdk2ap1 and molecular imaging genes. *American Association for Cancer Research 102nd Annual Meeting*. April 2-6, 2011. Orlando, FL.

28. Comeaux, B, **Zolochevska, O**, Figueiredo, ML. Examination of the oncogenic potential of XMRV in prostate epithelial cells. *American Association for Cancer Research 102nd Annual Meeting*. April 2-6, 2011. Orlando, FL.

29. Nelson, P, Zhang, H, Figueiredo, ML, **Zolochevska, O**, Feng, J-M, Yao, S, Guiterrez, DR, and Cheng, H. TRPM4 controls calcium signals in dental follicle stem cells. *International Association for Dental Research (IADR/AADR/CADR) 89th General Session and Exhibition*. March 16-19, 2011. San Diego, CA.

30. Nelson, P, **Zolochevska, O**, Figueiredo, ML, Hsu, W, Soliman, A, Feng, J-M, Zhang, H, Cheng, H. Characterization of transient receptor potential melastatin 4 in glucagon-secreting α-cells. *Phi Zeta Research Emphasis Day*. September 29, 2010. Baton Rouge, LA.

31. **Zolochevska, O**, Li, S, Figueiredo, ML. Monitoring sonoporation efficacy in prostate cancer by bioluminescence imaging for cancer gene therapy applications. *Phi Zeta Research Emphasis Day*. September 29, 2010. Baton Rouge, LA.

32. **Zolochevska, O**, Gimble, JM, Figueiredo, ML. Efficient delivery of prostate cancer gene therapy via adipose-derived mesenchymal stem cells. *Phi Zeta Research Emphasis Day*. September 29, 2010. Baton Rouge, LA.

33. Comeaux, B, Watzel, R, **Zolochevska, O**, and Figueiredo, ML. Examination of the oncogenic potential of XMRV in prostate cancer cells. *Phi Zeta Research Emphasis Day*. September 29, 2010. Baton Rouge, LA.

34. Djapni, RT, **Zolochevska, O**, and Figueiredo, ML. Development of new bone metastatic prostate cancer model for gene therapy applications. *17th Annual Summer Undergraduate Research Forum*. Baton Rouge, LA. July 29, 2010.

35. Comeaux, B, Watzel, R, **Zolochevska, O**, and Figueiredo, ML. Examination of the oncogenic potential of XMRV in prostate cancer cells. *17th Annual Summer Undergraduate Research Forum*. Baton Rouge, LA. July 29, 2010.

36. Nelson, P, **Zolochevska, O**, Figueiredo, M, Hsu, W, Soliman, A, Feng, J-M, Zhang, H, and Cheng, H. Characterization of transient receptor potential melastatin 4 in glucagon-secreting α-cells. *American Diabetes Association 70th Scientific Sessions*. June 25 - 29, 2010. Orlando, FL.

37. **Zolochevska, O**, Figueiredo, ML. Expression of the cell cycle regulator p27kip1 sensitizes prostate cancer cells to shHer2-mediated cell death mechanisms. *DNA Vaccines 2010: International Society of DNA Vaccines (Gene Therapy)*. March 2-4, 2010. New Orleans, LA.

38. **Zolochevska, O**, Li, S, Figueiredo, ML. Monitoring sonoporation efficacy in prostate cancer in vivo by bioluminescence imaging for cancer gene therapy applications. *DNA Vaccines 2010: International Society of DNA Vaccines (Gene Therapy)*. March 2-4, 2010. New Orleans, LA.

39. **Zolochevska, O**, Gimble, JM, Figueiredo, ML. Efficient delivery of cancer gene therapy via adipose-derived mesenchymal stem cells in vivo. *DNA Vaccines 2010: International Society of DNA Vaccines (Gene Therapy)*. March 2-4, 2010. New Orleans, LA.

40. **Zolochevska, O** and Figueiredo, ML. Novel tissue-targeted adenoviral vector for squamous cell carcinoma therapy expressing cell cycle regulator cdk2ap1 and molecular imaging genes. *DNA Vaccines 2010: International Society of DNA Vaccines (Gene Therapy)*. March 2-4, 2010. New Orleans, LA.

41. Martinez-Ramirez, EJ, **Zolochevska, O**, and Figueiredo, ML. p27 and MDA7 tumor suppressor gene therapy for prostate cancer treatment in vivo. *Louisiana NCRR/IDeA 2010 Biomedical Research Symposium*. Baton Rouge Marriot Hotel.

173

January 22, 2010. Baton Rouge, LA.

42. **<u>Zolochevska, O</u>** and Figueiredo, ML. A new Ad-based transcriptionally targeted vector for detecting and treating squamous cell carcinoma. *Center to Reduce Cancer Health Disparities (CRCHD) Professional Development Workshop 2009*. National Cancer Institute. August 5-6, 2009. Rockville, MD.

43. **<u>Zolochevska, O</u>** and Figueiredo, ML. A new Ad-based transcriptionally targeted vector for imaging therapeutic strategies for squamous cell carcinoma. *Frontiers in Imaging Meeting*. Vanderbilt University. June 2-5, 2009. Nashville, TN.

44. **<u>Zolochevska, O</u>** and Figueiredo, ML. A novel role for p12/CDK2AP1 cell cycle regulator in inhibiting cancer cell growth. In: *FASEB Experimental Biology 2009/American Society of Investigative Pathology (ASIP)*. April 18-22, 2009. New Orleans, LA.

45. **<u>Zolochevska, O</u>** and Figueiredo, ML. New orthotopic mouse models and Ad-based transcriptionally targeted vectors for squamous cell carcinoma therapy development. In: *FASEB Experimental Biology 2009/American Society of Investigative Pathology (ASIP)*. April 18-22, 2009. New Orleans, LA.

46. Martinez-Ramirez, EJ, **<u>Zolochevska, O</u>**, and Figueiredo, ML. New combination therapy using p27kip1 and MDA-7 tumor suppressor genes for prostate cancer. *Merck-Merial and NIH T35 Veterinary Scholars Symposium*. North Carolina State University. August 6-8, 2009. Raleigh, NC.

47. Shymanskyy, I, **<u>Zolochevska, O</u>**, Donchenko, G, Klimenko, A, Kuchmerovska, T. Association of impaired brain protein ADP-ribosylation with mitochondrial dysfunction in diabetes: evidence for the beneficial role of acetyl-L-carnitine supplementation. *European Association for the Study of Diabetes 44th Annual Meeting*. September 7-11, 2008. Rome, Italy.

ORAL PRESENTATIONS:

1. **<u>Zolochevska, O.</u>** Epigenetic modulation of synaptic resilience in Alzheimer's Disease. *Gordon Conference: Neurobiology of Disease*. August 4, 2018. Castelldefels, Spain.

2. **<u>Zolochevska O</u>**. Synaptic proteome of patients with Alzheimer's Disease and subjects who are Non-Demented with Alzheimer's Neuropathology. *The Department of Neuroscience and Cell Biology and Cell Biology Graduate Program.* December 12, 2014. Galveston, TX.

3. **<u>Zolochevska, O</u>**. Epigenetic Modulation of Amyloid Beta-Resistant Synapses in Non-Demented Subjects with Alzheimer's Neuropathology. *The Department of*

Neuroscience and Cell Biology and Cell Biology Graduate Program. July 29, 2015. Galveston, TX.

4. **Zolochevska O**. Synaptic proteome of individuals with Alzheimer's Disease and Non-Demented with AD Neuropathology. *The Department of Neuroscience and Cell Biology and Cell Biology Graduate Program.* August 5, 2015. Galveston, TX.

5. **Zolochevska, O**. Characterization of Synaptic Proteome of Non-Demented Subjects with Alzheimer's Neuropathology. *Joint meeting of the Lone Star Chapter and the South Central Chapter of the Society of Toxicology.* October 22-24, 2015. Houston, TX.

6. **Zolochevska, O**. Role of microRNA in modulation of synaptic amyloid-beta resistance in Non-Demented subjects with Alzheimer's Neuropathology. *3rd Annual Cell Biology Symposium.* May 4, 2016. Galveston, TX. - *1st place in Oral Session 1: Neuronal Development and Pathophysiology, Outstanding Predoctoral Fellow* and *Sigma Xi Award for the Overall Best Presentation.*

7. **Zolochevska, O**. MiRNA-4723 and -485 modulate synaptic resistance to amyloid beta in a cellular model. *4th Annual Cell Biology Student Symposium.* May 25, 2017. Galveston, TX. – *1st place in Oral Session 2: Pathophysiology, Injury, and Degeneration of the Neuron.*

8. **Zolochevska, O.** Role of miRNA in modulation of synaptic amyloid beta resistance in Non-Demented subjects with Alzheimer's Neuropathology. *The Department of Neuroscience and Cell Biology and Cell Biology Graduate Program.* August 8, 2017. Galveston, TX.

9. **Zolochevska, O.** Epigenetic modulation of synaptic resilience in Alzheimer's Disease. Mitchell Center Seminar Series. February 19, 2018. Galveston, TX.

Permanent address: 2295 Ashley Falls Lane, League City, TX 77573.

This dissertation was typed by Olga Zolochevska.